N° d'ordre :
N° de série :

UNIVERSITE KASDI MERBAH OUARGLA

Faculté des hydrocarbures, énergies renouvelables et science de la terre et de l'univers

Département de Géologie

Thèse

Présentée pour l'obtention du diplôme de

Doctorat sciences

Spécialité : Géologie

Présenté par :

Mohamed Ali ARBAOUI

Thème

Les problèmes de récupération des hydrocarbures en Algérie (traitement des dépôts du sulfate de baryum)

Sotenu publiquement le :
Devant le jury composé de :

BELKSIR Mohamed Salah	**MCA**	**UKMO**	**Président**
HACINI Messaoud	**Professeur**	**UKMO**	**Directeur de thèse**
ZATOUT Merzouk	**MCA**	**UKMO**	**Examinateur**
BOUDLEMAA Abderrazak	**MCA**	**U. Tlemcen**	**Examinateur**
HAMZIOUI Louanas	**Professeur**	**U. M'sila**	**Examinateur**
BENZAHI Khedidja	**MCA**	**ENS Ouargla**	**Examinatrice**

Order number :
Serial number :

A thesis submitted to the University Kasdi Merbah Ouargla for the degree of Doctor of Philosophy (PhD) in The Faculty of Hydrocarbons, Renewable Energies and Science of Earth and Universe

Geology Department

Presented by :
Mohamed Ali ARBAOUI

Theme

Hydrocarbon recovery problems in Algeria (treatment of barium sulphate deposits)

Discussed publicly on :

Before the jury composed of :

BELKSIR Mohamed Salah	**MCA**	**UKMO**	**Chairman**
HACINI Messaoud	**Professor**	**UKMO**	**Supervisor**
ZATOUT Merzouk	**MCA**	**UKMO**	**Examiner**
BOUDJEMAA Abderrazak	**MCA**	**U. Tlemcen**	**Examiner**
HAMZIOUI Louanas	**Professor**	**U. M'sila**	**Examiner**
BENZAHI Khedidja	**MCA**	**ENS Ouargla**	**Examiner**

Acknowledgements

I would like to thank in a very special way my PhD supervisor, **Pr. Messaoud Hacini** for his patience, understanding, advice and the confidence he always showed me during the realization of this work.

I am very appreciative to the honor we have done to **Mr. Mohamed Salah Beleksir** of Kasdi Merbah Ouargla University for having accepted to preside over the jury; that he finds here my deep gratitude and my sincere thanks.

My thanks also go to the examiners of our thesis **Mrs Merzouk Zatout, Abderrazak Boudjemaa, Louanas Hamzioui,** and **Ms Khadija Benzahi** for having devoted time to the examination of this work. I am very sensitive to the honor they gave me by participating in the jury of our thesis. Whose they find here the expression of my gratitude!

I would like to thank also all those who supported and helped me to perform this work especially **Mr Belarbi Noureldine**. Finally, I intend to dedicate this work to my parents and all the members of my family, as well as to the entire teams of Irara and Geology of Sahara laboratories.

ABSTRACT

Abstract

The main objective of this thesis is to predict, prevent and assess the effectiveness of barium sulphate scale treatment methods in the field of Hassi Messaoud during the injection of treated water. Scale deposition is one of the most critical oil field problems that water injection systems face, especially when two incompatible fluids are present. When two water volumes interact chemically and precipitate minerals when mixed, they are incompatible. Injection water with a high sulphate ion concentration and formation waters with a high barium ion concentration are obvious examples. As a result of mixing these water volumes, barium sulphate could precipitate. The formation of the barium sulphate scale is posing a challenge to oil and gas production. Once formed, it plugs oil pipelines, blocking tubes, valves, pumps, and other production flow systems, resulting in well abandonment and a significant economic loss. A detailed and comprehensive review is offered to understand the behaviours of this very insoluble material. Because of the incompatibility between these water volumes at the molecular level, several wells from the Hassi-Messaoud field were selected and analysed in the laboratory, then compared to the reference oil field water analysis to reach the forecasting study and provide the physical and chemical conditions for the formation of deposits. When the identification of the source of water, water quality factors, and laboratory compatibility tests was taken into account, a water injection process was successfully performed. When different waters are mixed, their compatibility must be determined before they are injected into oil wells. This work was undertaken to determine the composition of mineral scales that appear in raw water at various mixing volumes. The principal constituents of the scale were barium sulphate, according to the findings of testing for mixing different water volumes. The morphology of scaling crystals formed as shown by Scanning Electron Microscopy (SEM) was also presented. The analysis of selected wells samples for the period 2010 to 2020 showed that the efficacy of treatment by AD32 in HMD field is influenced by numerous factors and operational conditions. In this regard, an evaluation of the new device ENMAX was carried out and showed several limitations of this new technology.

Key words: barium sulphate, scale, Injection water, formation water, incompatibility, AD32 inhibitor, ENMAX.

ABSTRACT

Résumé

L'objectif principal cette thèse est de prédire, prévenir et évaluer l'efficacité des méthodes de traitement de dépôt du sulfate de baryum dans le champ de Hassi Messaoud lors de l'injection d'eau traitée. Le dépôt est l'un des problèmes les plus critiques auxquels sont confrontés les systèmes d'injection d'eau, en particulier lorsque deux fluides incompatibles sont présents. Lorsque deux eaux interagissent chimiquement et précipitent des minéraux lorsqu'elles sont mélangées, elles sont incompatibles. Les eaux d'injection à forte concentration d'ions sulfates et les eaux de formation à forte concentration d'ions baryum en sont des exemples évidents. Le mélange de ces eaux provoque la précipitation de sulfate de baryum. La formation de ce dépôt pose un défi à la production de pétrole et de gaz. Une fois ce dépôt formé, il obstrue les pipelines, boche les tubes, les vannes, les pompes et les autres systèmes de production, ce qui entraîne l'abandon de puits et une perte économique importante. Une présentation détaillée et complet est offert pour comprendre les comportements de cette matière très insoluble. En raison de l'incompatibilité de ces eaux à l'échelle moléculaire, plusieurs puits du champ Hassi-Messaoud ont été sélectionnés et analysés en laboratoire, puis comparé à l'analyse de référence pour atteindre l'étude de prévision et fournir les conditions physiques et chimiques pour la formation de dépôts. Lorsque l'identification de la source d'eau, les facteurs influent sur la qualité de l'eau et les tests de compatibilité en laboratoire ont été pris en compte, un processus d'injection d'eau a été effectué avec succès. Lorsque différentes eaux sont mélangées, leur compatibilité doit être déterminée avant d'être injectées dans des puits de pétrole. Ce travail a été consacré pour déterminer la composition des dépôts minérales qui apparaissent dans l'eau à divers pourcentages des mélanges de volume. Plusieurs échantillons provenant de différents points du champ de HMD ont été analysés pour déterminer la composition de chaque dépôt à l'aide d'analyses de laboratoire et de DRX. La morphologie des cristaux des dépôts formés comme le montre la microscopie électronique à balayage (MEB) a également été présentée. L'analyse des échantillons de puits sélectionnés pour la période de 2010 à 2020 a montré que l'efficacité du traitement par AD32 dans le champ de HMD est influencée par de nombreux facteurs et conditions opérationnelles. Dans ce contexte, une évaluation du nouveau dispositif ENMAX a été effectuée et a montré plusieurs inconvénients de cette nouvelle technologie.

Mots clés : sulfate de baryum, dépôt, l'eau d'injection, l'eau de formation, incompatibilité, l'inhibiteur AD32, ENMAX.

ABSTRACT

ملخص

الهدف الرئيسي من هاته الأطروحة هو التنبؤ وتجنيب وتقييم فعالية طرق معالجة كبريتات الباريوم في حقل حاسي مسعود أثناء حقن الماء المعالج. تعد الترسبات ا أحد أهم مشاكل التي تواجهها أنظمة حقن المياه في حقول النفط، خاصة عندما تكون هناك سوائل غير متوافقة. عندما يتفاعل نوعان من الماء كيميائيًا وتترسب معادن عند خلطهما، فيمكن القول انهما غير متوافقين. ومن الأمثلة على ذلك مياه الحقن ذات التركيز العالي من أيونات الكبريتات ومياه المكمن ذات التركيز العالي من أيونات الباريوم ويتسبب خلط هذه المياه في ترسب كبريتات الباريوم. يعد تشكل هذا الترسب تحديًا في مجال إنتاج النفط والغاز حيث وبمجرد تشكله، فإنه يتسبب في انسداد خطوط الأنابيب والصمامات والمضخات وأنظمة الإنتاج الأخرى، مما يؤدي إلى غلق الآبار وخسارة اقتصادية كبيرة. في هذا العمل قدمنا مراجعة مفصلة وشاملة لفهم سلوكيات هذه المادة غير القابلة للذوبان. بسبب عدم التوافق بين هذه المياه على المستوى الجزيئي، تم اختيار العديد من الآبار من حقل حاسي مسعود وتحليلها في المختبر، ثم مقارنتها بالتحليل المرجعي لمياه حقل النفط للوصول إلى دراسة تنبؤية ومعرفة الظروف الفيزيائية والكيميائية المؤدية لتكوين هاته الرواسب. وعندما أُخذ في الاعتبار تحديد مصدر المياه، والعوامل المؤثرة على نوعية المياه، واختبارات التوافق، أُجريت عملية حقن المياه بنجاح. عندما يتم خلط المياه المختلفة، يجب تحديد توافقها قبل حقنها في آبار النفط. وقد اضطلع هذا العمل بتحديد مكونات الرواسب المعدنية التي تظهر في المياه الخام عند مزج حجوم مختلفة. كانت المكونات الرئيسية للرواسب هي كبريتات الباريوم، وفقًا لنتائج اختبار خلط المياه المختلفة واظهرت النتائج أنه عند نسبة الخلط 70:30، يحدث الترسب الأقصى لكبريتات الباريوم وقد تم تحليل العديد من العينات من نقاط مختلفة في حقل حاسي مسعود لتحديد تكوين كل رواسب باستخدام التحليل المختبري وXRD.

كما تم تقديم مورفولوجيا بلورات الترسبات التي تشكلت كما هو موضح في المجهر الإلكتروني الضوئي (SEM)وقد أظهر تحليل عينات عدة آبار مختارة خلال الفترة الممتدة من 2010 إلى 2020 أن فعالية العلاج بواسطة AD32 في حقل حاسي مسعود تتأثر بالعديد من العوامل والظروف التشغيلية. في هذا الصدد، تم إجراء تقييم للجهاز الجديد ENMAX وأظهرت هاته التكنولوجيا الجديدة بدورها العديد من القيود والنقائص.

الكلمات المفتاحية: كبريتات الباريوم، الترسب، مياه الحقن، مياه المكمن، عدم التوافق، المثبط AD32، ENMAX .

Table of Contents

Table of Contents

List of Figures

List of Figures

List of Figures

List of Tables

Nomenclature

BV	Bed volume
c	Concentration
c	The speed of light
C	The concentration of salt at t=0
Co	Initial concentration of barium in inhibitor solution (at t = 0).
CB	Concentration of barium in blank solution (without inhibitor)
Ct	Barium concentration in the sample (at time t)
Cp	Concentration at thermodynamic equilibrium.
E	Energy, treatment efficiency
EDTA	Ethylene-diamine-tetra-acetic acid
EI%	Effectiveness of the inhibitor
H	Constant of Planck
I_0	Incident intensity
I	Transmitted intensity
l	Thickness
MIC	Minimum inhibition concentration
Q	Flow rate
RO	Reverse Osmosis
S	Solubility
SDI	Silt Density Index
SI	Saturation index
SR	Saturation rate
Sr	Degree of saturation
TDS	Total Dissolved Solids
TPH	Total Petroleum Hydrocarbons
TOC	Total Organic Carbon
TSS	Total Suspended Solids
K	Dissociation constante
Ks / Ksp	Solubility product
Kip	Constant of equilibrium between complex and free ions
υ	The frequency of radiation associated with the photon
WAC	Weakly acidic cation resin
WBA	Weakly Basic Anion Resins
λ	Wavelength
ε	Molar extinction coefficient or absorptivity

General Introduction

General Introduction

The oil industry seeks to obtain the best production yields and recover the maximum oil reserves in place. To achieve this goal, it tries to control all the problems that hinder productivity. However, during the life of a well, well productivity starts decreasing after a certain period of production due to natural depletion or possible damage in the near wellbore.

Improving the process of oil extraction in difficult geological, physical, and technological conditions is one of the main difficulties in the oil industry. This is due to the assumption that the majority of the country's high-yield oil fields are in late stages of development, as well as the growing proportion of hard-to-recover the total reserves. Due to high water cut production wellbore and formation of organic and inorganic deposits, oil extraction operations are significantly complex.

Oil field exploitation techniques are typically classified into three main steps: Primary recovery or natural drainage that uses the pressure initially existing in the reservoir to move fluids to the surface. The extraction of the fluids causes the pressure to drop, by the time, this pressure no longer allows a good recovery of the oil. A secondary recovery, also known as a conventional assisted recovery, is then carried out, which generally based on the injection of fluids associated with production. These fluids, introduced by the injector wells and capable of being liquid or gaseous, must be able to maintain the pressures necessary for operation. The combination of these two techniques makes it possible to obtain recovery rates that vary according to the type of reservoir and the choice of fluids.

Water injection is a widely used technique during the improved oil recovery stage because it is more cost-effective and straightforward than other enhanced oil recovery (EOR) methods. It also helps in the environmentally responsible disposal of unwanted produced water from oil and gas wells. The efficiency of the water injection is largely determined by the quality and compatibility of the water. (Hadia, 2006)

Injection water could come from different sources, including underground aquifers, produced water from wells, and surface waters like seawater and river water. The produced water is a mixture of the waters that were initially present in the oil reservoirs and distinct layers, which are classified as connate water (or formation water), saturation water of reservoir fluid, aquifer water, and injected water. (El-Said, 2009)

Water injection into oilfield reservoirs to maintain reservoir pressure and enhance secondary recovery is a well-known and well-practiced procedure. Furthermore, the degree of risk caused by mineral scale deposition in injection and production wells during such

procedures has been widely investigated. Scale deposition is one of the most critical oil field problems that water injection systems encounter, especially when two incompatible waters are present. When two waters interact chemically and precipitate minerals when mixed, they are said to be incompatible.

The formation of scale in surface and subsurface oil and gas production equipment have long been recognized as a significant problem. It has also been identified as a significant cause of formation damage in both injection and producing wells. Scale causes equipment wear and corrosion, as well as flow restriction, which reduces oil and gas production. Every year, scale problems cost the industry millions of dollars in production loss and damage. After corrosion and gas hydrates, scale is probably one of the top three water-related production problems. Every year, the worldwide cost of scale is expected to be more of USD 4 billion (Frenier and Ziauddin,2008).

Scale control can be the most expensive operational cost in some fields. In Algeria, the economic consequence of scale is expected to have the greatest influence on fields. These scale charges are expected to rise in the coming years as additional reservoirs mature and require pressure maintenance by water flooding to improve recovery.

The injected water contains SO_4^{-2} and water in the oil formation frequently has significant quantities of Ba^{+2}, Ca^{+2}, and Sr^{+2}. (Yuan, 1994). As a result, extremely insoluble alkaline earth metal sulphates [barite ($BaSO_4$), celestite ($SrSO_4$), and anhydrite ($CaSO_4$)] precipitate as an undesirable scale. $BaSO_4$, in particular, poses a significant scale difficulty because of its extremely low solubility. This led a major effort to develop chemicals substances that would either restrict crystal growth (scale inhibitors) or dissolve already-formed crystals (scale dissolvers) (Putnis, 1995).

Many experiments have been carried out to understand the morphology of barite crystals (Archibald, 1997), the nucleation and crystal growth process of barite (Pina, 1998), and the morphology and growth rate of etch pits formed during barite dissolution.

The pressure maintaining system in “Hassi Messaoud”; an oil field in Algeria, is generally provided by water injection. Also, the production of oil in this field is assisted by the injection of desalination water in the producing wells to dissolve the salts causing deposits on the walls at the bottom of the well. These salts are mainly obtained from reservoir water of very high salinity. The contact between the injection water “Albian” rich in sulphates (SO_4^{2-}) and the formation water “Cambrian” containing barium ions Ba^{2+}, calcium Ca^{2+}, and strontium Sr^{2+} causes a dangerous degradation by encrusting deposits of $BaSO_4$, $SrSO_4$, and $CaSO_4$.

General Introduction

Currently, there is a severe problem in Hassi Messaoud field due to the formation of Barium sulphate in the wells and the oil pipeline network. This problem leads to line blockage and oil production decrease. Approximately 200 km of pipelines are replaced every year due to the problem of scale deposition. Total production shortfall of the northern and southern zone of HMD filed due to the $BaSO_4$ deposits estimated by 838 tonnes in 2020, even the use of chemical treatment.

Prevention by chemical treatment with deposition inhibitors (AD 32, SCW85375, SCALETREAT837C, CHIMEC1264, and FQS11) is the only solution used to keep the production tool functional. Thus, to eliminate these deposits and prevent their recurrence, costly work is often necessary.

In this work, we are particularly interested in the study and evaluation based on the interpretation of the analyses of the Albian (formation water) and Cambrian (deposit water) in the field of Hassi-Messaoud. Then, their compatibility at different mixing ratios was evaluated from the view of scale formation in each of them. Our work aims to analyse barium sulphate deposits in the HMD field and to study the methods of treatment of these deposits.

In this context, we are opted to study and evaluate the preventive treatment of this deposit by using AD32 as an inhibitor of barium sulphate deposits, and the ENMAX device.

The obtained results allowed us to evaluate and optimize the different methods of treatment of BaSo4 and to propose new techniques to prevent the formation of this deposit. To better understand the scope of the treated subject, this thesis is structured in three chapters:

The first chapter presents a brief and recent bibliographic synthesis of scales in general and $BaSO_4$ in particular, as well as the different methods of treatment of barite deposit. This chapter also presents theoretical background about ENMAX devices.

The second chapter is devoted for materials and physico-chemical analysis methods used to carry out this work, such as: gravimetry method, FAAS, compatibility test, XRD, SEM....

To present and interpret obtained results of this work, the third chapter is subdivided to four parts. The first one presents the results of the analysis of waters, Albian, Cambrian, and mixture (Albian +Cambrian) water, then a study of scale prediction in the field of HMD. The second part includes analyses of several deposits from different points in the field of HMD to determine the composites and morphology aspects of this scale using the gravimetric method, XRD, and SEM. The third part aims to evaluate the current methods of treatment of $BaSO_4$,

which are AD32 and ENMAX devices. This part also gives a comparative study between different inhibitors used in oilfields.

A general conclusion illustrates the strong points of this work focussing on the method of treatment of $BaSO_4$ deposit in HMD field and a summary of the results found and the prospects envisaged.

Summary of related literature

Summary of related literature

In recent years, more research has been devoted to the study of the formation of scale deposits in oil fields. Bezerra et at., 1990 notice that The Namorado field's producing wells have formed barium and strontium sulphate scales due to the chemical incompatibility of injected seawater and formation water. According to Betero et al., 1988, the first need for appropriate injection water is that it does not damage well injectivity or reservoir fluid properties. Before being injected into the injection wells, injection water must be free of suspended particles, organic matter, oxygen, and acid gases (CO_2 and H_2S). According to Moghadasi et al. (2003a), Scale formation in Iranian oilfields has been identified as a major operational problem, causing formation damage either at the injection or producing wells. Scale causes equipment wear and corrosion, as well flow limitations, which reduces oil and gas production.

Strachan et al. (2004) mention that, even at low water cuts (1%), barium sulphate scale was a major problem in the BP Magnus field. BP Magnus began performing pre-emptive scale squeeze treatments on newly completed wells in the late 1990s to avoid scale deposition and maintain well production during water breakthrough. Nancollas and Liu, (1975) confirm that, based on available information on thermodynamic conditions and precipitation kinetics, barium sulphate scale (barite) can be easily precipitated in oil fields. Jordan et al., 2006b said that, scale squeeze treatments and continuous chemical injection are two chemical methods for controlling scale that have been developed. Understanding chemical location and the efficiency of the treatment chemicals is a critical aspect of the success of such treatments. Smith et al., 2000 reported that, for achieving a successful design of combination scale removal and scale inhibition treatment, several difficulties must be solved, such as; Cost, Corrosion control, System compatibility, Inhibitor adsorption and Process compatibility.

Lindlof and Stoffer (1983) conducted a laboratory investigation to examine the potential of strontium sulphate and calcium sulphate scaling in the Arab-D reservoir in Saudi Arabia after the injection of seawater. When the two waters mix in the pore channels during displacement of one by the other, laboratory experiments revealed no detectable change in permeability due to incompatibility effects between Arab D formation water and seawater. They reported that mixing Arab D water with seawater in various amounts resulted in the precipitation of strontium sulphate. Vetter et al. (1982) and Todd et al. (1989) developed a predictive calculation for the precipitation of sulphate salts from incompatible mixtures due to changes in pressure and temperature in oil reservoirs.

Summary of related literature

Works of Tomson et al. (2009) have shown that the presence of calcium ion in the injection or formation waters during barite precipitation promotes increased supersaturation and reduces the effectiveness of the EDTA inhibitor. Jones et al. (2007) used different techniques (Turbidity, FTIR, and molecular modelling) to explain the mechanism of interaction between EDTA and barium sulphate molecule. Ethylene diamine tetra-acetic acid (EDTA) is a known complexing agent that interacts through complexation with cations in solution. Christian Roque (1996) studied the control of the parameters of use and monitoring of the inhibitor agent to quickly solve the extrapolation problems related to a future generalized anti-deposition treatment in the whole field of TFT. Zerrouk Lalmi (2008) studied the inhibition of calcium sulphate deposition by three commercial products (NALCO65 61, AD32, and SI4012) and a synthesized ferrocene family compound.

Karima Larbaoui (2017) studied the inhibitory power of two families of compounds and their effect on barium sulphate deposition. These compounds are polyelectrolytes based on phosphonates and polyacrylates-esters, which are commercial deposit inhibitors.

Chapter I : LITERATURE REVIEW

Chapter I : LITERATURE REVIEW

I.1 Introduction

The use of water as an injection liquid in oil recovery or as a thermal fluid in cooling systems poses several challenges and problems such as corrosion and scaling. The scale is the most problematic in the series of complications encountered in the industrial sector. It has remained, over the years, a major threat that calls for further examination. Disorders found in water-carrying installations are essentially linked to its composition, its pH, its temperature, but also to the nature of the material and the operating conditions of the water transport systems (Bin Merdhah et al., 2008).

Deposition accumulation is a process with considerable negative consequences in oil and gas reservoirs with adverse effects on fluid flow in wells and reservoir rocks. The clear consequence of the formation of the encrusted deposits is the progressive restriction of the flow of fluids which can lead to the total blockage of production facilities. This process essentially changes the permeability of the sediments by plugging the pores of the reservoir rock by the deposits of solid substance (Moghadasi et al., 2002).

Economic losses from deposits can be substantial, industrial and environmental, damage causes are mainly:

- The reduction of the cross-section of the pipes with the degradation of the surface by the adherent scale increases the pressure losses and consequently the energy expenditure related to the circulation of the fluids (Imhamed, 2012).
- The accumulation of deposits compromises safety by causing damage to production equipment, such as electric pumps, also caused a health hazard, because some deposits are formed from natural radioactive material (NORM) (Mackay, 2003).

I.2 Waters in the oil fields

I.2.1 Injection water

It is the oldest process (late nineteenth century) and still the most used. Its purpose is not only to recover but also to accelerate production, in addition to decreasing its decline. The way used is often a pressure hold. Injection can be either of the distributed type in the oil zone or of the peripheral type in an existing aquifer. In terms of water sources, the most often are aquifers which locate at shallow depths of seawater or surface water on land (lakes, rivers).

In addition, the water must be injectable: sufficient permeability and compatibility with the reservoir water. Indeed, the mixture of injected water with the water in place can cause inscrutable precipitates ($BaSO_4$) that block the wells. There are two categories of injection water (Granier, 1998).

I.2.1.1 Washing water

It is usually injected into the base of the tubing to clean the wells from time to time and dissolve the salt 'sodium chloride' deposits found there. Some formation waters may contain 350 g/l of sodium chloride and thus be so close to saturation, so a very small temperature variation or low evaporation of water due to the fall causes, a significant precipitation of NaCl on the walls of the tubing can appear. This deposit increase till the blockage and reduction of the tubing section that leads to the production drop. In order to put the wells back into production, we intervene on the NaCl, simply sending; a quantity of freshwater.

Sometimes water injection is a serious problem of incompatibility with reservoir waters. In fact, reservoir waters may contain barium, calcium, and strontium ions, when they are put in contact with water, either for washing or for maintaining pressure, which contain sulphated ions. The result is the formation of deposits in the facilities (Granier, 1998).

I.2.1.2 Pressure maintaining water

It is used as a means of production when the absolute static pressure at the wellhead decreases rapidly during the exploitation of a reservoir, and that the recovery in place will only reach a very small percentage of the estimated reserves if an artificial process is not used to make up for the lack of natural drainage (Granier, 1998).

I.2.2 Reservoir waters

It should be noted that the production of crude oil is always accompanied by the production of oil, gas, and a quantity of water more or less important depending on the reservoir. The presence of water is due to various causes, namely natural causes either, from the source rock itself, which can retain considerable quantities of it. The latter is generally very charged with salts until supersaturation. The predominant salt is sodium chloride, but it is always accompanied by varying amounts of calcium, potassium, magnesium, barium, and strontium salts in the form of carbonate sulphates, bicarbonates, and chlorides. The reservoir water accompanies the crude oil in the production field; this reservoir or formation water can come either from the aquifer at the base of the oil fields or from the source rock itself.

There are different types of reservoir water, such as:

- ***Condensation water:*** which corresponds to the fraction of water in the steam phase accompanying the reservoir fluids. They are theoretically less loaded with chemical elements. They are produced at the wellhead by condensation in small quantities relatively.

- ***Formation waters:*** commonly attributed to the aquifer of the deposit and accompany the formation of hydrocarbons. They are varied and classified according to the dominant chemical elements they contain.
- ***Interstitial waters:*** waters found in small spaces between the tiny grains of a rock.
- ***Connate waters:*** "connate" means born, produced or generated together. Connate water can be considered as interstitial water of syngeneic origin (formed at the same time as the parent rock). Connate water is, therefore, fossil water that is not in contact with the atmosphere during much of a geological period (Granier, 1998).

I.2.3 Groundwater Properties

The geological nature of the soil determines the chemical composition of the groundwater. Water is constantly in contact with the earth on which it stagnates or circulates, so the balance develops between the composition of the soil and that of the water: i.e.., water circulating in a sandy or granitic substratum is acidic and has a few minerals. Water circulating in limestone contains the alkalinity of bicarbonates (Granier, 1998; Dégremont, 1991).

The following table is a comparison between the characteristics of the surface water and those of groundwater:

Table I.1: Groundwater and surface water characteristics (Dégremont, 1991).

Characteristic	**surface water**	**groundwater**
Temperature	Varies according to the seasons.	Relatively constant.
Turbidity	Varying levels, sometimes elevated.	Low or zero (except in limestone soils).
Minerals	Varies with soil, precipitation, effluent, et.	Constant, generally more high than surface water.
CO_2 Aggressive	Often nil.	Often present.
O_2 Dissolved	Absent in highly polluted water.	Often nil.
Nitrate	Generally low level.	Perfect high level.
Silica	Moderate proportions.	Often high level.
Living organisms	Bacteria, viruses, plankton	Iron bacteria usually.

I.2.3.1 Main characteristics of groundwater

- ***Low turbidity:*** because it benefits from a natural filtration in the different formations of the salt they crossed.
- ***Constant temperature:*** because it is protected from solar radiation and the atmosphere.

- ***Low color index:*** it is not in contact with plant substances (color source).
- ***Often high hardness:*** groundwater may come into contact with rock formations containing bivalent metals such as (Mg^{2+}, Ca^{2+}, etc..,) the elements responsible for the hardness.
- ***High concentrations of iron and manganese***.

I.2.3.2 Physico-chemical properties of water

Water is a chemical compound that results from the combination of two hydrogen atoms and one oxygen atom to form the H_2O molecule. It is this composition of water that is at the origin of its specific properties; the main ones are the following:

- ✓ Water is a clear, odourless liquid.
- ✓ Its molar mass = 18 g/mole or 55 moles H_2O/l.
- ✓ Its density is 1000 Kg/m^3 at 4°C.
- ✓ Viscosity = 1 cSt.
- ✓ It's the best solvent.
- ✓ It dissolves mineral gases and salts and contains living organisms in its liquid state.

I.2.3.3 Composition of raw water

A. ***suspended solids:*** Their nature can be:

Mineral: This is the case with sand, silt and clay.

Biological: This is the case with bacteria and organic products.

A very brief classification of the elements in the water makes it possible to establish the table below

Table I.2: Substances in water.

State of the elements	Nature of the elements
Suspended matter	Sand, mud clay, debris rocks, organic, mineral and vegetable matter.
Emulsion matter	Colloidal organic matter, mineral oil, clay colloidal.
Solubilized organic matter	Vegetable waste, nitrogen, nitrogen products synthesis, soluble organic, etc.
Mineral salts	Bicarbonate carbonates, sulphates, calcium, magnesium, sodium, etc.
Living microorganism	Fungi, worms, bacteria, viruses, etc..
Gas	Oxygen, nitrogen, carbon dioxide ammonia.

B. *Dissolved solids (salts)*

The most common dissolved solids encountered are:

- ✓ Bicarbonates,
- ✓ Chloride,
- ✓ Sulphate,
- ✓ Silicate,

There are also:

- ✓ Fluorides F,
- ✓ Nitrates NO_3,
- ✓ NO_2 nitrites,
- ✓ The dissolved gases,
- ✓ H_2SO_4 sulphuric gas or hydrogen sulphide.

I.2.4 The incompatibility of injection water and reservoir water:

The typical incompatibility between the formation waters of oil reservoir and the sulphate of injection water resulted problems in the forms of calcium and/or strontium and/or barium. Like what happens in the Hassi Messaoud field during the Albian water injection, for maintaining pressure or washing salt oil wells. Water injection is still one of the most widely used techniques for the secondary recovery of oil and the success of this one is primarily due to the compatibility of the injection water and the reservoir water. Because they should in no case cause a reduction of the permeability of the reservoir rock nor even corrosion of the bottom and surface installations.

The problem of mixing the injection water and the reservoir water is the basis of the incompatibility problem, which gives precipitates according to the following reactions:

$CaCl_2+Na_2SO_4 \longrightarrow CaSO_4+2NaCl$

$CaCl_2+Mg\ SO_4 \longrightarrow CaSO_4+ MgCl_2$

$SrCl_2+ Na_2SO_4 \longrightarrow SrSO_4+2NaCl$

$SrCl_2+ Mg\ SO_4 \longrightarrow SrSO_4+ MgCl_2$

$BaCl_2+ Na_2SO_4 \longrightarrow BaSO_4+2NaCl$

$BaCl_2+ Mg\ SO_4 \longrightarrow BaSO_4+ MgCl_2$

$CaCl_2+2NaHCO_3 \longrightarrow CaCO_3+2NaCl+CO_2+H_2O$

Knowing that water can be chemically pure, despite these different components; it has an ionic balance between its cations and anions. By adding another water containing other ions, this balance is violated. So, the formation of insoluble compounds that precipitate even this equilibrium is restored. That said, two types of water are said to be compatible if the reaction

between the chemical components does not give the mixture insoluble compounds (Raymon,1999).

I.3 Overview about deposits

I.3.1 Origin of deposits

I.3.1.1 Deposits originally natural

Natural deposits are shown in the following table (Manuel de traitement des eaux d'injection, 1973):

Table I.3: Deposits originally natural.

From water	From air
- Silt	- Gas
- Mud	- Dust and ground dust
- Natural organic substance	- Organic matter (vegetation)
- Dissolved minerals	- Microbiological organisms
-Microbiological and macro-biological organisms	

I.3.1.2 Deposits originally artificial

Artificial deposits are shown in the following table:

Table I.4: Deposits originally artificial (Manuel de traitement des eaux d'injection, 1973)

From water	From air	From the system
- Particles entrained after water has passed through the clarifier	- Organic gas	- Corrosion products
- Pollutants	- Sulfurized hydrogen	- Inhibitors of corrosion and their reactive
- Phosphate	- Sulfur dioxide	- Erosion products
- Detergent	- Carbon dioxide	- Other chemical treatment products
- Sewage effluents	- Ammonia (NH_3)	

I.3.2 The conditions of formation of scale:

Before drilling, in the reservoir, the minerals in the formation waters are dissolved in balance with those that constitute the reservoir rock. It is only at the time of drilling a well and during the exploitation of this well we can say that minerals are likely to precipitate in the reservoir, due to changes in thermodynamic (T, P) or chemical conditions.

Calcite scale ($CaCO_3$) formation conditions are often present in hydrocarbon field production systems and formation waters, especially when the latter has high concentrations of dissolved calcium. The two most common types of calcium (Ca) depositions are calcium carbonate ($CaCO_3$) and calcium sulphate ($CaSO_4$).

According to Vetter (1987) the calcium carbonate scale appears in the first place due to changes in CO_2 partial pressure, temperature, and pH of production fluids whereas, the formation of calcium sulphate tartar is mainly associated with the mixing of the two incompatible waters, injection and formation waters. (Moghadasi et al., 2003b ; Todd & Yuan, 1989 ; Moghadasi et al., 2003a).

The iron deposition is a major problem in hydrocarbon reservoir which has been ignored for the most part because of the difficulty in identifying and preventing it. Fe deposits are less present in the oil fields than Ba and Ca deposits. The family of Fe deposits consists of six classes of anions: carbonates, sulphides, sulphates, oxides, hydroxides, and fluorides. It is the most diverse group of all deposit groups.

Barium deposits are represented by two main mineral constituents: barium sulphate ($BaSO_4$) and barium carbonate ($BaCO_3$) deposits. Barium sulphate, barium or barite, is the most common deposit in the barium group. Precipitation of barium sulphate occurs when two incompatible types of water are mixed (for example, formation water and injection water containing the Ba^{2+} cation and SO_4^{2-} anion respectively, leading to $BaSO_4$ precipitation). Barium carbonate occurs primarily as a result of the decompression of CO_2 gases in formation waters saturated with Ba^{2+}. It should be noted that Barium deposits are considered the most stable concerning their chemical dissolution (Jordan et al., 1994; Graham et al., 1997).

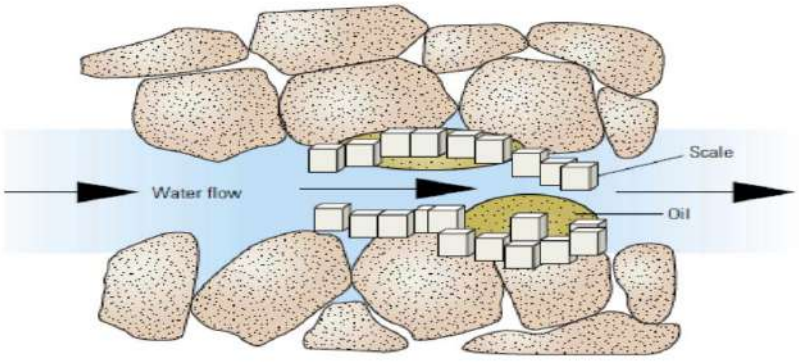

Figure I.1: Scale deposition restricts the flow of fluid through the formation, resulting in a loss of permeability (Crabtree et al., 1999).

I.3.3 The main causes of deposit formation

The main causes of deposit formation in oil fields are:

- **Pressure drops**

The formation water of the bottom of wells, as well as the production process progresses, is subject to continuous pressure reduction. When the pressure is sufficiently reduced, some dissolved gases escape.

Boak (2012) emphasizes that the decrease in the concentration of one of these gases causes an imbalance leading to the formation of deposits. Indeed, the reduction of carbon dioxide CO_2, for example, disturbs the bicarbonate-carbonate equilibrium, which increases the probability of formation of the deposit of calcium carbonate and the restriction of the flow of fluids.

- **Temperature change**

The study of factors that impact the scale potential such as pH, temperature, and mixing ratio, Aziz et al (2016) found that calcite and aragonite were the major scale potential to precipitate.

Some surface equipment heats up, such as motors or pumps' heat exchangers, causing the formation of deposits (Jordan et al., 2000). Indeed, as an example, the formation of calcium carbonate in some equipment is due to the decrease in its solubility with the increase in temperature.

However, Boak's (2012) studies have shown that for $BaSO_4$, although solubility increases with increasing temperature, barium sulphate deposition occurs even at high temperatures. In general, Bin Merdhah et al (2008, 2012) found that a temperature rises from 40° to 90° C causes an increase in the solubility of $BaSO_4$ and a decrease in the solubilities of $CaSO_4$ and $SrSO_4$. For $CaSO_4.2H_2O$ gypsum, Nancollas and Yuan (1975) confirm that has a maximum solubility at 43°C, which decreases as we deviated from this temperature value.

Autoscaling

Autoscaling occurs when the natural water in the reservoir undergoes a change in pressure and/or temperature during its production. Normally, an increase in temperature tends to increase the water solubility of a mineral. This means that more ions are dissolved at high temperatures. Similarly, a decrease in pressure tends to decrease the water solubility of minerals. The temperature trend is not valid for all minerals. Calcium Carbonate ($CaCO_3$) has an inverse trend with increasing water solubility with decreasing temperature.

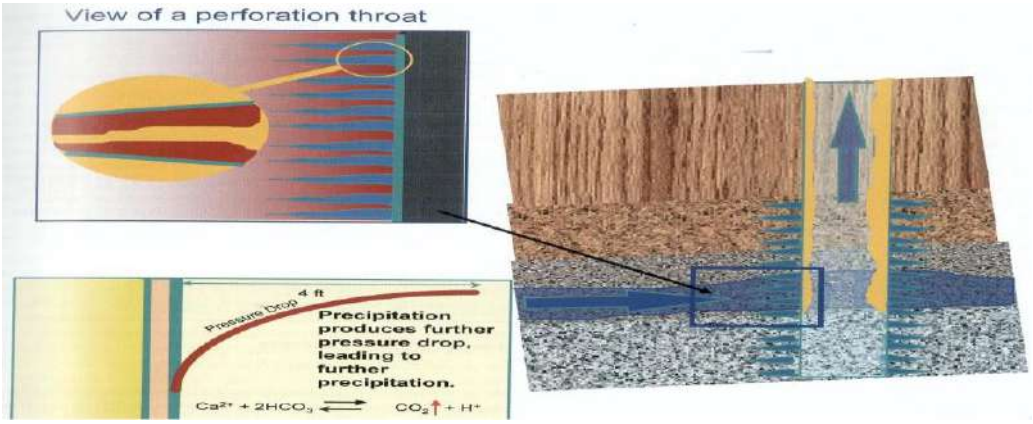

Figure I.2 : Autoscaling of calcium carbonate in a well (Crabtree et al., 1999).

- **Change in mineral characteristics**

A change in the mineral characteristics of water could lead to the formation of deposits due to the change in the ionic forces of the ions in solution. The total concentration of salts (total salts) in water is an important factor. For example, the solubility of calcium carbonate increases with increasing total dissolved salts. The presence of dissolved chlorides (NaCl) or sulphate ions or other ions than those calcium in water increases the solubility of $CaSO_4.2H_2O$ gypsum or $CaSO_4$ anhydrite. Hennessy (2002) in his study "The effect of additives on the co-crystallisation of calcium with barium sulphate" find that the solubility of barium sulphate in water is also enhanced by the presence of dissolved foreign salts.

- **Mixing of incompatible waters**

During secondary recovery, water from production wells, containing various minerals, mixed after the breakthrough, with injection water causes a change in mineral characteristics due to the incompatibility of the two types of waters leading to deposition formation. In many cases, the instability of calcium carbonates or sulphates and barium sulphate is a direct consequence of this amalgam, as is often the case in hydrocarbon fields in the North Sea. Indeed, when two incompatible waters, formation water containing barium ions and seawater containing sulphate ions are mixed, barium sulphate deposition is formed (Bader, 2006).

Figure I.3: Seawater mixing with formation water (Frenier & Ziauddin, 2008).

As already mentioned in the introduction, the case of the HMD field is a concrete example, in Algeria, the appearance of $BaSO_4$ deposition as a consequence of mixing injection water incompatible with the reservoir water. From the first years of oil production in the field of HMD, the pressure drops, hydrocarbon production decreases, and the problem of salted wells was appeared. In order to maintain an economic production level, the technicians at HMD field proceeded to search for injection water for pressure maintain and washing salted wells. The injection of Albian water began in 1980. Most often, it contains sulphate ions in the form of Na_2SO_4. The reservoir water associated with oil in the producing reservoir is most often loaded with salt and contains strontium cations, calcium and a significant amount of barium in the form

of $BaCl_2$. The predominant salt is sodium chloride. The interaction between the reservoir water (Cambrian charged with barium Ba^{2+}) and the injected water (Albian charged with sulphate SO_4^{2-}) causes $BaSO_4$ to precipitate throughout the production line, from the bottom of the wells to the surface installations.

Due to problems related to the mixing of various fluids, intervention becomes necessary and increasingly expensive. The most practical treatment for preventing or controlling scale formation is the injection of chemicals products called inhibitors. Checking the compatibility of the reservoir and injection water, is necessary before proceeding to the injection operation also designing adequate methods of treatment with inhibition products.

I.3.4 Study of water incompatibility

Water can be chemically pure, despite its various components. It has an ionic balance between its cations and anions. By adding another water containing other ions, this balance can be broken, so we have the formation of insoluble compounds that precipitate, the waters are said to be incompatible.

Two waters are said to be compatible if the reaction between the chemical components does not give the mixture insoluble compounds. The elementary chemical analysis allows us to make a theoretical approach through certain physico-chemical parameters such as: solubility product, ionic force, temperature and pressure. It simply consists of bringing two determined waters into contact (injection water and reservoir water) and the observation of what is happening either;

- Visual, and/or
- Electrochemical: recording the variation of pH and conductivity, and/or
- Analytical (gravimetric): filtration of a precipitate, calcination of the resulting deposit, dosage of the elements contained in the filtrate.

The study of water compatibility at a laboratory can be conducted under surface conditions (atmospheric pressure - 1 atmosphere - and ambient temperature - 25°C) or underground conditions (high pressure and high temperature).

I.3.5 Prediction of deposit formation

In order to predict the formation of certain types of deposits, it is necessary to have an accurate information on the conditions of their appearance in production wells. To do this, several forecasting models are available and cited in the literature (Alwi et al., 2013; Chen et al., 2007; Dai et al., 2013; Kan et al., 2013; Tomson et al., 2009).

BinMerdhah (2010) reports that the Deposition formation prediction is possible by calculating the solubility product of the deposition compound under a wide range of thermodynamic conditions. These thermodynamic conditions are essentially pressure and temperature with variations in the chemical compositions of the solutions. The effects of ions, in excess in the solution, are the only ones to be considered in predicting solubility. Solubility indicates the degree of precipitation (deposition) or scale-forming capacity.

The calculation of solubility is an extremely valuable tool, but its exact value depends enormously on the user's experience and appreciation. It is clear that the acquisition of significant solubility measurements is an important factor for deposition prediction.

Figures I.4 and I.5 illustrate an example of a scaling tendency calculation. The equilibrium amount of precipitates are shown as function of % seawater in the produced seawater/formation brin mixture.

At composition of 10 % sea water a larger amount of barium sulphate will precipitate at a lower supersaturation. For 50 % sea water less barium sulphate will precipitate however the supersaturation is higher (figure I.5).

The higher super saturation at 50% sea water compared to 10% indicate a stronger thermodynamic driving force for precipitation of barium sulphate scale. Effective inhibition may be more difficult to achieve when comparing 50/50 FW-SW to 10% SW situation, and normally a higher inhibition threshold concentration will be required.

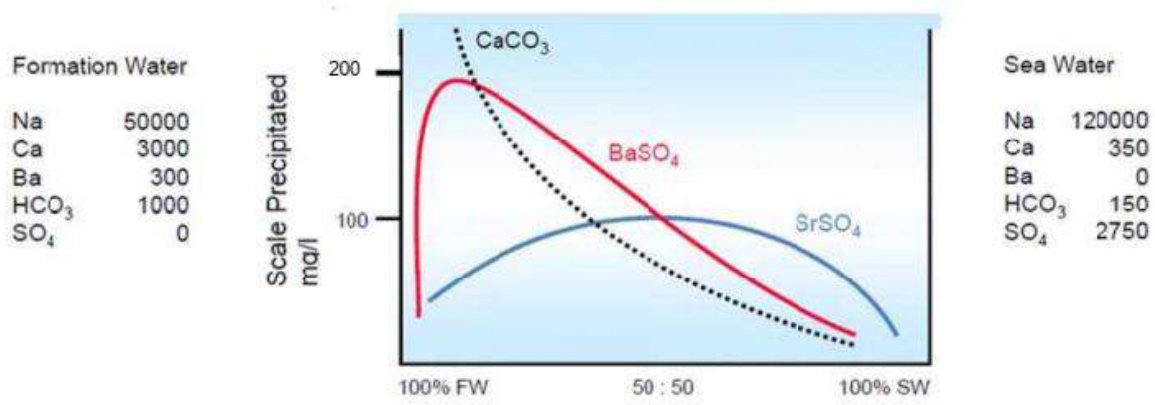

Figure I.4: predicted scale precipitation upon mixing of formation water and sea water. (Montgomerie, 2014).

As seawater breakthrough increases the severity of scaling reaches a peak and then declines. This indicates that the inhibitor dosage needs to be adjusted to account for the changing scaling tendency.

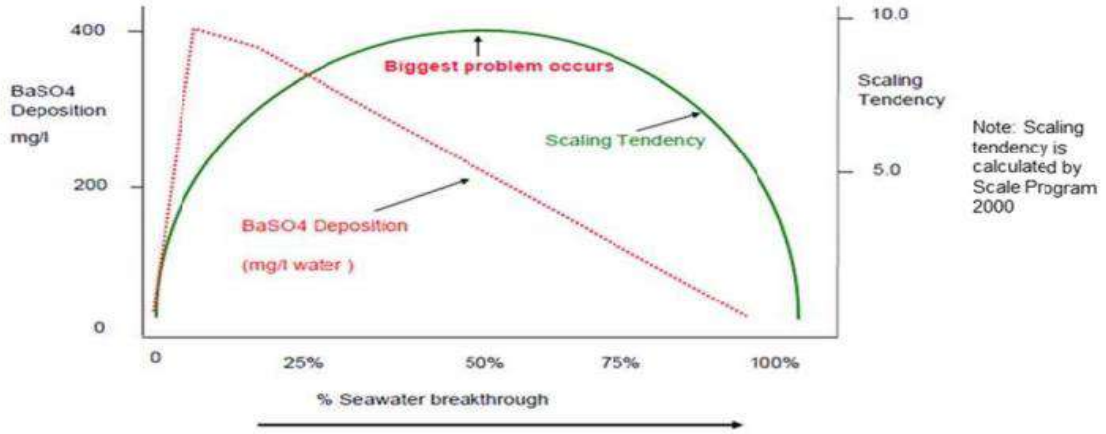

Figure I.5: calculated amount of $BaSO_4$ and scaling potential upon mixing of formation water and sea water (Montgomerie, 2014).

As can be seen, the most precipitation of barium sulphate occurs approximately 90/10 FW/SW. When the amount of precipitation begins to decrease, the precipitation ratio remains at 50/50. The thermodynamic driving force is stronger at 50/50, according to the scaling tendency.

I.3.6 Deposit formation steps

happens as follows:

I.3.6.1 Supersaturation:

A degree of saturation of the solution must be achieved for precipitation of a new solid phase from a liquid phase to take place. This degree of saturation is an important parameter that conditions the entire crystallization process. However, in many cases, exceeding the solubility product K_S does not automatically induce deposition. Experience has shown that a value that exceeds K_S is not sufficient for the formation of a solid phase. In the case of calcium carbonate, even if the product $[Ca^{2+}]$. $[CO_3^{2-}]$ is greater than K_S, but the difference in concentration between these two values is not sufficient, the spontaneous evolution of water towards calcocarbonic equilibrium will not take place: it is the phenomenon of supersaturation. As in any crystallization process, a deposit is formed in two stages: nucleation and crystalline growth. Growth stage studies are very numerous, while little work is done on nucleation. This is probably due to the complexity of the system, which has so far failed to provide satisfactory mathematical modelling of nucleation (Teghidet, 2012).

By applying the laws of thermodynamics relative to chemical equilibrium, we could explain the phenomenon of precipitation. By applying the law of mass action to an aqueous solution AB, the latter dissociates more or less according to the following reaction:

$$AB \rightleftharpoons A^+ + B^-$$

$K = [A^+][B^-]/[AB]$

K: dissociation constant

$[A^+]$ and $[B^-]$: concentration expressed in mol ion/l

[AB]: concentration expressed in mol ion/l

Ks: solubility product of AB

*If a salt solution CD is added to the AB solution, the mixture will contain the ions: A^+, B^-, C^-, D^+

*Assuming that the AC salt is poorly soluble, all A^+, C^- ions will remain in solution if the equation: $[A^+][C^-] < Ks$ is satisfied. Otherwise, the salt will precipitate until this equation is satisfied.

*The solubility product is a characteristic of salt and thermodynamic conditions; any variation of the latter will also vary the solubility product and will therefore cause precipitation.

*To initiate nucleation, it is necessary to exceed the solubility product. This exceedance is characterized by the degree of saturation which defined as follows:

$$Sr = C_{salt}/Cp_{salt}$$

C: the concentration of salt at t=0 Cp: concentration at thermodynamic equilibrium.

I.3.6.2 Nucleation (germination)

In a supersaturated solution compared to a phase, the phase may precipitate more or less rapidly depending on the conditions of the growing environment:

- supersaturation and concentration values,
- nature and concentration of impurities, etc.

Since several types of germination are possible, it is useful to recall here some definitions:

- primary nucleation: the appearance of the crystals of the consideration phase in a solution that lacked it. Primary nucleation is also divided into two types: homogeneous and heterogeneous.
- secondary nucleation: secondary nucleation, where new germs come from crystals of the same phase, already existing in the solution.

a. Homogeneous nucleation:

Homogeneous germination is a complex process not yet well known. Indeed, the microscopic entities constituting the germ must not only agglomerate in the same place, resisting a strong tendency to redissolving, but they must grow and be organized according to a well-determined network. Homogeneous nucleation can occur within the supersaturated

solution if the random displacement of the ions under the effect of thermal agitation creates a configuration initiating the orderly stacking of the future crystal. This phenomenon, although highly unlikely, always ends up happening. One of the characteristics of homogeneous nucleation is that it requires the growth of germs and an organized agglomeration in the same place (Teghidet, 2012).

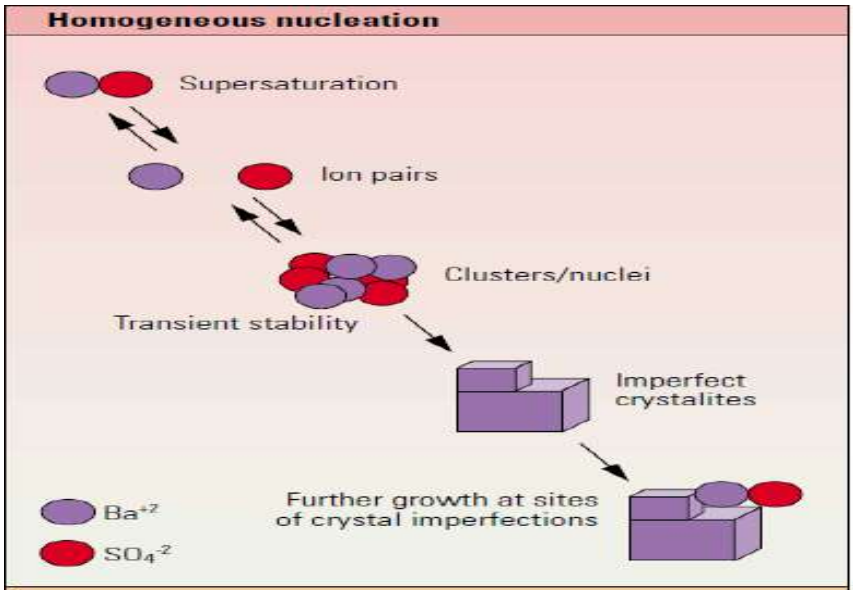

Figure I.6: homogeneous nucleation (Crabtree et al.,1999).

b. Heterogeneous nucleation:

In general, heterogeneous nucleation is easier and faster than homogeneous germination. It is triggered by contact with a wall or suspended solid.

The formation of a crystalline germ in heterogeneous phase presupposes the presence at the same time and place:

- The supersaturated liquid phase.

A number of free ions in a configuration that allows growth to initiate (Teghidet, 2012).

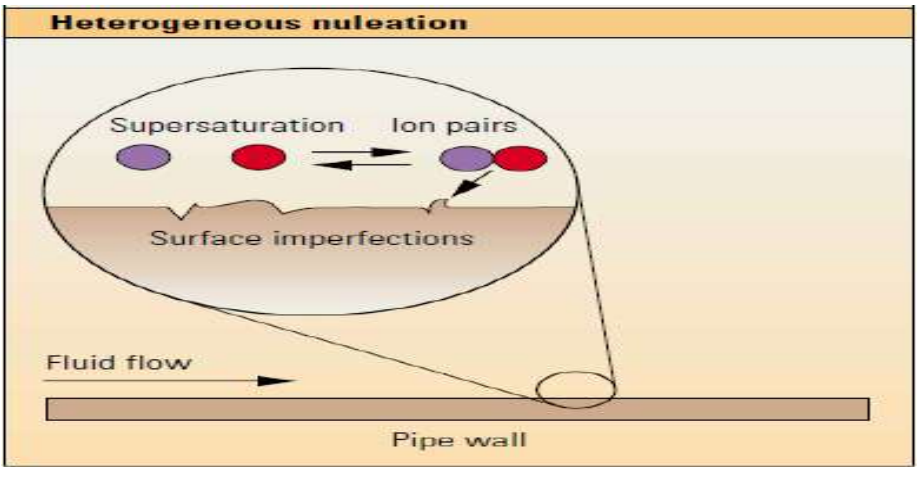

Figure I.7: heterogeneous nucleation (Crabtree et al., 1999).

I.3.6.3 Crystal growth:

When the germs form, there will be:

- Homogeneous growth: it is the nutrition of these germs by the supersaturated solution by transfer of matter;
- Heterogeneous growth: it is the formation of the second layer by adsorption of the ions of the supersaturated solution, which subsequently give a deposition adhering to the metal wall.

The increase in temperature increases both nucleation and crystalline growth, these two kinetic factors (germination and growth) can be influenced by various parameters, in particular: the nature of the material on which the deposition is made, surface condition (porosity, coating, wettability, etc.), hydrodynamic condition.

I.3.7 Solubility and supersaturation

Solubility is defined as the limiting amount of solute that may dissolve in the solvent under physical conditions. Mineral salts dissolved in water are present in their ionic form. The solubility of a particular solid is reached only if the number of cations is equal to the number of anions or when the solution is in stoichiometric equilibrium. If an excess of ions occurs, the solubility of the salt is significantly reduced, the supersaturation of total salt in the solution becomes higher. The solubility of salt varies greatly from case to case: while many salts are fully soluble such as Na_2SO_4, a number of salts are partially soluble and others are completely insoluble such as barium sulphate. Supersaturation represents the excess salt content in the solubility and thus represents the amount available for precipitation from the solution until the solution returns to its equilibrium state. The precipitate may remain suspended or form a deposit adhering to a surface.

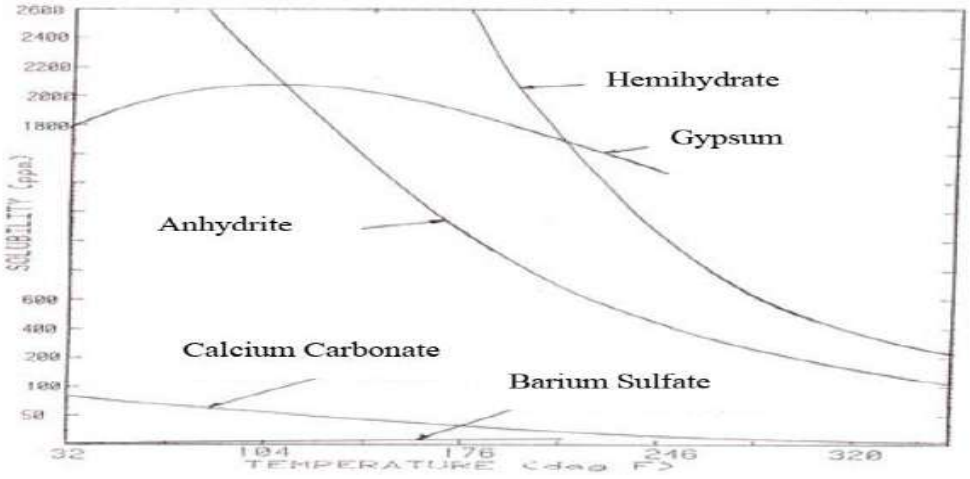

Figure I.8 : Solubilities of common scales (Connell, 1983).

Although the solubility curves (Figure I.8) of these crystalline forms versus temperature show that above about 40 ºC (104 ºF), anhydrite is the chemically stable form, it is known from experience that gypsum is the form most likely to precipitate up to a temperature of about 100 ºC (212 ºF). Above this temperature, hemihydrate becomes less soluble than gypsum and will normally be the form precipitated. This, in turn, can dehydrate to form a scale at temperatures below 100 ºC and hemihydrate forms above this temperature (Connell, 1983).

In the case of a solid ionic compound (AB), which dissociates into A^- and B^+ indicates the concentration in gram ions/litre, the equilibrium constant of the dissolution reaction is called the solubility product and is noted as Ks (T), it depends only on the temperature in general. The solubility product is used to explain, and predict whether a precipitation reaction is occurring and whether precipitation is complete. When the product of the concentrations of the two ions in solution exceeds the value of the corresponding salt solubility product, the salt precipitation continues until the product of the concentrations of the two ions in solution equals the solubility product.

- Salts are said to be highly soluble when "S" is around 10^{-1} mol/l; salts are said to be poorly soluble when "S" is around 10^{-4} mol/l.
- The lower K_S, the less soluble the salt.

Table I.5: Solubility products of a few frequent deposits in the field of HMD (Lembarki,2018)

Deposit Name	**Ion product**	**Solubility products at 25°C**
FeS	$[Fe^{2+}].[S^{2-}]$	$3,2 .10^{-18}$
$BaSO_4$	$[Ba^{2+}].[SO_4^{2-}]$	$1,1.10^{-10}$
Ca SO_4	$[Ca^{2+}].[SO_4^{2-}]$	$6,1.10^{-5}$
$SrSO_4$	$[Sr^{2+}].[SO_4^{2-}]$	$2,8.10^{-7}$
Ba CO_3	$[Ba^{2+}].[CO_3^{2-}]$	8.10^{-9}
$CaCO_3$	$[Ca^{2+}].[CO_3^{2-}]$	$4,8.10^{-9}$
Mg CO_3	$[Mg^{2+}].[CO_3^{2-}]$	$1,0.10^{-5}$

I.3.7.1 Relation between solubility and solubility product

Whether dissociation of the ionic solid from the formula A_xB_y. Salt solubility:

S = $[A_xB_y]$ dissolved. We can write:

$$AxBy\,(solid) \quad \leftrightarrow \quad AxBy\,(dissolved) \quad \leftrightarrow \quad x\,A^{+y}\,(aq) + y\,B^{-x}(aq)$$

$$C_0 = 0 \qquad 0 \qquad 0$$

$$C = s \qquad xs \qquad ys$$

The ionic concentrations $[A^{+y}]$ and $[B^{-x}]$ can then be expressed according to the solubility 'S' of the salt: $[A^{+y}] = xs$ and $[B^{-x}] = ys$

The expression of the solubility product is:

$K_s = [A^{+y}]^x . [B^{-x}]^y$

And can therefore be written:

$K_s = (xs)^x . (ys)^y$ where $K_s = x^x . y^y . s^{(x+y)}$

Thus, we obtain: $s = [K_s / x^x y^y]^{1/x+y}$

I.3.7.2 Factors affecting solubility

If we want to dose anion A^- with a C^+ cation, the following reaction will be used:

$$A^- + C^+ \rightarrow AC$$

where AC is the insoluble precipitate.

The solubility product $Ks = [A^-] . [C^+]$ is a known constant.

The presence of foreign ions leads to an increase in the solubility of the precipitate which due, in fact, to the increase of the ionic force. The gravimetric analysis will therefore be less accurate in the presence of foreign ions.

The pH plays an important role. For example, if the solution is basic, many metals precipitate as hydroxide. In this case, the formation of the precipitate will not be quantitative. Generally, pH plays a role in precipitation involving an acid-based agent such as organic acids, sulphides (e.g., FeS, $Fe(OH)_2$ and $Fe(OH)_3$), phosphates or carbonates. Secondary reactions may disrupt the dosage.

The purpose of the gravimetric analysis is to transform all the anions A^- into an insoluble compound AC or $[A^-] = Ks/[C^+]$ so we see that when the amount of reagent C^+ increases, A^- decreases. In order to increase the precision, we should add an excess of reagent (C). But the addition of excess will be harmful because of the increase in ionic force. Solubility is a function of the solubility product and varies in the same direction.

I.3.8 Precipitate formation

The precipitate begins to emerge when the solubility limit is reached. If the reagent is added quickly, the precipitate is formed immediately. The number of germs (initial crystals) formed is then very important; these many germs will give birth to very small crystals. The surface of such a precipitate being large, it favours the phenomena of absorption and adsorption of foreign ions. It is, therefore, better to slowly add the reagent. Thus, the number of starting germs is relatively small. As the reagent is added, the precipitate will agglomerate on the previously formed germs. These will tend to grow rather than multiply, which will also be more favourable for the separation of the precipitate formed. To obtain a better crystallization, it is therefore necessary to let the precipitate rest for a certain time.

I.3.9 Difference between precipitation and surface deposition

Deposition is the portion of precipitate that attaches to a surface, such as the walls of the tubes or the inner surface of the rock. Scale deposition is generally associated with precipitation. It is recognized that precipitation does not necessarily lead to deposition, but deposition is often considered to result from precipitation followed by precipitation adhesion to the surface. (Boak, 2012).

The precipitation process is related to the solubility product of a compound containing an ion that is considered undesirable. If an excess of this ion is introduced, the solubility is slightly modified. One of the fundamental principles of precipitation is that the size of the precipitate increases if the chemical reaction continues to occur on previously precipitated particles. Thus, the precipitation of minerals scales occurs through the germination and growth of crystals.

I.3.10 The parameters influencing the formation of deposits:

I.3.10.1 Effect of temperature:

Landolt-bornstien (1985) (cited in Moghadasi et al., 2004b) showed that it has a very important effect on the solubility and crystalline growth of calcium, barium and strontium sulphate. An increase in temperature reduces the solubility of $CaCO_3$, $SrSO_4$ and $CaSO_4$, but on the contrary, it causes a large dissolution of $BaSO_4$ (Moghadasi et al., 2003a).

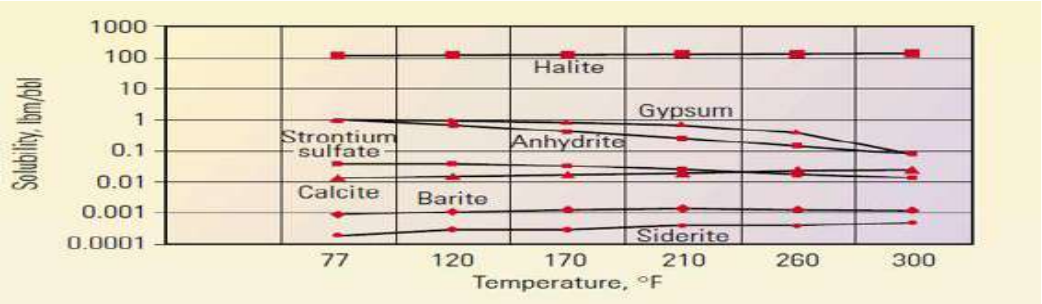

Figure I.9 : Influence of temperature on solubility (Crabtree at al., 1999).

I.3.10.2 Effect of dissolved salts

Salts dissolved in water promote the solubility of $BaSO_4$, just as in the case of $CaCO_3$ and $CaSO_4$. For example, 100 000 mg/L NaCl increases $BaSO_4$ solubility from 2.03 to 31 mg/L at 25°C and from 3.9 to 65 mg/L at 95°C.

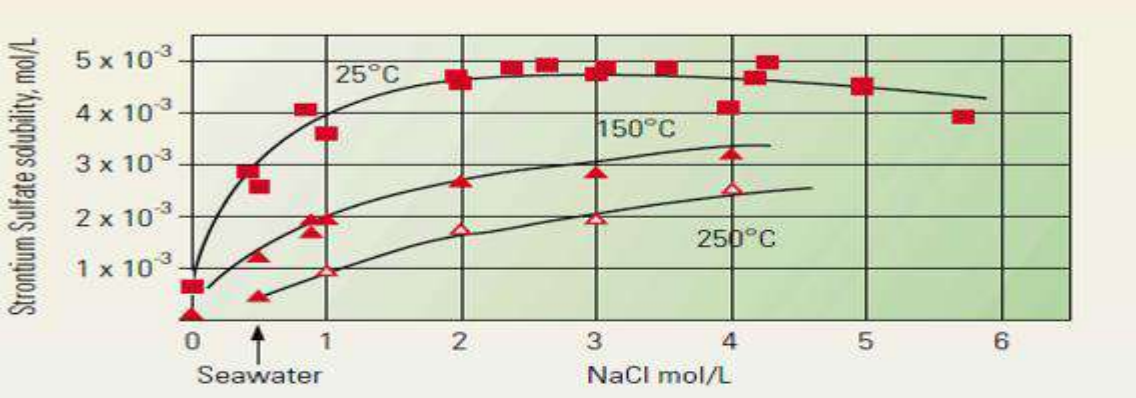

Figure I.10 : Influence of salinity on solubility (Crabtree et al., 1999).

I.3.10.3 Pressure effect

The variation in pressure causes variations in the concentration of the dissolved gas which may modify the precipitation conditions. The great variations in pressure occur during the ascent of effluents to the surface in the producing wells, which causes partial evaporation of water leading to rapid precipitation of $BaSO_4$ and $CaSO_4$, on the other hand, the decrease in pressure promotes the formation of $CaCO_3$ deposits (Connell, 1983).

The solubility of scale formation in a two-phase system increases with increased pressure for two reasons (Moghadasi et al., 2004b):

- Increased pressure increases the partial pressure of CO_2 and increases the solubility of $CaCO_3$ in water.
- Increased pressure also increases the solubility due to thermodynamic considerations.

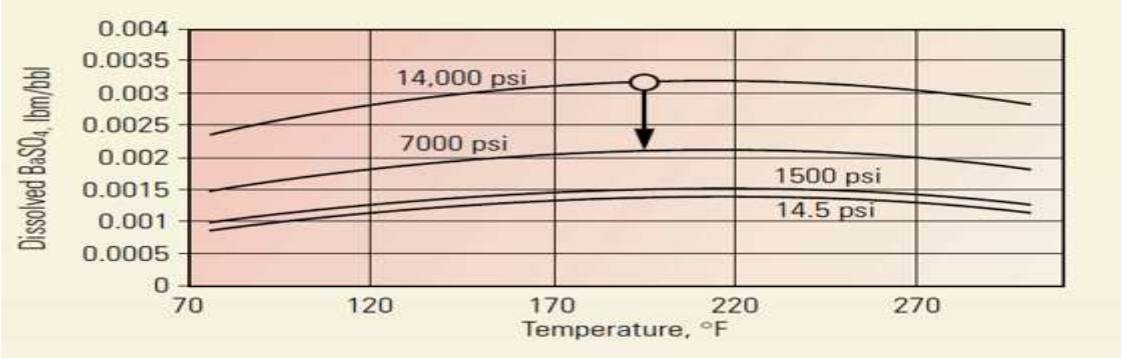

Figure I.11 : Influence of pressure on solubility (Crabtree et al., 1999).

I.3.10.4 pH effect

The solubility of the salts increases with the decrease in pH. This is due to the high activity of the H^+ ions. Indeed, when we have the presence of an acidic pH, the activity of H^+ (which has for origin the dissociation of weak acids like H_2SO_4), is very strong, it easily attacks the deposit, but the presence of a basic pH causes the formation of oxides which increases the mass of the deposit and decreases the solubility (Moghadasi et al., 2004b).

I.3.10.5 Effect of ionic force

The solubility of calcium sulphate is strongly affected by the presence and concentration of other ions in the system. The solubility of calcium sulphate is an order of magnitude greater than that of strontium sulphate, which in turn about an order and a half of magnitude greater than that of barium sulphate, as shown in the figure.

For example, figure I.12 indicates that the solubility of strontium sulphate may be greater than 950 mg/l. This solubility, however, is true only when the solution is stoichiometrically balanced, that is, when the number of strontium ions is equal to the number of sulphate ions. If an excess of either ion is introduced, the solubility is remarkably reduced. This is known as the common ionic effect (Lindlof & Stoffer 1983). Solubility reaches maximum in highly concentrated brines.

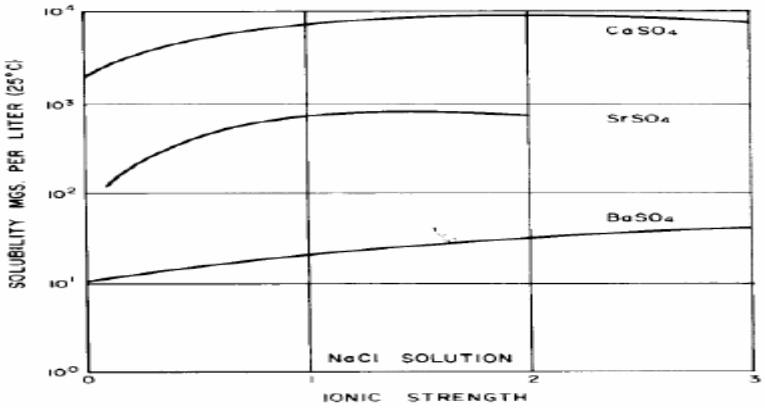

Figure I.12: Relative solubilities of three sulfates in brine (Lindlof & Stoffer, 1983).

I.4 Barium Sulphate

Barium sulphate $BaSO_4$ is a white compound that has been widely used in the industry for many years. It is present in quantities in the form of ore, referred to as 'baryte'. It is involved in the manufacture of glass, certain paints, floor coverings, and the paper industry. According to Pacary (2008), Barium sulphate is often considered a reference precipitate in the study of precipitation. A great deal of work is devoted to the study of this system (Aoun et al., 1996; Wong et al., 2003; Uehara-nagamine & Armenante, 2001). But barium sulphate mainly is

known as one of the problems that pose on the extraction sites, especially offshore of gas and oil.

Some chemical analyses used the formation of precipitate $BaSO_4$ to determine the SO_4^{2-} concentration in a solution. It was, later, recognized that in such procedures, $BaSO_4$ is not pure and may contain different anions and cations; the cause of this contamination is adsorption. $BaSO_4$ is contaminated with various foreign ions when it precipitates in some salt mixing systems (Pacary 2008).

Figure I.13: Deposits of $BaSO_4$.

Barium sulphate formation is a simple reaction of addition exothermic given by the following equation:

$$Ba^{2+}(aq) + SO_4^{2-}(aq) \text{ ----> } BaSO_4(s)$$

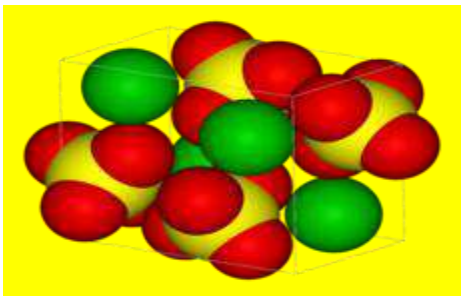

Figure I.14: Barium Sulphate Complex, Yellow=Barium Atom, Red= Oxygen Atom, Green=Sulphur Atom

I.4.1 The origin of $BaSO_4$

In the field of Hassi Messaoud, the formation of $BaSO_4$ deposit is caused by the direct contact between the reservoir water (Cambrian) loaded in barium (Ba^{2+}), and the injected water (Albian) loaded in sulphate element (SO_4^{2-}).

This contact may take place during continuous washing to avoid salt deposits or during the injection of fresh water into the reservoir to maintain the pressure of the reservoir.

The table below contains the composition of Albian and Cambrian water.

Table I.6: Average analyses of Albian and Cambrian waters (Data bank SH, 2019).

	Albian (mg/l)	**Cambrian (mg/l)**
$(HCO_3)^-$	170	0
CO_3^{2-}	0	0
Cl^-	420	210 000
$(SO_4)^{2-}$	600	0
Ca^{2+}	210	36 000
Mg^{2+}	70	6 500
Ba^{2+}	0	800
Sr^{2+}	0	970
Na^+	250	80 000
K^+	40	6 000
Total Iron	0	5 500
pH	7.0	3.5
Density at 25°C	1.00	1.230
depth (m)	1050-1350	3300-3400

I.4.2 Physico-chemical properties of barium sulphate

Barium sulphate is a crystalline mineral chemical body composed of sulphate anion and barium cation, it has the chemical formula $BaSO_4$, and has the following properties:

- A relative molecular weight of 233.4,
- Molar volume of 51.863 cm^3/mol
- A relative density of 4.5 (15 °C),
- A melting point of 1580 °C
- It is almost insoluble in water with a solubility of 0.00022 at 18 °C and 0.0041 at 100 °C.
- It is slightly soluble in concentrated sulphuric acid and soluble in an alkaline metal carbonate solution in which it is converted into barium carbonate.
- It is insoluble in other types of acids or bases. In nature, it exists in the mineral form of baryte.

I.4.3 Crystalline structure of barium sulphate

The crystals of $BaSO_4$ like those of $SrSO_4$ are, on the one hand, orthorhombic with very close mesh, On the other hand, they are porous in nature and tend to absorb foreign ions which can co-precipitate. However, $CaSO_4$ is orthorhombic, monoclinic with mesh very different from those of $BaSO_4$ and $SrSO_4$.

Barium sulphate crystallizes in the orthorhombic system (Pmma group). Its mesh parameters vary according to the authors. (James &Wood, 1925) obtained: a = 8.85 Å; b = 5.43 Å; c = 7.13 Å

I.4.4 Growth kinetics of Barium sulphate deposition

The first work on the nucleation kinetics of barium sulphate was proposed by Nielson (1961). His experiments have made it possible to study the nucleation kinetics of $BaSO_4$ by counting the number of particles produced by microscope and by measuring the induction time by varying the initial supersaturation. According to Nielsen and Toft (1984), diffusion at the interface becomes limiting when the growth rate becomes greater than 10^{-8} m/s, and the growth rate then varies linearly with over-saturation (Nielsen,1958). When oversaturation is too high, the transfer of the matter to the interface becomes the limiting step in the growth process.

I.4.5 Solubility of $BaSO_4$

In fact, the sulphate salt of $BaSO_4$ has the lowest solubility. At 25°C, Rosseinsky (1958) measures by conductimetry a solubility equal to 1,04. 10^{-5} mol/l or 2,5 mg/l. The solubility product of $BaSO_4$ at 25°C is $1{,}10.10^{-10}$. The table below lists some solubility products at 25°C of some sulphates reported in the literature.

Table I.7: Solubility and solubility product of three deposits sulphate-based.

Elements	**$BaSO_4$**	**$SrSO_4$**	**$CaSO_4$**
solubility product K_{sp}	$1\ ,1.10^{-10}$	$2{,}8.10^{-7}$	$6{,}1.10^{-5}$
solubility 'S' (mol/l)	$1{,}04.10^{-5}$	$5{,}3.10^{-4}$	$7\ ,8.10^{-3}$

The solubility of $BaSO_4$ in concentrated sulphuric acid (density 1.853) is 15.89 g in 100g of saturated solution at 25°C. Solubility drops rapidly when the sulphuric acid solution is diluted (0.05 g per 100 g diluted solution containing 83% concentrated acid).

The solubility of $BaSO_4$ increases with increasing temperature. Thus, experiments show that the solubility of barium sulphate in distilled water at 25°C is between 2.3 mg/l and 3.9 mg/l. Less precipitation occurs at high temperatures.

Table I.8: Solubility of $BaSO_4$ and temperature.

T (°C)	**0,77**	**3,33**	**18**	**26,75**	**34**
$BaSO_4$ (mg)	0,171	0,207	0,230	0,266	0.291

We have verified that these values do not vary much from one to another, in particular, the data of Cowan and Weintritt (1976) can be cited.

Table I.9: Solubility of $BaSO_4$ and temperature.

T (°C)	0°	10°	18°	30°	50°
$BaSO_4$ (mg/100ml)	0.115	0.20	0.226	0.285	0.336

I.4.6 Saturation rate of $BaSO_4$

The ability to precipitate can be measured in several forms; saturation index (SI), supersaturation (S), and saturation rate (SR). The multi-deposition thermodynamic prediction model used in this study is based on saturation rates defined by the following equation:

$$SR = \frac{[Ba^{2+}]0[SO_4^{2-}]0}{Ksp} \quad (I.1)$$

$[Ba^{2+}]_0$: Initial barium ion concentration (mol/l)

$[SO_4^{2-}]_0$: Initial sulphate ion concentration (mol/l)

Ksp: Barium sulphate solubility product, depends on temperature T, pH and ionic forces.

SR : Depends on several experimental conditions, including the mixture of injection and formation water, temperature (T), pH, and ion strength of the species in solution.

The thermodynamic driving force of nucleation and growth is supersaturation. Due to the high ionic force in supersaturated solutions (up to 0.5 mol/l), concentrations are replaced by ionic activities for the calculation of supersaturation. According to the method described by Vicum et al., (2003), precipitation of barium sulphate from aqueous solutions of barium chloride and sodium sulphate is as follows:

$$BaCl_2 + Na_2SO_4 \longrightarrow BaSO_4 + 2NaCl \quad (I.2)$$

The supersaturation Sa based on activity is defined as follows:

$$Sa = \sqrt{\frac{a_{SO_4^{2-}\ free} \cdot a_{Ba^{2+}\ free}}{Ksp}} = \gamma\pm . \sqrt{\frac{c_{SO_4^{2-}\ free} \cdot c_{Ba^{2+}\ free}}{Ksp}} \quad (I.3)$$

With the solubility product value Ksp = 9.82 x 10^{-11} at 25°C according to Monnin (1999). The activities and concentrations of free ions indicate that for the calculation of supersaturation the free ion activities in solution should be used. The average of activity coefficient γ± can be calculated as a function of the ionic force using the semiempirical method proposed by Bromley (1973) as a developed version of the limit law of Debey-Hückel and its valid for ionic forces up to 6 mol/l. In addition, the formation of a metal sulphate complex (pair of ions) $BaSO_4\ (aq)^0$, as discussed by Monnin, reduces the number of barium and sulphate free ions, so the actual supersaturation is considered.

Constant of equilibrium between complex and free ions is given by;

$$K\ ip = \frac{c_{Ba\ free} \cdot c_{SO4\ free} \cdot \gamma\pm^2}{c_{BaSO4\ (aq)}\ ^0 \cdot \gamma_{\ BaSO4\ (aq)}\ ^0} = 5{,}50\ .10^{-3}\ mol/l \quad (I.4)$$

I.4.7 Effect of certain parameters on $BaSO_4$ formation

The solubility of $BaSO_4$ increases with increasing temperature. Thus, experiments show that the solubility of barium sulphate in distilled water at 25°C is between 2.3 mg/l and 3.9 mg/l. Less precipitation occurs at elevated temperatures (Bin Merdhah, 2008, 2010, and 2012). The reverse was observed for $SrSO_4$ (Yuan et all., 1994; Nancollas, 1985).

Salts dissolved in water promote the solubility of $BaSO_4$, as in the case of $CaCO_3$ and $CaSO_4$. For example, 100 mg/l NaCl increases $BaSO_4$ solubility from 2.03 to 31 mg/l at 25°C and from 3.9 to 65 mg/l at 95°C (Bin Merdhah, 2007).

The solubility of the salts increases with the decrease in pH and this is due to the high activity of the H^+ ions. Indeed, in the presence of an acidic pH, the activity of H^+ is so strong that it easily attacks the deposit, on the other hand with a basic pH it is found that the formation of hydroxides increases the mass of the deposit and decreases the solubility.

The presence of salts in the solution decreases the activity coefficients of the Ba^{2+} and SO_4^{2-} ions and thus increases the solubility of $BaSO_4$. This decrease in activity coefficients results a decrease in supersaturation (Flouret, 2013).

I.4.8 Heterogeneous formation of $BaSO_4$

The monitoring of barium sulphate formation in situ by measurements of DRXS X-ray diffraction on stainless steel determined the crystalline faces of barytin and concluded that growth of $BaSO_4$ surface planes follows the same trend regardless of supersaturation and temperature. (Mavredaki et al., 2011).

The characteristics of deposition can be controlled by electrochemical methods (Emmons et al., 1999; Moritz and Neville, 2000) such as chrono-electrogravimetry (CEG), chrono-amperometry (CA), and electrochemical impedance (SIE). It is also possible to study deposits by non-electric chemical methods such as measurement of critical pH, thermal methods (evaporation), fast controlled of precipitation, degassing, and continuous filling on polymer or tube. However, the various methods used are not representative of the actual scaling phenomenon.

I.4.9 Possible locations for $BaSO_4$ scale deposits

However, barium sulphate $BaSO_4$ precipitation is not limited to petroleum reservoirs. Deposits may occur on wells, tubing, surface facilities, or in refinery equipment used for oil processing. Sulphate deposition can form throughout the production system depending on where the injection water and formation water mix.

In Bader list where scale deposits could take place in a production system with water injection:

Case 1: At the surface water injection facility where incompatible sources of waters are mixed prior to injection.

Case 2: In injection wells where the injected water starts to mix with the reservoir formation water.

Case 3: Downhole in the reservoir where the injected water displaces reservoir formation water.

Case 4: Downhole in the reservoir where the mixed injected water and formation water are about to reach the range of producing wells.

Case5: Downhole in the reservoir where the mixed waters are within the range of producing wells.

Case 6: At the connection of a branched zone where each branch produces different water.

Case 7: At the manifold of a producing zone where water is produced from different blocks within the same producing zone.

Case 8: At topside facility where produced fluids are mixed from different zones to separate oil and gas from produced waters, or in pipelines that transport produced fluids to on-shore processing facilities.

Case 9: And if applicable in disposal wells where produced water is injected for final disposal.

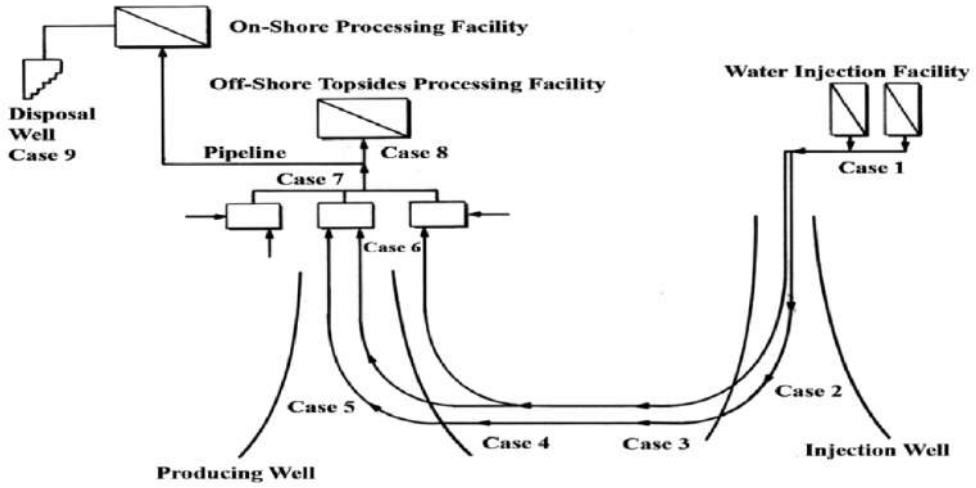

Figure I.15: Possible locations for $BaSO_4$ deposition (Bader, 2006)

I.4.10 Impact of $BaSO_4$ deposits on production

In the oil industry, the various problems of deposits that occurred during the exploitation of oil have created many problems, with all the economic consequences and the resulting production constraints.

These deposits represent a serious problem in the slowdown of production, and against which industrialists struggled for many decades. Deposits can be encountered in the underground installations as they can be found in the surface installations as indicated in the

photos taken from different places in the field of Hassi-Messaoud; in lines (pipes), separators, chokes, concentric, and in tubing of production.

Figure I.16: Deposits of $BaSO_4$ in the field of Hassi Messaoud.

In the well:

- Plugging of perforations.
- Proven precipitation around wells
- Limited effects in open-hole wells

At well level 3210-3220m

Inside the side valves

Deposits outside of CCE1 1'900 at 3385m

Deposits Inside Line 2'7/8, snubbing

Figure I.17: $BaSO_4$ deposits in the well.

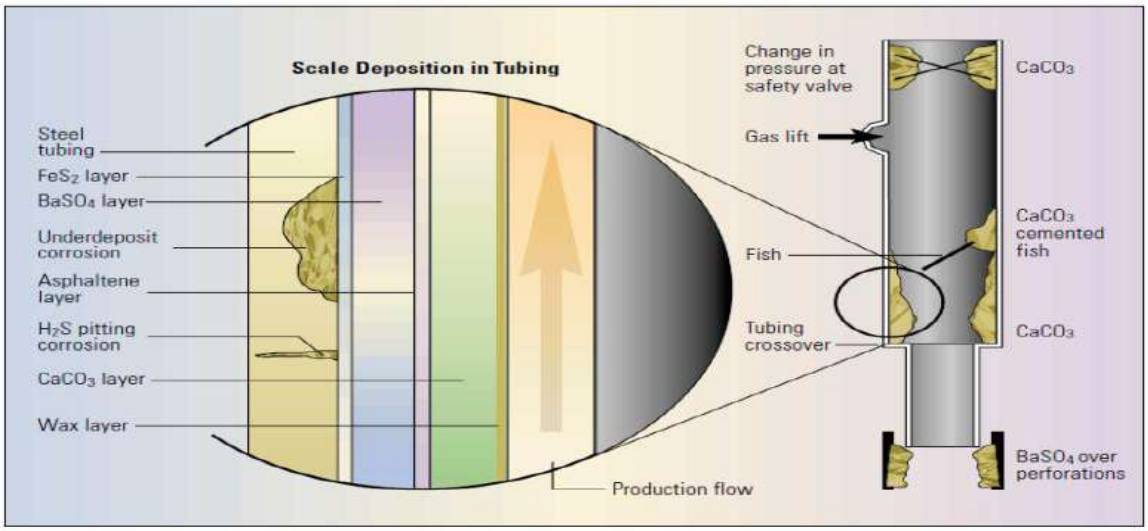

Figure I.18: location of deposits in the tubing

In the reservoir:

- Precipitation unlikely in formation.

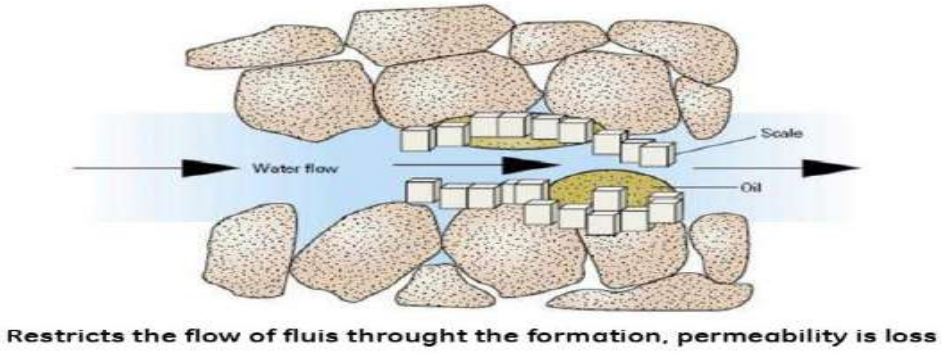

Figure I.19: location of deposits in the rock reservoir.

In the separation centre:

- Pump plugging
- Line plugging
- Manifold plugging
- Automatic valve blockage

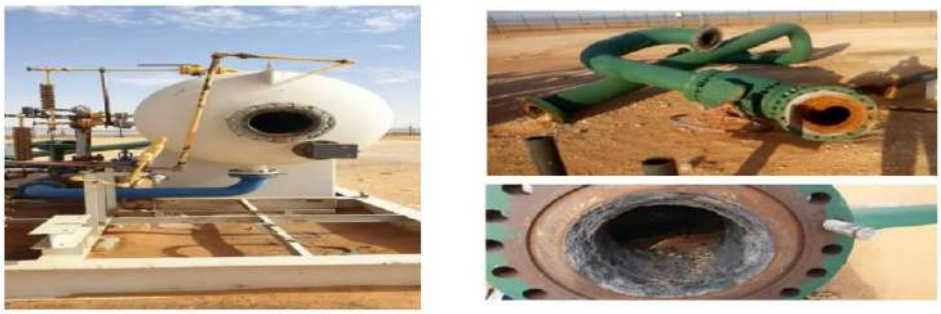

Figure I.20 : $BaSO_4$ deposits in the separation centre.

I.4.10.1 Loss of production caused by $BaSO_4$ deposits in the HMD field

This problem can be summarized in the following points:

- Reduction of the section of the pipes with the degradation of the surface, these adhering scales increase the losses of load and, consequently, the energy expenditure related to the circulation of fluids.
- Reduced well productivity
- Tubing and line blockage cause stops in production
- Production losses (in tonnes) Case E1C
- Equipment malfunction
- Formation of deposits leads to large investments in repair and workover of the equipment of bottoms of producers and injectors well
- Clogging of reservoir rock around producing wells.

I.5 Methods of treatment of $BaSO_4$ deposit

I.5.1 Curative treatment

I.5.1.1 Milling

It is done by mechanical partition using scraper, it is used to scrape the walls on which barium sulphate was deposited, but it can cause cracks at the tubing level during the operation. This operation is performed by the wire line units, work over, and snubbing.

Figure I.21: Milling tool

I.5.1.2 Jetting (hydraulic jet)

Scale Blaster operation with Coiled Tubing has proved its effectiveness since November 1999 for the interior cleaning of strainers and openings. Scale Blaster is a mechanical treatment by the coiled tubing unit used mainly for cleaning barium sulphate deposits at the level of perforations and obstructions inside the tubing. It consists of using a viscous fluid with sand and high pressure (Lalmi, 2008).

The properties of Sterling Beads are:

- Not abrasive

- More effective on very hard deposits and cement plugs
- To remove hard and inert deposits such as $BaSO_4$
- Positive cleaning with One-pass
- Secure technique.

Figure I.22: Sterling Beads (Lalmi, 2008).

The tool (Jett Blaster**)** used for the Scale Blaster operation consists of a nozzle in the head that ensures their passage, two (2) side nozzles that cause the tool to rotate, and drift for control the cleaning.

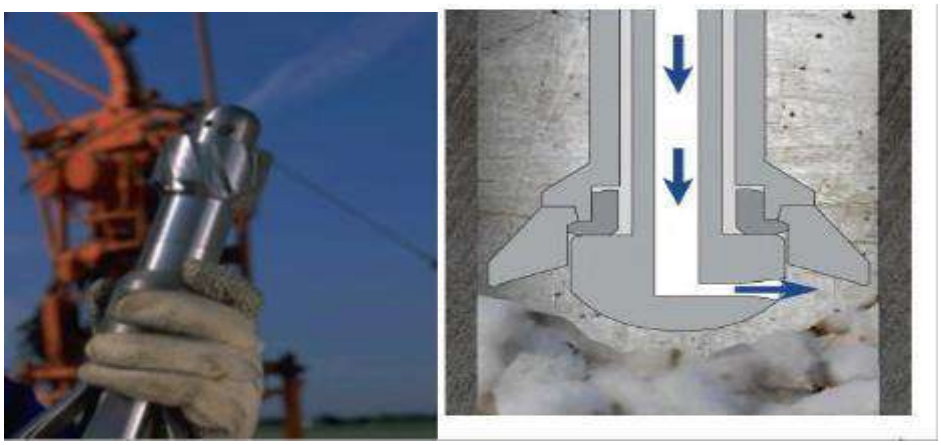

Figure I.23: Jett Blaster (Lalmi, 2008).

I.5.2 Preventive treatment

I.5.2.1 The additive process (by continuous injection of an inhibitor)

The continuous injection method of an inhibitor is performed in injector and producer wells. This technique allows uninterrupted pumping of an inhibitor at the bottom of the concentric at a certain depth. The inhibitor is diluted to achieve a good distribution and to avoid precipitation near wells caused by the concentrated inhibitor (Rondon, 2010).

I.5.2.2 Squeeze of inhibitor solution in formation

The technique of inhibitor squeeze consists of stopping the production of the well to be treated, then injecting a certain volume of inhibitory aqueous solution into the reservoir and closing the latter to allow the inhibitor to adsorb onto the rock. This operation may take a few days to a few weeks before the well is back into production, depending on the state of damage

caused by precipitation in the reservoir area around the wells. When production resumes, the inhibitor is gradually released into the water.

However, to be effective, it must be released into the production waters at a sufficient rate to prevent the formation of deposits. This value is called the minimum inhibition concentration (MIC): the lowest inhibitor concentration for which deposits do not form/grow.

This mechanism is also referred to as the "threshold effect", defined as the inhibition of deposition precipitation by very low concentrations. Beyond that, the product loses its inhibitory action by the phenomenon of desorption by reacting as a sequestering agent (complexing agent) (Rondon, 2010).

I.5.2.3 Deposit inhibitors

An inhibitor is a substance that is added in small quantities in any medium to slow down or prevent the evolution of certain deposition phenomena. They are compounding whose action is to inhibit a chemical reaction, i.e., to slow or stop it.

Deposit inhibitors are compounds used at concentrations below stoichiometry for inhibition against the formation of crystalline deposits. In general, they are used in the industrial field, and, in particular, in the petroleum sector (producing wells, hydrocarbon reservoirs, water circuits, and production facilities in general). Deposit inhibitors are also used in water treatment (sanitary water, industrial process water, boiler water, etc.) (Rondon, 2010).

I.5.2.4 Mechanisms of action of inhibitors

The mechanisms of action of inhibitors are classified into three categories, described below:

- **Inhibition of nucleation:** thermodynamic destabilization of nuclei by adsorption of inhibitor molecules at their growth sites.
- **Dispersion of crystals already formed:** suspension of aggregates formed by electrostatic or steric stabilization due to the adsorption of macromolecules, such as poly electrolytes, on their surface (Figure a).
- **Slowing/blocking crystal growth:** by adsorption of inhibitor molecules at growth sites of formation deposits. (Figure b).

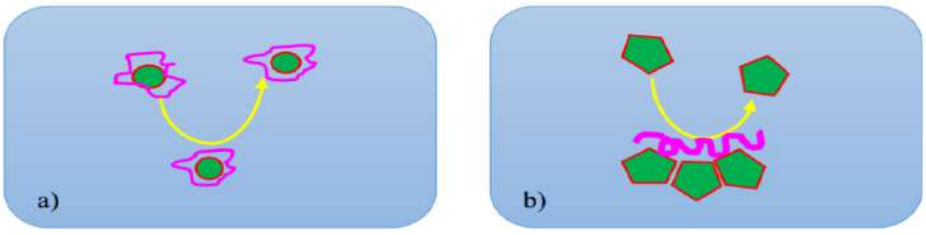

Figure I.24: (a) dispersion of formed nuclei and (b) stabilization of growing deposits (Rondon, 2010).

I.5.2.5 Properties of deposition inhibitors

- Inhibitory activity results in slowing or preventing the precipitation reaction.
- Good stability is characterized by the fact that the inhibitor does not evolve in the operating conditions (thermodynamics: pressure and temperature) to avoid the loss of its effectiveness.
- The deposit inhibitor must have good resistivity to keep all properties during treatment.
- The chosen deposition inhibitor must comply with the safety (toxicity) and environmental (biodegradability) requirements.
- Even if the inhibitor has all the mentioned priorities and characteristics, it must be cost-competitive so as not to be a heavy burden on the production process.

I.5.2.6 Types of inhibitors

➢ **Mineral formulation inhibitors**

They are most often used in near-neutral environments, even in alkaline environments, and more rarely in acidic environments. The products dissociate in solution, and their dissociation products ensure the inhibition phenomena (anions or cations).

➢ **Inhibitors of organic formulation**

Available in several varieties. The main ones are: Amines; polyphosphates; phosphoric esters; polyesters and polyacrylic acids.

The most well-known anti-deposition products are:

- **Ethylene diamine tetra acetic acid (EDTA):**

It is a known complex agent that interacts with a multitude of cations. EDTA is often used to study the solubility of deposits such as barium sulphate, or calcium sulphate. Different techniques are used to elucidate the mechanism of interaction between EDTA surfaces and barium sulphate. The chelation between EDTA and Ba^{2+} is performed according to the reaction (Kieffer et al., 2009):

$$Ba^{2+} + EDTA^{4-} \rightarrow Ba\text{ - }EDTA^{2-} \quad \text{(I.5)}$$

The equilibrium constant gives by :

$$K_{Ba-EDTA} = \frac{[Ba-EDTA^{2-}]}{[Ba^{2+}]\,[EDTA^{4-}]} \quad \text{(I.6)}$$

$K_{Ba\text{-}EDTA}$= 6,02 × 10^7 at 25°C. (Dean & Patnaik, 2004).

- **Phosphates with Linear chain :**

They are the first inhibitors used, and they are characterized by p-o-p bonds; the most well-known compounds in this class are:

- Pyrophosphates, metaphosphates and polyphosphates.

- Organic phosphate esters are effective inhibitors.
- Phosphonates. (Jones et al., 2003, 2002 ; Boak, 2012)

The formulations of these inhibitors are illustrated in the table below:

Table I.10: Developed formulas of the main deposit inhibitors.

Inhibitor name	Developed formula
EDTA	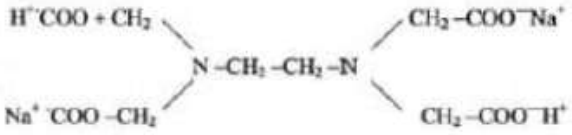
polyphosphates	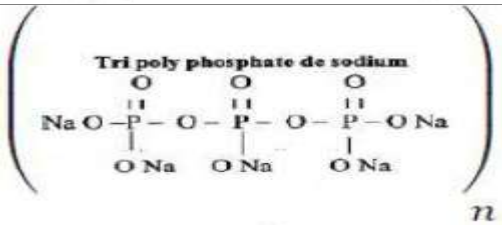
organophosphates	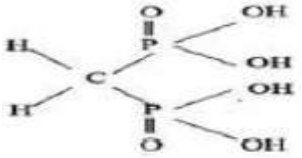
polyacrylates	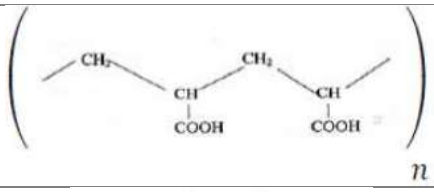
Organic phosphate esters **R : hydrocarbon radical (methyl, ethyl, …etc.)**	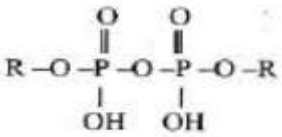
Phosphonate **R: radical (methyl, ethyl, …etc.)**	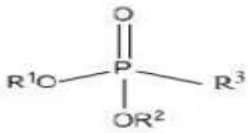

I.5.2.7 Chemical dissolution

The purpose of using chelating agents such as EDTA and DTPA is to transform insoluble barium sulphate into barium carbonate or other compounds it is easier to dissolve than using an acid. The stability of the metal complex can be controlled by the concentration of hydrogen ions (i.e., pH).

This is generally done by dissolving the sodium hydroxide in the solution to increase the pH of the medium. An increase in pH will promote the removal of EDTA and DTPA molecules (i.e., removal of hydrogen atoms) to the form $(EDTA)^{4-}$ or $(DTPA\ ions)^{6-}$.

These complexes ion can adhere to barium sulphate and remove Ba^{2+} ions accordingly, leaving the SO_4^{2-} ions in the solution.

$$BaSO_{4(s)} + 2Na^{+}_{(aq)} + CO^{2-}_{3(aq)} \leftrightarrow BaCO_{3(s)} + 2Na^{+}_{(aq)} + SO^{2-}_{4(aq)}$$

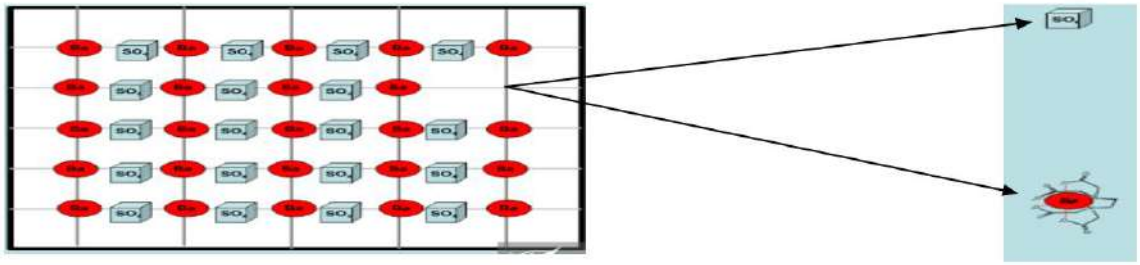

Figure I.25: The EDTA complex provides barium sulphate for dissolution. (Environmental Science and Technology, 1999)

I.5.2.8 Factors influencing the performance of deposition inhibitors

The inhibitory properties of deposition inhibitors can be significantly affected by a number of factors, including chemical and environmental structures. (Graham, G.M. 2001b et al.).

- *Changes in experimental conditions* such as pH, temperature, and hydrodynamic conditions. (Quddus et al., 2000 ; Shaw et al., 2013a, 2013b).

the presence of other chemicals and the composition of solutions or other factors such as over-saturation may have a significant effect on the performance of deposition inhibitors (Yuan et al., 2001; Jones et al., 2003)

- *the presence of bivalent cations*, such as Ca^{2+} and Mg^{2+} or even Zn^{2+} (Kan, 2012), may lead to an incompatibility between the system and certain anti-deposit products; This causes the decrease of their concentration in the solution and hence their efficacy (Dyer, et al., 1999; Graham et al., 1997a, 2001b, 2003c; Shaw et al., 2013a, 2013b; Quddus et al., 2000; Yuan et al., 2001).

An increase in calcium concentration seems to considerably improve the performance of certain scaling inhibitors such as phosphonates (Sweeney et all., 1993), while the presence of magnesium ions is significantly detrimental to them (Boak et al., 1999; Graham et al., 2003c).

- The major problem with deposit inhibitors in the oil industry is the reduction of their efficiency due to the presence of Fe^{2+} and Fe^{3+} ions in reservoir waters.

Fe^{2+} ions in the presence of oxygen in the air oxidize to Fe^{3+}, and they precipitate in the form $Fe(OH)_3$. Due to the adsorbent power of the latter vis-à-vis, other ions in the solution prevent the inhibitor from playing its role.

- *The pH of the solutions appears to influence the inhibitor*. According to the study of Jones et al (2003), It may have an influence on the degree of ionization of the acid functions and consequently on the flexibility of the macromolecule of the anti-deposit.
- *Functional groups of inhibitors play an important role in their mechanism of action.*

Amjad (1994) found that the position of the functional group in a structural chain is very important because a functional group can be more effective if it is located at the end of the chain rather than in the middle.

I.5.2.9 $BaSO_4$ inhibition

The morphology, composition, number and size of barite crystals are affected by the presence of the deposition inhibitor at a concentration greater than, equal to or less than the minimum concentration of inhibitor MIC (Aoun et al., 1999).

The mechanisms through which inhibitor complexes act to control tartar formation are related to the performance of these inhibitors, determined in relation to the residual concentration in solution after a certain period of residence (Boak, 2012, Graham et al., 2003c). The effectiveness of $BaSO_4$ inhibition is given by the following equation:

$$EI\ \% = \frac{C_t - c_{.B}}{C_0 - c_{.B}} . 100 \qquad (I.7)$$

with

EI%: Effectiveness of the inhibitor

C_t: Barium concentration in the sample (at time t)

C_B: Concentration of barium in blank solution (without inhibitor)

C_o: Initial concentration of barium in inhibitor solution (at t = 0).

I.5.2.10 The most used inhibitors in HMD field

The following inhibitors represent the most used products in the HMD field; AD32, SCW85375, SCALETREAT837C, ALPHA 7241, CHIMEC1264 and FQS113.

a. **CHIMEC1264:** It is a polyfunctional liquid product used specifically for inhibiting the formation of calcium sulphate deposits, as well as barium sulphate deposits. It contains a balanced mix of anti-incrusted, and it has considerable efficiency for protecting metal surfaces from corrosion.

Figure I.26: The inhibitor CHIMEC1264

Characterizations of the CHIMEC1264 inhibitor:

Table I.11 below shows the physical-chemical properties of the CHIMEC1264 inhibitor.

Table I.11: Physical and chemical properties of CHIMEC1264.

Nature	**Phospho-organic**
Appearance	Liquid
Colour	yellow
Freezing point	< 0 °C
Viscosity at 20°C	< 50
Boiling point	100 °C
Solubility in water	Full solubility
Density at 20°C	1.07 (g/cm^3)

b. **FQS113:** It is an amber liquid injected into the desalination system to prevent the formation of barium sulphate $BaSO_4$ deposits and also calcium sulphate $CaSO_4$ deposits.

Figure I.27: The inhibitor FQS113

Characterizations of the FQS113 inhibitor:

Table I.12 below shows the physical-chemical properties of the FQS113 inhibitor.

Table I.12: Physical and chemical properties of FQS113.

Nature	**Phosphonate**
Appearance	liquid
Colour	Amber
Odour	Smell of an amine
pH	3.5 - 4.5
Dynamic viscosity	38 - 48 cPs
Solubility in water	Full solubility
Flash point	>200 °F (>93 °C)

c. GYPTRON SA 860N inhibitor

The inhibitor GYPTRON SA 860N is an industrial liquid used for inhibiting the formation of barium sulphate deposits, The use of this inhibitor is part of the procedure for approval and acquisition of new treatment products.

The table below shows the characteristics of this inhibitor.

Table I.13: Physical and chemical properties of GYPTRON SA 860N

Nature	**Phosphonate**
Appearance	liquid
Colour	brown
pH	5 - 6
Density	1.22 – 1.25
Solidification temperature	-12 °C
Solubility	Soluble in water
Chemical stability	Stable under normal conditions
Kinematic viscosity	4.7 mm^2/s (40 C°)

I.5.2.11 The inhibitor AD32

It is the main inhibitor used in the field of Hassi Messaoud, it is a deposition inhibitor used for the treatment of water circuits to avoid precipitation of salts, calcium, strontium, barium, iron and other cations in association with sulphates, carbonates and oxides. The AD32 inhibitor is particularly recommended for crude oil lines and for water injection circuits to control the scaling in tubing, pumps, pipes...etc. (Lembarki., 2017)

Figure I.28: The AD32 inhibitor.

Characterizations of the AD32 inhibitor

Table I.14 shows the physical-chemical properties of the AD32 inhibitor.

Table I.14: Physical and chemical properties of AD32.

Nature	**Phosphonate**
Appearance	liquid
Solidification temperature	-5 °C
pH	6 - 8
Active substance	25%
Flash point	100°C
Density	1225-1275 Kg/m^3
Viscosity	10 m Pa/s
Solubility	soluble in water and organic solvent (insoluble in hydrocarbons)

AD32 Inhibitor Operating Instructions

It is injected directly into the system to be inhibited, pure or diluted in water, preferably in continuous injection using a dosing pump.

Figure I.29: system of injecting inhibitors in CIS station (HMD field).

I.5.2.12 Control of corrosion and mineral deposits in the HMD field

The exploitation of the HMD field is characterized by the diversity of problems encountered and the complexity of the phenomena involved. Several factors may be responsible for these problems, such as corrosion in all its electrochemical and bacterial forms also organic and mineral deposits. However, in order to remedy these problems and to prevent deterioration of the equipment, means of control are used:

1. Treatment of washing water with a deposition inhibitor (AD 32, ALPHA 7241) to prevent the formation of mineral deposits.
2. To avoid chemical and electrical-chemical corrosion caused by several factors: H_2O, CO_2, S^{2-} a film-forming corrosion inhibitor is injected currently NORUST720.
3. Washing water also presents a problem of bacterial corrosion that manifests mainly inside concentric. Hence the use of several bactericides in alternation to avoid the effect of habituation: BACTIRAM 3084, UMP B 52, SERVOCK 494, currently FQS50. (Kafi, 2009).

I.5.2.13 The Treatment Stations

The water treatment units (chemical injection stations) are designed to treat the washing water of salted oil wells as well as the treatment of the pressure-maintaining water. They are eight (08) in number and located in different areas on the Hassi-Messaoud field.

The treatment stations are controlled remotely, which allows having information and the possibility to intervene quickly on:

- Concentration of treatment products
- Programming bactericidal injection continuously or by shock
- Corrosion rate
- Bin level
- Start and stop pumps etc.,

- Injected water flows

All this information will make it possible to optimize the chemical treatment.

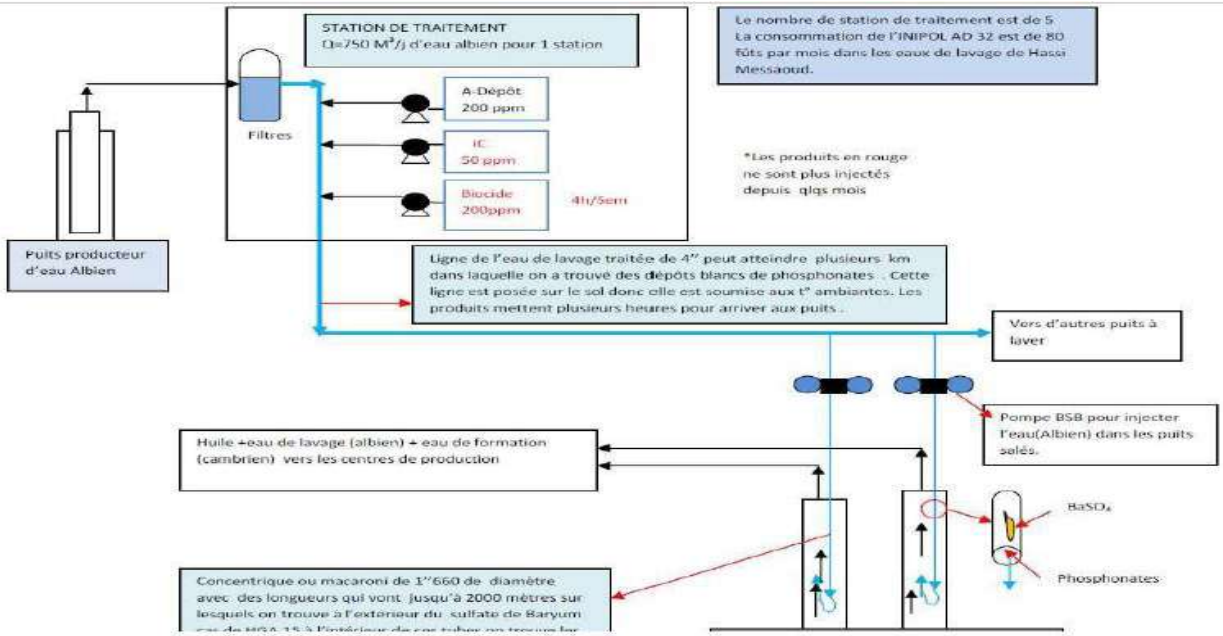

Figure I.30: Simple schema of water injection circuit.

I.5.2.13.1 Desalting network

- ***Salt oil well washing station:***

The purpose of water treatment units (chemical injection stations) is to treat the washing water of salted oil wells as well as the treatment of pressure-maintaining water. They are five (05) in number, and they are located in different areas on the Hassi-Messaoud field.

A. **Station Z14** is located in the central zone of the HMD field (inside the IRARA base) and processes the salt oil wells of the eastern zone. It includes 6 tanks of 1000 liters.

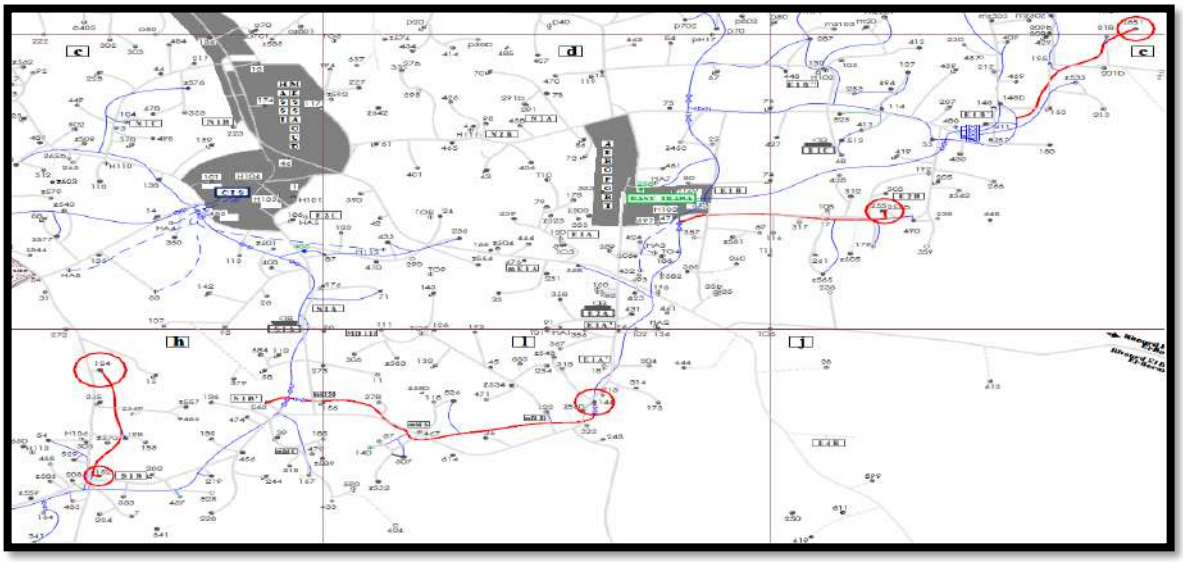

Figure I.31: Desalination water network (station Z14).

Figure I.32: Z14 station tanks

Figure I.33: dosing pump **Figure I.34:** sampling valve **Figure I.35:** inhibitor injection line

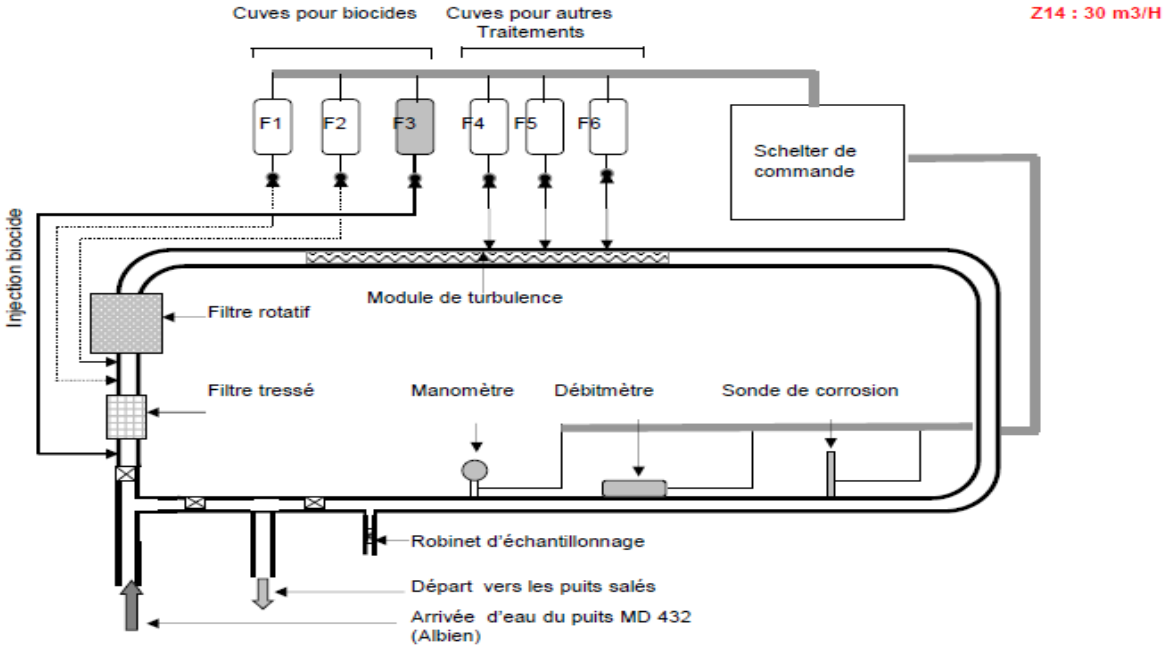

Figure I.36: Z14 Water treatment station schematic.

B. **CINA station** is located in the central area of the HMD field (inside the Industrial Center North) and treats the salted oil wells of the North area. It includes five tanks of 1000 liters and one of 2000 liters.

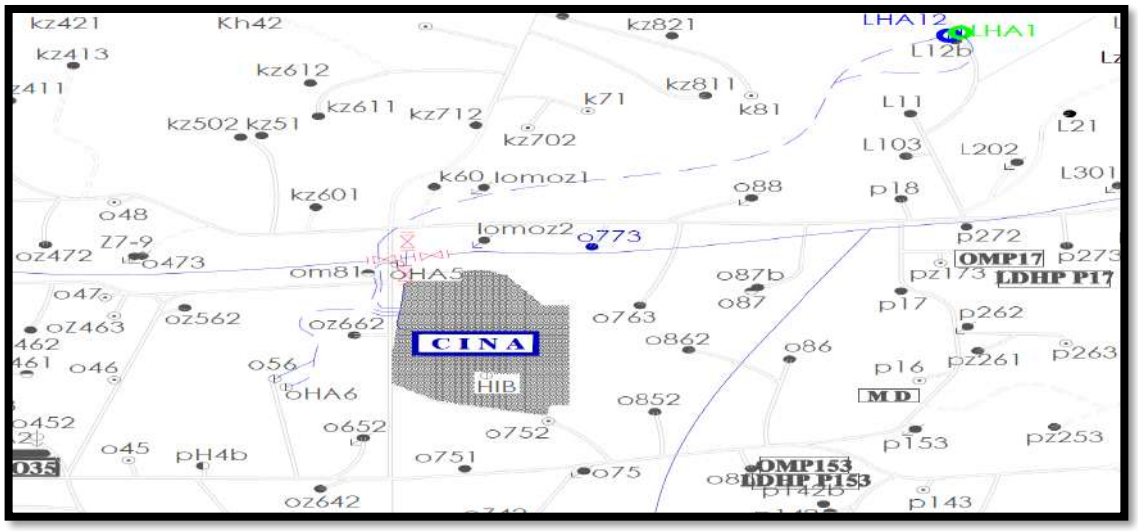

Figure I.37: desalination water network (CINA station).

The capacity of this unit varies between 30 and 35 m^3/h.

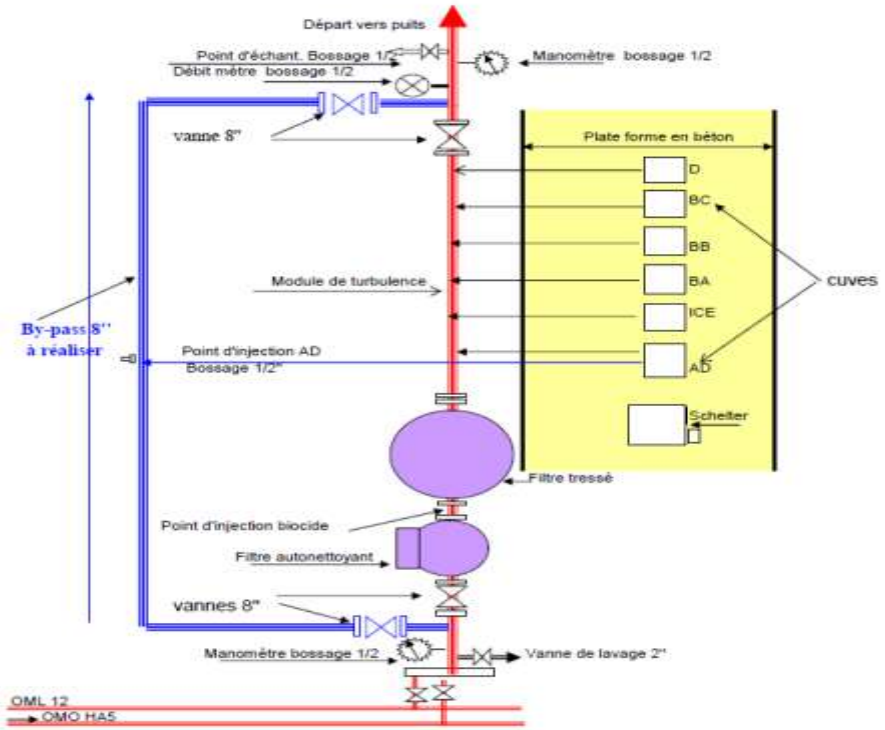

Figure I.38: Water wash injection plant in CINA

C. **Station W1C** is located in zone complex of the field of HMD (interior the satellite station W1C) and treats the salted oil wells of zone 1. It includes 6 tanks of 1000 liters and one of 3000 liters.

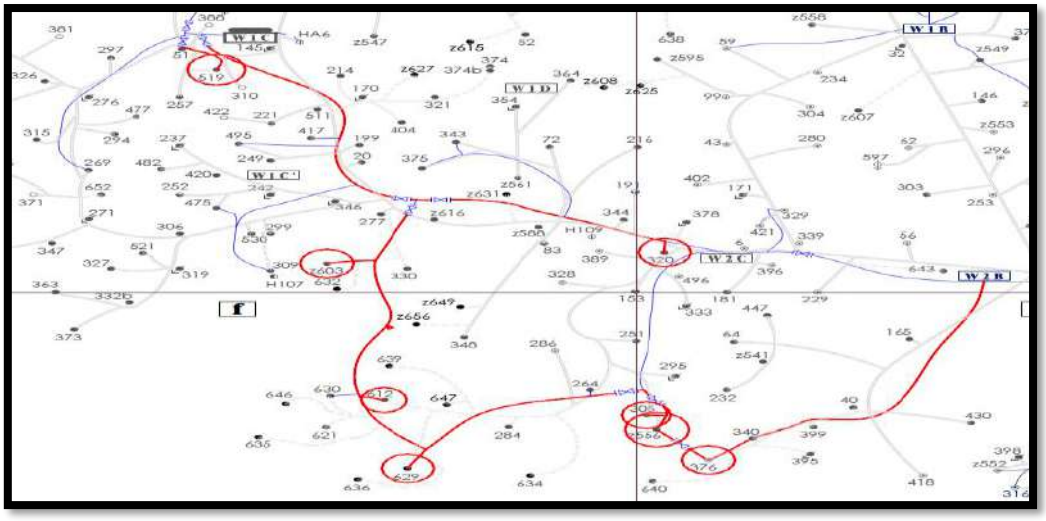

Figure I.39: desalination water network (station W1C).

The capacity of this unit equals 16 m^3/h.

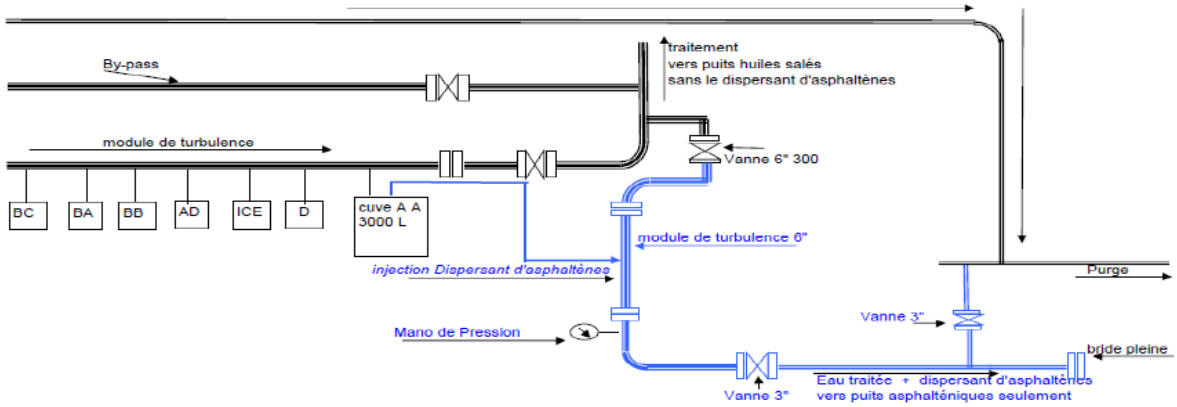

Figure I.40: Station W1C.

D. **CIS station** is located in the central zone of the HMD field (interior the South Industrial Center) and treats the salt oil wells of the West zone. It includes 5 tanks of 1000 liters and one of 2000 liters.

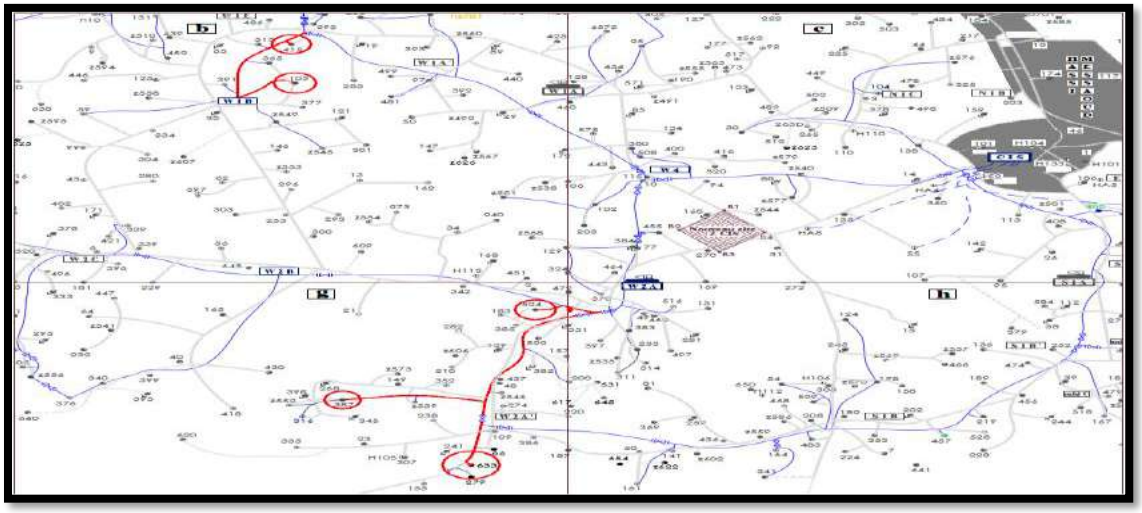

Figure I.41: desalination water network (CIS station).

The capacity of this station is 30 m^3/h.

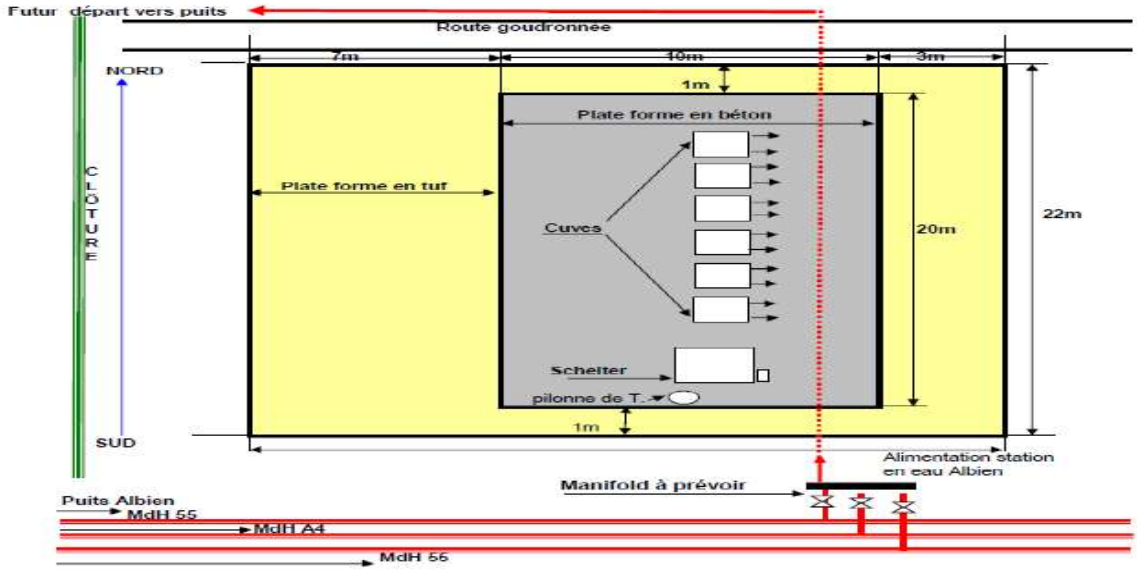

Figure I.42: CIS station.

E. **HGA station** is located in the Complex area of the HMD field and treats the salt oil wells of the HGA field. It includes 3 tanks of 1000 liters.

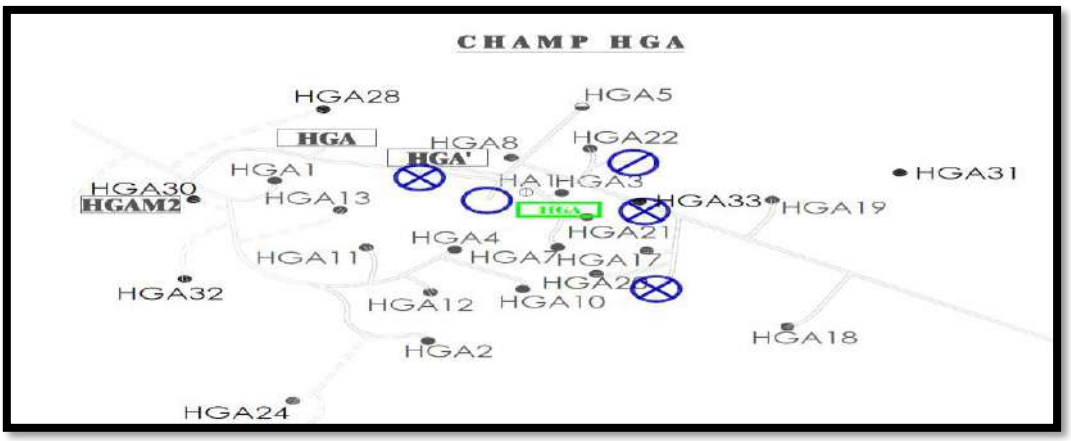

Figure I.43: desalination water network (HGA station).

The capacity of this unit varies between 2 and 5 m^3/h, and the maximum capacity is 10 m^3/h.

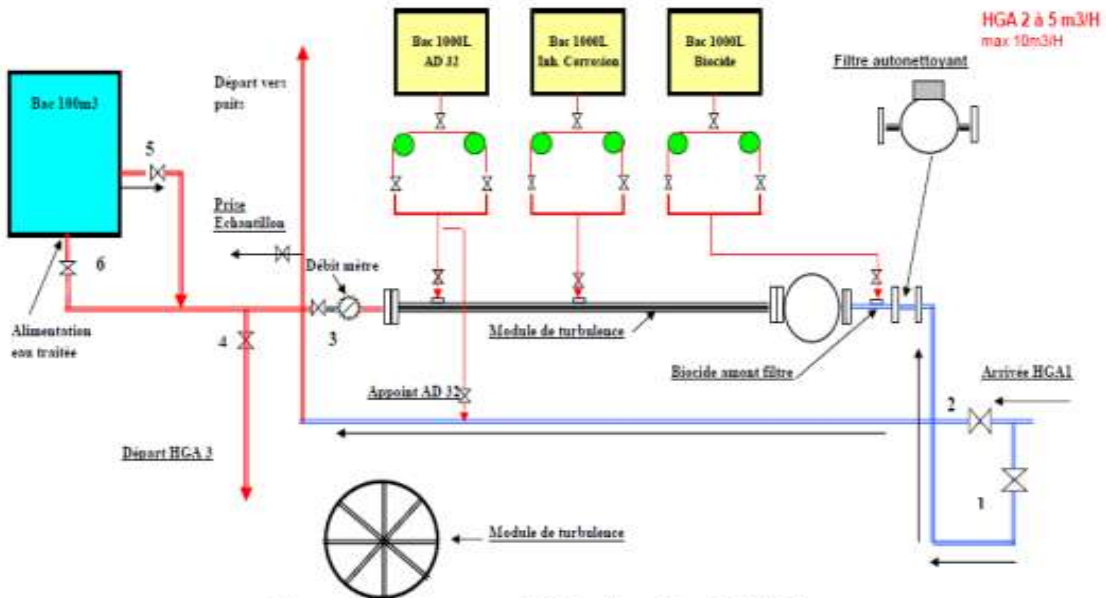

Figure I.44: HGA station

- ***Pressure maintaining station***

a) **Station E2A** is located in the central zone of the HMD field and treats the injector wells of the eastern zone. It Includes 4 tanks of 3000 liters.

b) **OMP 53 Station** is located in the central area of the HMD field and treats the northeast injection wells. Includes 2 tanks of 3000 liters and 2 tanks of 5000 liters.

c) **Station OMN 77** is located in the central zone of the HMD field and treats the injection wells of the North zone. It includes 4 tanks of 5000 liters.

Skides

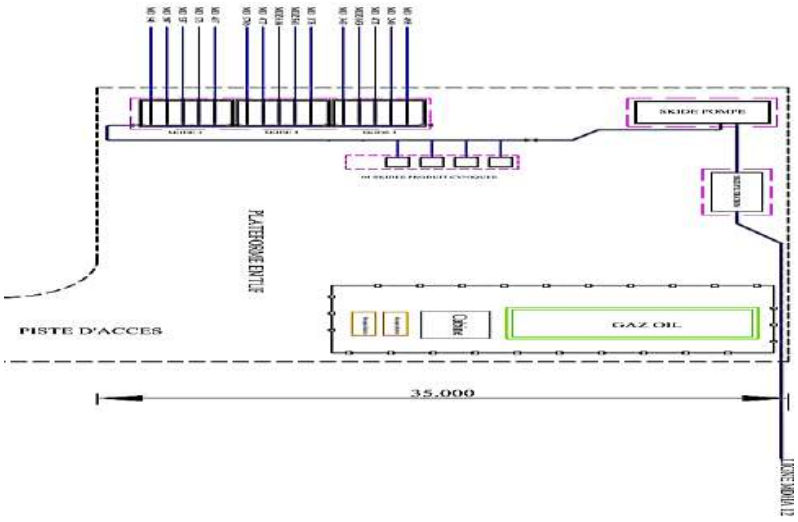

Figure I.45: Skides Schematic.

Shelter of control

Filter

Inhibitor pumping

Inhibitor injection

Control Valves of Wells

Figure I.46: MD141 Skid for HP Pressurized Desalination (BONATTI) HMD.

I.5.3 ENMAX CPRS Tool

ENMAX Corrosion Prevention System (CPRS) is a complete series of tools used for the prevention of scale, paraffin, asphaltene deposits and rust in oil and gas industry and any heat or cooling water systems in other industries.

The Enmax CPRS consists of nine dissimilar metals such as copper, zinc and nickel, etc., and forms a special catalyst when placed in contact with fluids, the metals (alloys) act as a special catalyst to enable a change in the electrostatic potential of the fluids, also inhibiting the binding forces between particles in the fluids. It is based on suspending solids and inhibiting the formation of scales, paraffin and corrosion. The metals are non-sacrificial during the reaction process.

Figure I.47: ENMAX Tool.

The photos below indicate the device, it was already used in many companies like Shell in Nigeria, Austrian Oil Company, Many Chinese oil companies.

Figure I.48: Installation of ENMAX (Enmax Technology (Shanghai) Co, 2012).

I.5.3.1 The functions of ENMAX CPRS

The following points represent the main function of ENMAX tool:

- Prevention and elimination of paraffin and asphaltene.
- Preventing and removing scale or slowing scale deposits.
- Prevention and elimination of corrosion by oxidation as rust.
- Change the surface tension of the gas/liquid phase to improve the efficiency of degassing (H_2S, CO_2).

- Sterilize, remove algae and improve water quality.
- Improve fuel combustion efficiency and minimize emissions pollution (Enmax Technology (Shanghai) Co, 2012).

I.5.3.2 The characteristics of ENMAX CPRS:

The characteristics of ENMAX tool are:

- Non-magnetic, non-electric, and no chemicals required.
- Respectful of the environment.
- Suitable for HP and HT operations.
- Less downtime and equipment replacement costs.
- Minimal cost because there are no chemicals products.
- Increase the efficiency and lifetime of the equipment.
- Improved fuel quality and emissions.
- Easy installation and free maintenance.

I.5.3.3 How ENMAX CPRS works

Enmax CPRS includes nine dissimilar metals, such as copper, zinc, nickel, etc., which can form a special catalyst. When fluids pass through CPRS units, metals allow a change in the electrostatic potential of fluids, for that a polarization effect is produced on the molecular liquid and reduces the bond between negative and positive ions in addition between the suspension particles.

This catalytic action will keep particles in suspension and prevent ions from binding to each other to form scales and paraffin deposits. This action will also break down the existing paraffin or scale deposit and escape with the fluids (Enmax Technology (Shanghai) Co, 2012).

I.5.3.4 The working conditions of ENMAX

The table below summarizes the conditions under which ENMAX tool can work.

Table I.15: ENMAX working conditions (Enmax Technology (Shanghai) Co, 2012).

Working distance	5 – 10 KM
Fluid temperature	Up to 700 ℃
Equipment Surface Temperature	Up to 500℃
Liquid ratio	Based on Pipeline Size and C.P.R.S selection.
Lifetime unit	5-10 years
Fluid pH	3~10
Chloride	≤15000mg
Unit head loss	5% for standard fixed ID units, 2% or 0 for variable ID units
Operating pressure	Low to high pressure, to match system pressure.
Granulometry for passing through	≤7mm
Types of deposits to be treated	Ca, Mg, Ba, Sr, scales, Br...etc.

I.5.3.5 ENMAX CPRS application range

ENMAX CPRS is useful for the following cases:

- Oil and gas production wells and water injection wells.
- Oil/gas production, storage, and transportation facilities.
- Cooling water systems and installations.
- Hot water systems and facilities.
- Civil water systems and facilities.
- Fuel treatment for industrial engines

Figure I.49: ENMAX CPRS application range (Enmax Technology (Shanghai) Co, 2012).

I.5.3.6 Types of application of CPRS units

There are two types of application of CPRS, the first is installed in the down hole and the second on the surface.

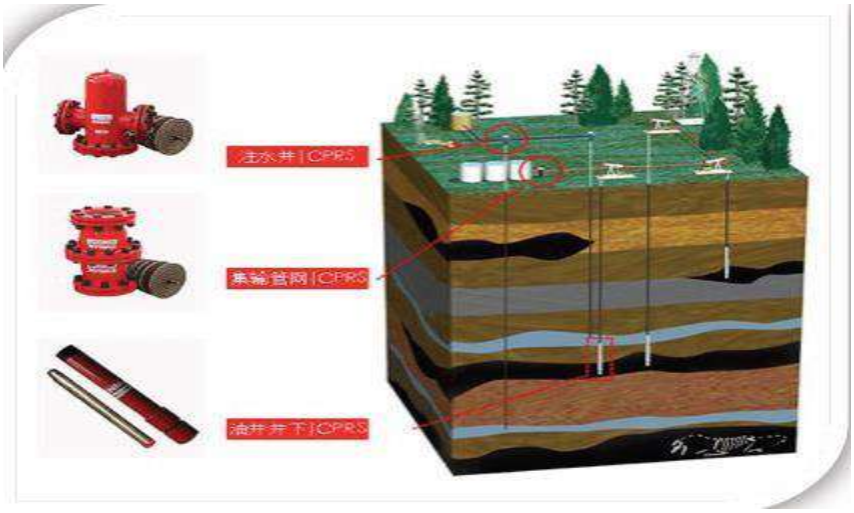

Figure I.50: Type of ENMAX CPRS units (Enmax Technology (Shanghai) Co, 2012).

a. The down hole CPRS units

Enmax CPRS units for Oil Well Bottom are typically installed at the bottom of oil production wells or water injection wells for the prevention and disposal of paraffin, asphalt, and corrosion.

Figure I.51: ENMAX style disc.

Figure I.52: ENMAX bar style.

Applications

Enmax CPRS bottom units will operate in all depositing wells and are suitable for any pumping system, including submersible electric pumps. Each application is designed for a specific well depending on the size of the tubing and the volume of fluid.

Installation

As a general rule, Enmax CPRS bottom units operate either below the pump inlet or above the pump discharge, or as a tail joint at the end of the tube train. The CPRS can also be installed in a well without pulling on the tubing. It can be placed in the well completion with an adjusting nipple using the appropriate adjusting tool with a cable.

Figure I.53: CPRS Downhole unit (Enmax Technology (Shanghai) Co, 2012).

b. The CPRS surface units

The industrial units of the CRPS are mainly installed on the oil field collection and transport pipelines to solve deposition and corrosion problems and improve water quality. The systems are mainly installed on ground pipelines and are called "surface units."

Figure I.54: The CPRS surface unit

Applications

The CRPS surface units are suitable for:

- Oil field collection and transport pipelines or water injection lines to solve paraffin, scale, and corrosion problems.
- Industrial heated water or cooling water circulation loops in petrochemical and chemical plants, power stations, iron and steel plants and other industrial facilities for the prevention and disposal of scale, corrosion and improvement of water quality.

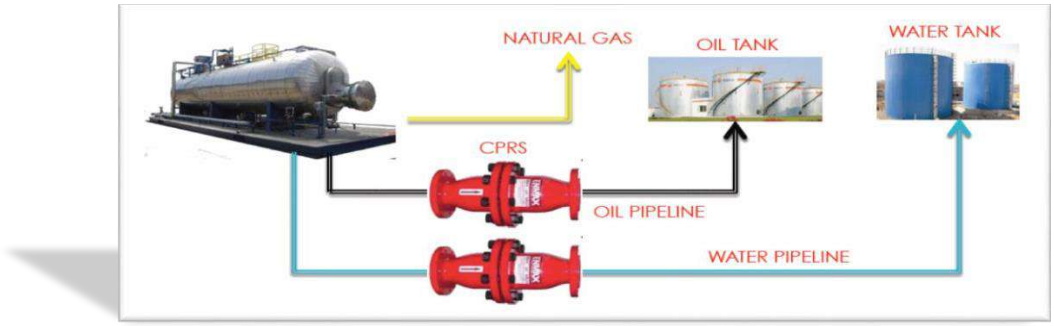

Figure I.55: Using of ENMAX in the transportation of oil fields.

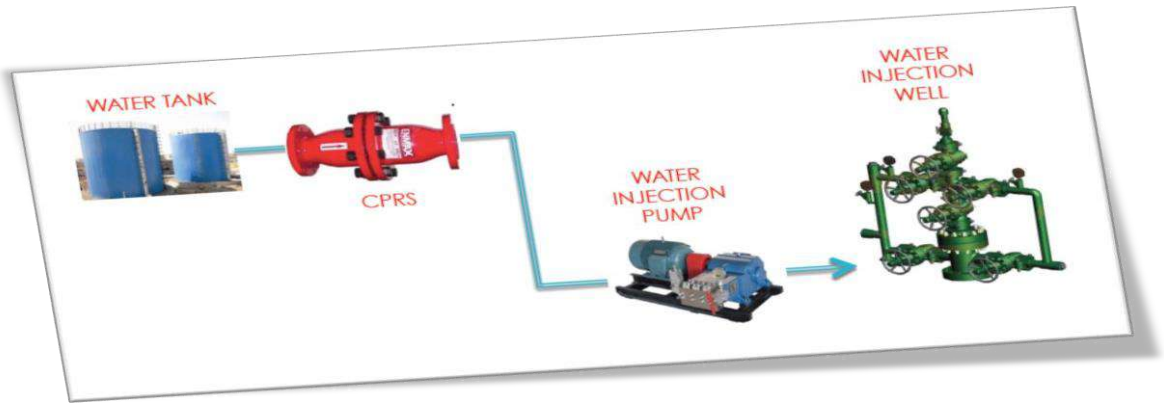

Figure I.56: Using of ENMAX in water injection

Installation

CPRS units can be installed on the mainline or bypass line. The units are delivered with complementary flanges at each end, with a complete set of bolts and caps, the installation on-site will be very easy and simple.

Figure I.57: Installation of ENMAX

Chapter II : Methods, Products and Equipment

II.1 Introduction

In order to realize the present thesis, we have adopted the following methodology:

- Sampling of reservoir, injection and mixed water.
- Sampling of deposits from different points of wells and several zones of the HMD field.
- Analyses of samples using different methods.
- Interpretation of results of analyses using the classical method.

It should be noted that the fieldwork has been carried out at Sonatrach company. And for sample analyses, it has been realized in Sonatrach and the geology of Sahara laboratories.

II.2 Water analysis

II.2.1 SDI measurement for Albian wells

$$\text{SDI} = \left(1 - \frac{t_i}{t_f}\right) * \frac{100}{T} \qquad \text{II.1}$$

t_i =initial time in seconds required to collect 500 ml of sample.

t_f = Final time in seconds required to collect the second sample after the test time.

T=total test time (15 min).

Figure II.1: Measure SDI of well

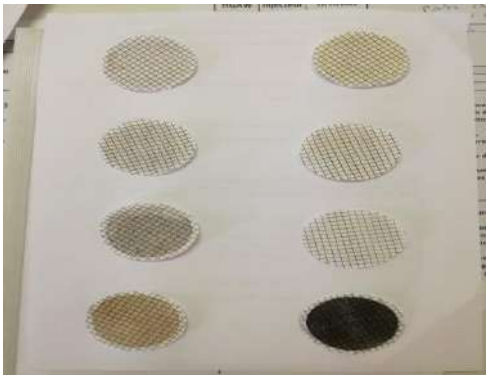

Figure II.2: membranes of SDI

II.2.2 Sample Preparation

The samples were filtered through a 0.2 µm Pall IC Acrodisc syringe filter, prior to all analyses except the determination of total species concentrations.

II.2.3 Methods

pH by pH electrode

The pH was determined by potentiometer measurement using a Multiline Sen Tix 41 combined pH electrode with integrated temperature probe. The electrode consists of a glass electrode and a reference electrode in a single unit. Hydrogen ion activity is registered via a hydrogen sensor and the signal is converted to a digital read out by the pH-meter. The temperature at which measurements were made was recorded.

Density by Density Meter

Density was measured using an Anton Paar DMA-4500 density meter.

Chloride by Potentiometric Titration/ volumetric

Chloride (total halide) was determined by potentiometric titration on a Metrohm 888 Titrando using a Metrohm silver titrode and 0.1 M silver nitrate as titrant calibrated with a 1000 mg/l chloride standard.

Potentiometric Titration is an electrochemical measurement method involving an electrochemical reaction. This method used to measure chloride ions is based on the monitoring of the potential difference between two electrodes when adding a saturated solution of silver nitrate.

$$E = f\ (V_{added}\ \text{of}\ AgNO_3) \qquad \text{II.2}$$

This potential is directly related to the chloride ion concentration, which varies according to the following reaction:

$$\mathbf{Ag^+ + Cl^- \rightarrow AgCl\downarrow} \qquad \text{II.3}$$

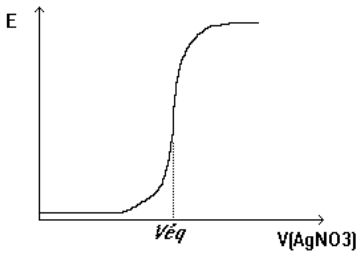

Figure II.3: Evolution of the potential according to the added volume.

Anions by Ion Chromatography

The anions of interest were separated from each other and other interferences by ion chromatography and detected by a combination of suppressed conductivity and UV.

Cations by ICP-OES and analysis of heavy metals by ICP-MS

All cations and elemental species were determined by ICP-OES using a Perkin-Elmer Optima 8300 instrument calibrated with certified standard reference materials.

Fluoride by Ion Selective Electrode

Fluoride was determined by ion selective electrode using a Thermos Scientific Orion 4 Star bench top ion meter and Thermos Scientific fluoride selective electrode, calibrated with standards prepared in TISAB.(Basset, 1978).

Turbidity

Turbidity was measured on a HACH Turbidimeter, wavelength 860 nm.

FNU stands for Formazin Nephelometric Units and signifies that the instrument is measuring scattered light from the sample at a 90-degree angle from the incident light. Method is based on NSEN ISO 7027.

Total Suspended Solids (TSS) by Filtration / Gravimetry

TSS was determined through the filtration of a known mass (weighed accurately to 0.1 mg) of shaken sample through a weighed filter (0.2 µm).

Total Dissolved Solids (TDS) by Evaporation / Gravimetry

TDS was determined through the evaporation of a known mass of filtered (0.2 µm) sample, sequentially at 110ºC, 140ºC and 180ºC.

Calcium, magnesium, and iron by complexometric

The complexometric method is used to determine the alkaline cations Mg^{2+} and Ca^{2+}, The specific-coloured indicator used in this assay is Eriochrome Black T. It is complex with these cations and gives the solution a red coloration. The introduction of ethylene-diamine-tetra-acetic acid (EDTA) leads to the formation of the EDTA-metal complex. As EDTA is added, the metal becomes detached from the indicator. At the equivalence, the whole indicator is in free form in the medium and takes a blue coloration. This colour change, therefore, indicates that all metal cations have been complexed mole to mole by EDTA.

The two reactions can be summarized as follows:

$$Ind^- + M^+ \rightarrow IndM \qquad \text{II.4}$$

$$IndM + EDTA \rightarrow M(EDTA) + Ind^-_{free} \qquad \text{II.5}$$

Thus, we can calculate the content of these two ions by applying the following relation:

$$[Ca^{2+}] = [EDTA].\ M_{Ca}.\ V_{eq2}/Vp \qquad \text{II.6}$$

$$[Mg^{2+}] = [EDTA].\ M_{Mg}.(V_{eq1}-V_{eq2})/Vp \qquad \text{II.7}$$

with M_{Ca} and M_{Mg} respectively, the molar masses of calcium and magnesium (Charlot, 1966)

sulphates by gravimetry

Sulphate ions are determined by gravimetry. This quantitative method consists in precipitating, in an acid medium, the sulphate ion by the barium ion in the form of barium sulphate according to the following reaction:

$$BaCl_2 + SO_4^{2-} \longrightarrow \underline{BaSO_4} + 2Cl^- \qquad \text{II.8}$$

The sulphate content is determined by measuring the mass of the barium sulphate precipitate formed, previously dried in the oven at 110°C.

The sulphate concentration, expressed in g/L, is given by the following relationship (Skoog, 1997):

$$[SO_4^{2-}](g.L^{-1}) = \frac{m_{BaSO_4} \times M_{SO_4} \times 1000}{V_p \times M_{BaSO_4}} \qquad \text{II.9}$$

$$[SO_4^{2-}](g.L^{-1}) = \frac{m_{BaSO_4} \times 96{,}066 \times 1000}{V_p \times 223{,}426}$$

$$[SO_4^{2-}](g.L^{-1}) = \frac{m_{BaSO_4}}{V_p} \times 411{,}548 \qquad \text{II.10}$$

Determination of metallic elements by Flame atomic absorption spectrometry

Atomic absorption spectrometry allows the determination of many inorganic materials (Cd; K; Fe; etc.). It applies to the qualitative and quantitative analysis of approximately 70 elements. Its sensitivity, its speed, its simplicity, its exceptionally high selectivity, and the moderate cost of its equipment are all additional advantages of this method (Skoog, 1997).

When an atom is excited by an input of energy, the electrons of the outer layer of this atom can go from an E_0 energy state to a higher energy state E_1, being able to take only a discontinuous sequence of values, following quantum theory. These electrons then jump to an unstable higher level, further away from the nucleus, and they tend to return to their initial level by a transition during which they emit a photon of energy E defined by the relation:

$$\mathbf{E = E_1 - E_0 = h\upsilon = hc / \lambda} \qquad \text{II.11}$$

with:

h: constant of Planck;

c: the speed of light;

λ: the wavelength associated with the photon;

υ: the frequency of radiation associated with the photon.

Atomic absorption spectroscopy is based on the principle that a population of atoms in the E_0 state can absorb photons of hυ energy and that an estimate of the number of photons absorbed can be related to the concentration of the element in the solution to be analysed. Figures II-4 and II-5 show the principle of atomic absorption (Skoog, 1997).

I_0 : incident intensity

atomic cloud

I : transmitted intensity

Figure II.4: General principle of atomic absorption.

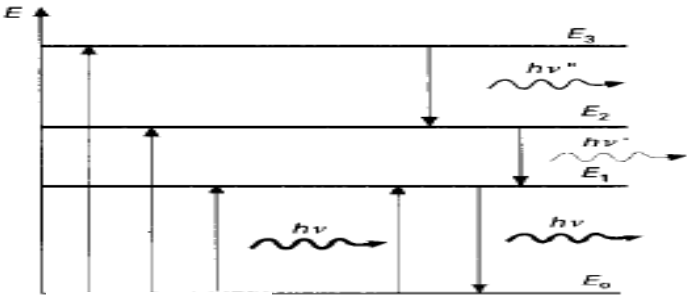

Figure II.5: Simplified diagram of possible energy levels and transitions.

The main components of a flame atomic absorption spectrometer FAAS are:

A source of light: A hollow cathode lamp is used. Its role is to produce light radiation at the wavelength characteristic of the element to be measured (emission line). The photons emitted will be partially absorbed by the atomic cloud created in the atomizer.

A light modulator: It allows for eliminating parasitic lights due to the flame.

A flame atomizer: It consists of a nebulizer that transforms the sample into a fog or aerosol. Then, it injects into a burner.

A monochromator is used to eliminate all radiation other than the λ_0 wavelength.

A detector coupled to an electronic system to record and process signals.

Besides these essential elements, we find one or other complement according to the degree of development of the device. These are:

- A light beam divider in dual beam devices.
- A corrector of non-specific absorptions.
- A system for visualizing specific and non-specific signals (Skoog, 1997).

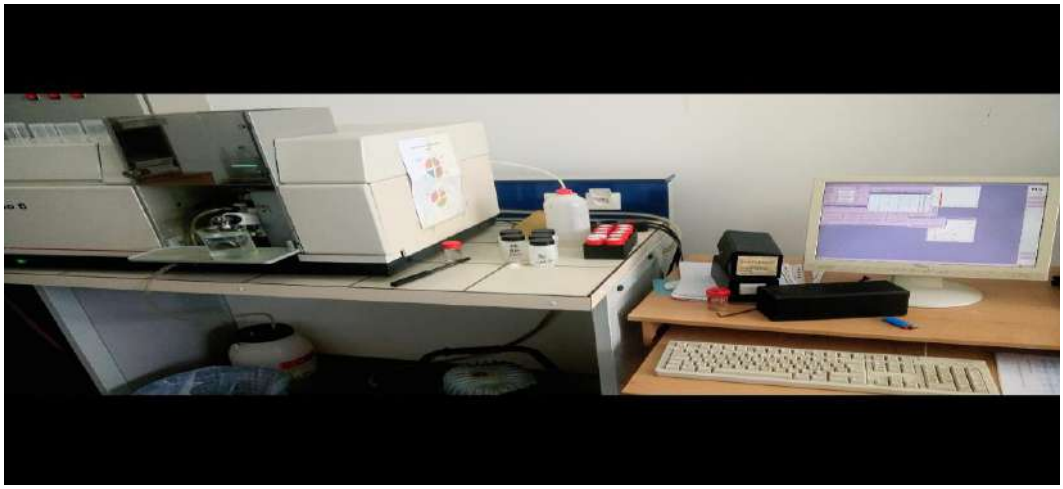

Figure II.6: FAAS apparatus

UV–visible spectrophotometry

Quantitative analysis of monophosphates can be performed by measuring the amount of light absorbed by the solution (phosphate solution with yellow vanadomolybdic reagent).

A light beam of wavelength λ passing through a solution of thickness l and concentration c in an absorbing compound, the absorbance or optical density of this solution is given by the law of Beer-Lambert:

$$D = \log I_0 / I = \varepsilon . l . c \qquad \text{II.12}$$

with ε: molar extinction coefficient or absorptivity (Standard methods for the examination of water and wastewater, 1995).

II.2.4 Water compatibility test under surface conditions

A water injection process was successfully performed when the identification of the source of water, water quality considerations, and laboratory compatibility tests were considered.

When different waters are mixed, it is necessary to evaluate their compatibility prior to the injection into oil wells. A conventionally test performed in the laboratory to estimate formation damage by scale formation in the wellbore and facility. The individual waters may be quite stable under all system conditions and present no scale problems. However, once they are mixed, the reaction between ions dissolved in the individual waters may form insoluble products that cause permeability damage in the vicinity of the wellbore. The obtained results from the test for different mixtures of waters can be used to know the type of scale in the reservoir, composition of mineral scales that occur in a raw water, and different volume mixings.

sampling method

- Purge the sampling valve with a high constant flow rate to eliminate all accumulated deposits.
- Fill the polyethylene vial, which is rinsed with distilled water, and let it overflow at least three times.
- Rinse the cap and close the bottle.
- Label the bottle with the point (wellhead, separator outlet, etc.), date, and time of sampling.
- Specify sampling temperature and pressure.

Figure II.7: sampling method.

Test method

- Place the nine (09) beakers labelled on the multi-posted stirring plate.
- Put the injection water in the beakers from the first to the last: 10ml, 20ml,30 ml….. 90ml, and agitate them on the multi-post stirrer.
- Add reservoir water (90ml, 80ml, 10ml) to these beakers from first to last.
- Keep beakers in continuous agitation for one hour and then let them rest for one hour.
- Filter each solution through an ash-free filter using the filtration device.
- Place the filters containing the precipitate in platinum crucibles that have been previously washed hot with hydrochloric acid, rinsed with distilled water, put in the oven at 850° C for 20 minutes, cooled in a desiccator for 20 minutes, and then weighed.
- Calcine the precipitate at 850°C for 30 minutes.
- Remove from oven, leave in a desiccator for 20 minutes and weigh it.
- Deduct the critical rate of deposition: The rate of mixing where the maximum weight of deposits has been obtained.
- Analyse the filtrate to determine the content of $Ba^{++}$by gravimetry procedure.

Figure II.8: Steps of water compatibility test

II. 3 Treatment product compatibility test

To prevent problems that may arise from using two or more products at once, a compatibility study between products used simultaneously in oil production is necessary. Possible incompatibility between two or more products may lead to production problems (foaming, deposits, loss of efficiency, and clogging of pipes).

We will present the results of compatibility testing of three treatment products currently in use in the HMD filed. This study is about the corrosion inhibitor Cortron CP 7130 of the firm Champion Technology, the bactericide FQS THPS 75 of FQS, and the anti-deposit INHIPOL AD32 of CECA.

Method of test

The method used is that proposed by the IFP, which consists of mixing equal volumes of the products under test conditions and studying the behaviour of the mixture after one minute, 03 hours, and 48 hours of contact.

The tests were conducted under ambient conditions at 04°C and 70°C.

II.4 Control of the concentration of the deposit inhibitor (AD32)

II.4.1 Principle of monitoring of concentration

The AD 32 inhibitor is based on phosphonates, so the method is based on the oxidation of phosphonates $(PO_3)^{3-}$ to phosphates $(PO_4)^{3-}$ using ammonium molybdate $((NH4)_6Mo_7O_{24}$, $4H_2O$ in the presence of potassium antimony tartrate $KSb_5C_4H_4O_6$), a blue complex appears, which is absorbed by a spectrophotometer at a wavelength of 640nm.

II.4.2 Procedure of monitoring of concentration

Oxidation of phosphonates

In a beaker, add to the test sample 3ml of H_2SO_4 10N and 1ml of $KMnO_4$ 0.2N, then, complete to 50ml with distilled water and heat the solution until a brown precipitate appears.

$$2KMnO_4 + 3H_2SO_4 + 5(PO_3)^{-3} \longrightarrow 2MnSO_4 + K_2SO_4 + 5(PO_4)^{3-} + 3H_2O \quad \text{II.13}$$

$$2KMnO_4 + H_2SO_4 \longrightarrow K_2SO_4 + Mn_2O_7 + H_2O \quad \text{II.14}$$

$$Mn_2O_7 \longrightarrow 2MnO_2 + 3/2\ O_2 \quad \text{II.15}$$

Figure II.9: Oxidation of phosphonates

Discoloration of the solution

The brown precipitate hinders the analysis; therefore, it will be discoloured by a few drops of ascorbic acid $C_6H_8O_6$, 4%.

$$5(2MnO(OH)_2 + 2H_2SO_4 \longrightarrow 2MnSO_4 + O_2 + 4H_2O \quad \text{II.16}$$

$$C_6H_8O_6 + 5O_2 \longrightarrow 6O_2 + 4H_2O \quad \text{II.17}$$

$$10MnO(OH)_2 + 10H_2SO_4 + C_6H_8O_6 \longrightarrow 10MnSO_4 + 6CO_2 + 24H_2O \quad \text{II.18}$$

Transfer the solution to a 50ml volumetric flask, add 5ml of ammonium molybdate (2%) and 4 ml of the reducing solution (50% Antimony potassium tartrate and 50% ascorbic acid); a blue complex is obtained.

$$(NH4)_6Mo_7O_{24},4H2O + C_6H_8O_8 + KSbC_4H_4O_6 + PO_4^3 \longrightarrow$$

$$(NH4)_3PO_4.4MO_3O8.12\ H_2O.\ \text{(Phosphomolybdic complex)} \quad \text{II.19}$$

leave for half an hour and proceed to the photo colorimeter (wavelength = 650 nm). We note the zero with distilled water, then we take the value of the absorbance of the sample and then the concentration.

Figure II.10: Discoloration of the solution and Control of the anti-deposit concentration by the UV-Visible specctro-photometer

II.5 ENMAX tool

There is currently a critical problem in the Hassi Messaoud field due to the formation of barium sulphate and asphalt in wells and networks. Due to the previous problem The ENMAX tool has been installed for a free trial period in the 6" flow line of well MD-411 and in the 8" main line of manifold E1B to satellite E1C to evaluate the performance and efficiency of this device.

the evaluation of ENMAX includes the following elements:

- ***The pressure and the daily flow upstream and downstream of the tool.***
- ***Laboratory Analysis of Sample.***
- ***Analysis of deposit coupons upstream and downstream of ENMAX.***

II.6 Deposit analysis

II.6.1 laboratory analysis protocols

acid attack

- Wash, dry and grind the sample,

Figure II.11: Acid attack- step 1.

- Take 1g of the sample in 100 ml of Aqua Regia and evaporate the solution completely.

Figure II.12: Acid attack- step 2.

- Add 20 ml of HCl and evaporate dry, then 10 ml of distilled water boil for 1mn.

Figure II.13: Acid attack- step 3

- After filtration, the precipitate is kept, and the filtrate is reduced to measure calcium, magnesium, iron, sulphates, phosphates, sulphides, sodium, etc.

Figure II.14: Acid attack- step 4

Alkaline attack

- Insoluble residue is calcined in a muffle oven at 800°C in a platinum crucible.

Figure II.15: Alkaline attack- step 1

- Weigh the contents of the crucible

Figure II.16: Alkaline attack- step 2

- Add sodium carbonate. Melt in the oven. Remove the crucible and let cool in the desiccator.

Figure II.17: Alkaline attack- step 3

- Boil distilled water in a beaker.

Figure II.18: Alkaline attack- step 4

- Put the crucible in the beaker and boil it until the calcination dissolved in the water.

Figure II.19: Alkaline attack- step 5

- After filtration (the filtrate contains silica and sodium sulphate and the filter contains the barium carbonate).

Figure II.20: Alkaline attack- step 6

- After boiling, add H_2SO_4.A white precipitate is formed indicating the presence of barium sulphate.

Figure II.21: Alkaline attack- step 7

II.6.2 X-Ray Diffraction

The X-ray diffraction (XRD) allows for identifying the phases present in the sample by comparison with the international diffraction maps, determining the mesh parameters of a crystalline network and atomic positions, as well as, calculating the size d_{DRX} of crystals.

The sample is subjected to a monochromatic X-ray beam produced by a copper anti-cathode with wavelength λ=1.5418 A°, bombarded by electrons (emitted by a tungsten filament) accelerated under a voltage of 45 kV.

The diffractometer is equipped with Soller slits at the front of the sample holder rotating uniformly around an axis located in its plane, thus allowing to increase the number of possible rotations of the reticular planes in such a way as simultaneously obtain all susceptible beams to diffract.

The diffractometer is coupled to a microcomputer that allows the processing of diffractograms.

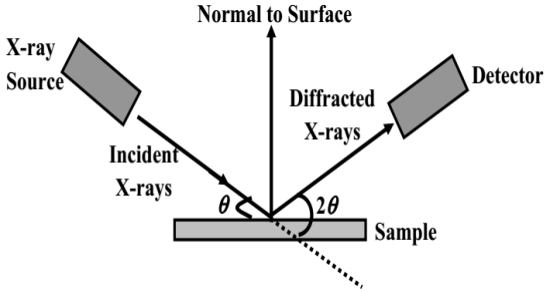

Figure II.22: XRD working principle

II.6.3 Scanning Electron Microscopy with Energy Dispersive X-Ray Analysis (SEM-EDX)

Scanning electron microscopy (SEM) is based on the principle of electron-matter interactions, capable of producing high-resolution images of the surface of a sample.

The SEM principle consists of a beam of electrons scanning the surface of the sample to be analysed, which re-emits certain particles. These particles are analysed by different detectors that allow to reconstruction a three-dimensional image of the surface.

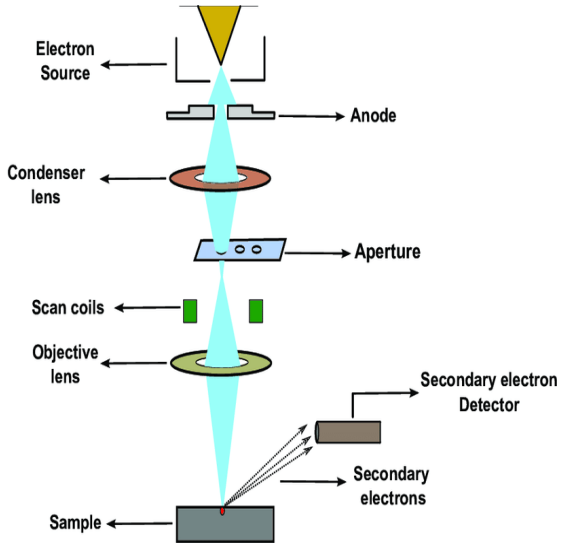

Figure II.23: SEM working principle

Chapter III : Results and Discussions

Part 1 : Albian, Cambrian, and Mixed Water Analysis (HMD field)

III.1 Albian water analysis

III.1.1 SDI results for Albian wells

The SDI (silt density index) is a technique for describing water's fouling tendency. The DuPont Company developed the test in the 1970s to perform the quality control of electronic grade water. The SDI is calculated by measuring the rate of plugging of a 0.45m pore size membrane during constant pressure (30 psi) filtration. Figure III.1 shows the standard SDI measurement apparatus.

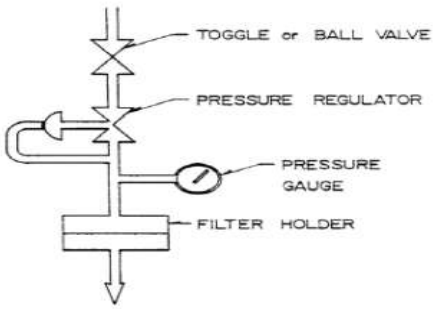

Figure III.1: Apparatus for measuring SDI.

To execute the calculation based on the following equation, several data points along the filter process must be recorded:

$$SDI = \frac{\%P30}{T} = \left(1 - \frac{t_i}{t_f}\right) * \frac{100}{T} \qquad \text{III.1}$$

The plugging rate of the membrane at 30psi pressure is shown in percent (P30%). The time parameter t_i is calculated as the amount of time it takes to collect the first 500mL of filtrate. After T (15 minutes) of filtering, the time t_f required to collect the final 500mL of filtrate is calculated. The SDI result is then calculated and displayed in percent every minute. Figure III.2 illustrates a schematic diagram of filtration showing the component of SDI calculation.

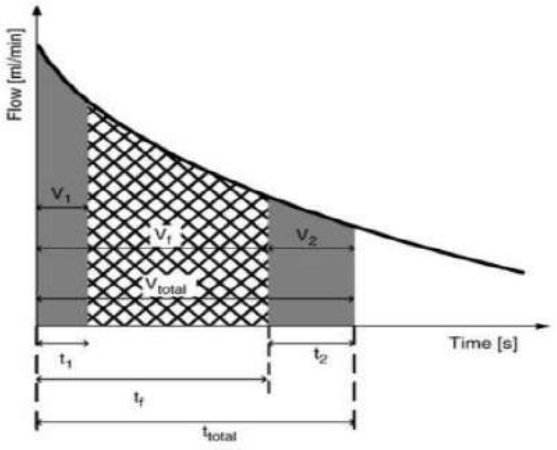

Figure III.2: Schematic diagram of filtration for SDI calculation.

For a specific type of water, parameter T is frequently reduced from 15 to 5 or 10 minutes; for example, salt water, which has a typical total plugging even before 15 minutes of filtration.

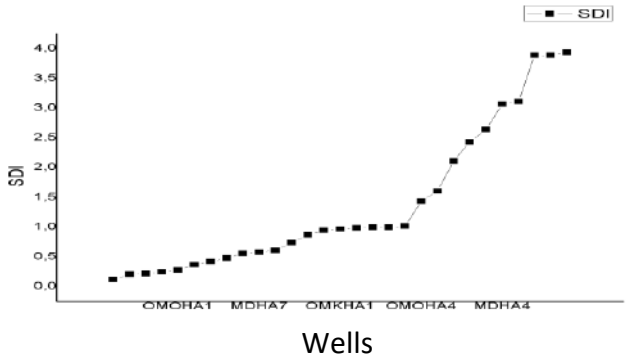

Figure III.3: SDI variation for different Albian wells in the HMD field.

the quality of water could be defined by the value of SDI, according to the following margin:

SDI (0-3): Non clogging water, can be used directly without specific treatment.

SDI (3-5): Low clogging water, requires the use of a physical treatment such as prefilters.

SDI >5: Highly clogging water, further water treatment is required like MFT and UF.

The nature of fouling prediction by SDI is relating the fouling occurrence of microfiltration membrane fouling during water sample filter. After filtration, the contaminated SDI membrane is shown in Figure III.4. The presence of particle foulant, as represented by the SDI, fouled the membranes generally by cake deposition on the membrane surface. A considerable amount of iron is present in Albian water, judging by the yellow colour of the foulant trapped on the membrane.

III.1.2 Monitoring the concentration of the various elements of Albian water in the HMD field

In this part, we try to monitor the variation of different elements that caused deposits in the field of HMD in the period (1994-2018). We chose several Albian wells from different points in this field. Results are shown in the following graphs.

1. **Well : MDHA 113 (1994-2018), depth : 1100 m.**

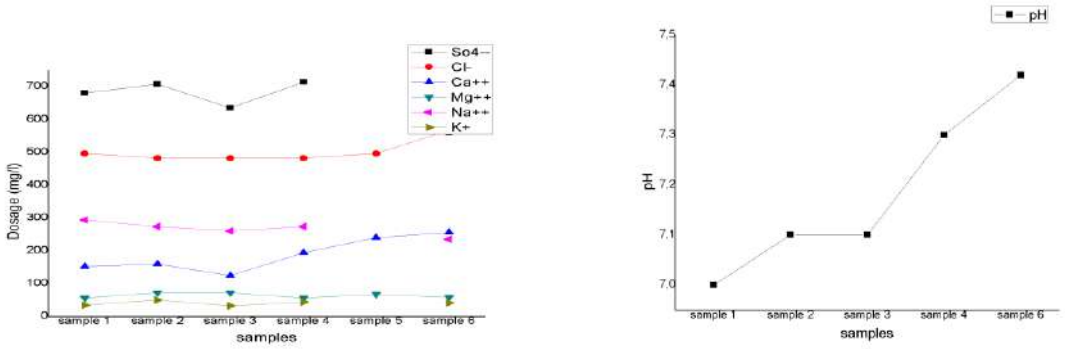

Figure III.5: Monitoring the concentration of the various elements of MDHA 113 well.

2. **Well: MDHA 115 (1994-2018), depth: 1100 m.**

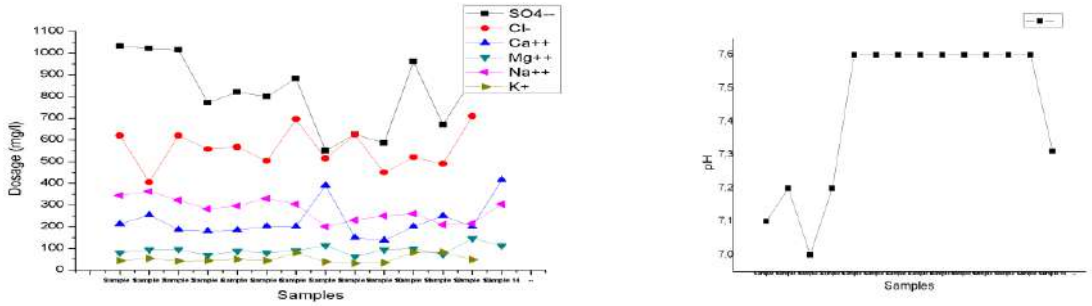

Figure III.6: Monitoring the concentration of the various elements of MDHA 115 well.

3. **Well: MDH 432 (1994-2018), depth: 1100m.**

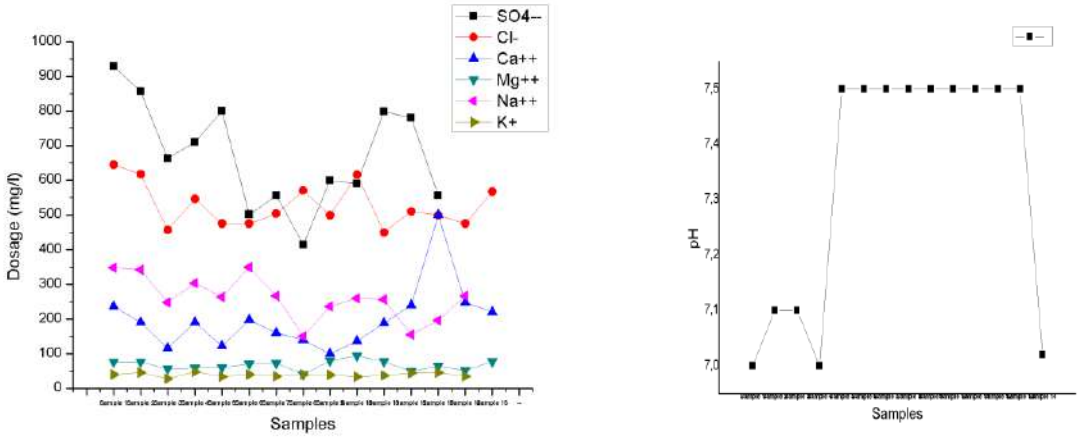

Figure III.7: Monitoring the concentration of the various elements of MDHA 432 well.

4. **Well: OMNHA 1 (1994-2018), depth: 1100m.**

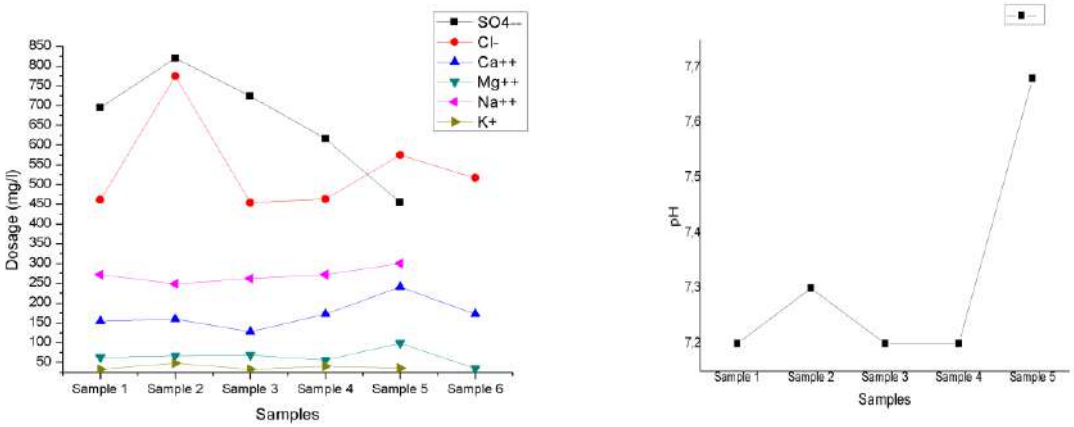

Figure III.8: Monitoring the concentration of the various elements of OMNHA 1 well.

5. **Well: OMNHA 2 (1994-2018), depth: 1100m.**

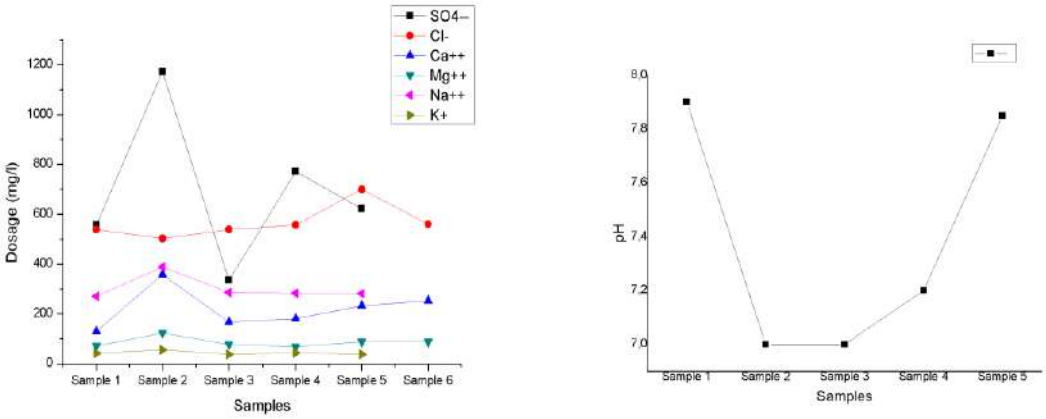

Figure III.9: Monitoring the concentration of the various elements of OMNHA 2 well.

III.2 Cambrian water analysis

III.2.1 Monitoring the concentration of the various elements of Cambrian water in the HMD field

In this part, we try to monitor the concentration of the various elements of water which sampled from 22 wells. The following figures represent the concentration of elements for each well.

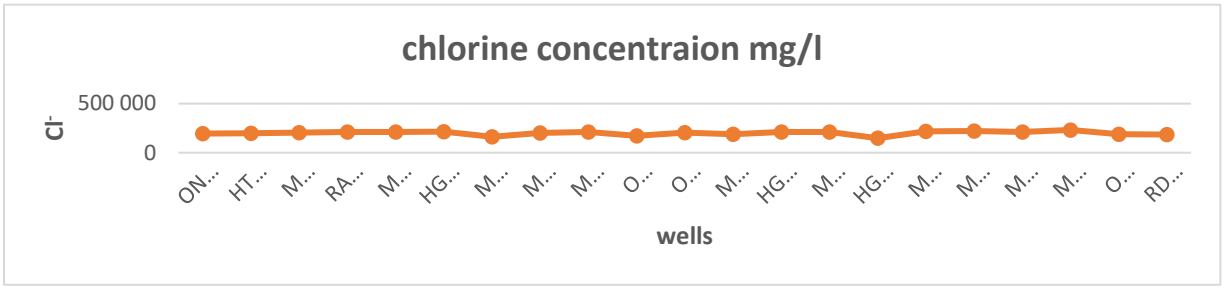

Figure III.15: Monitoring the concentration of chlorine for Cambrian water.

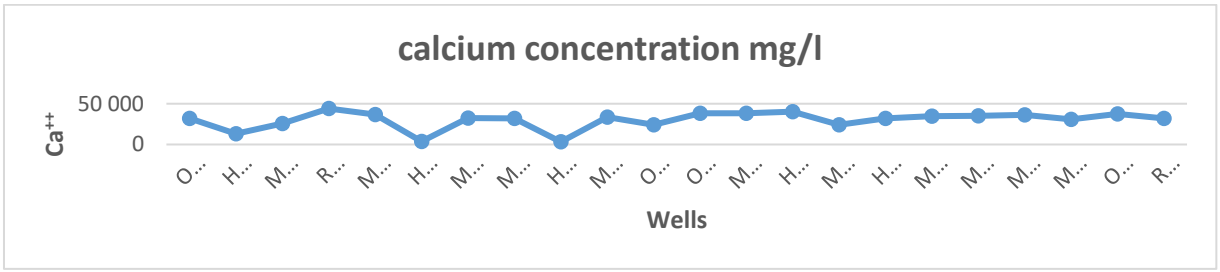

Figure III.16: Monitoring the concentration of calcium for Cambrian water.

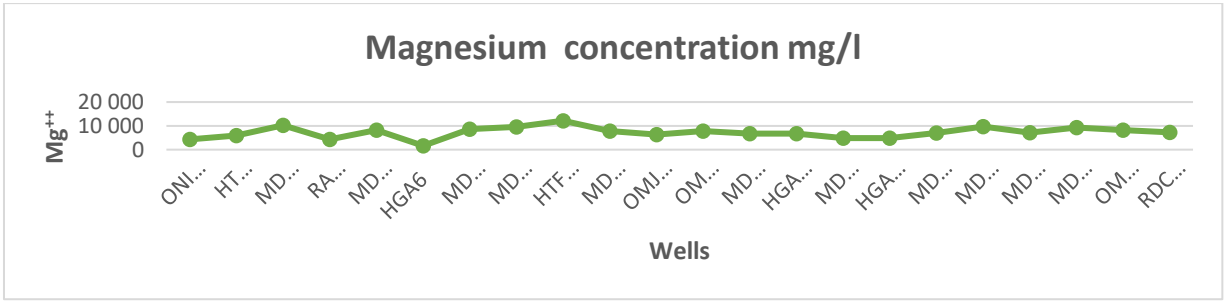

Figure III.17: Monitoring the concentration of magnesium for Cambrian water.

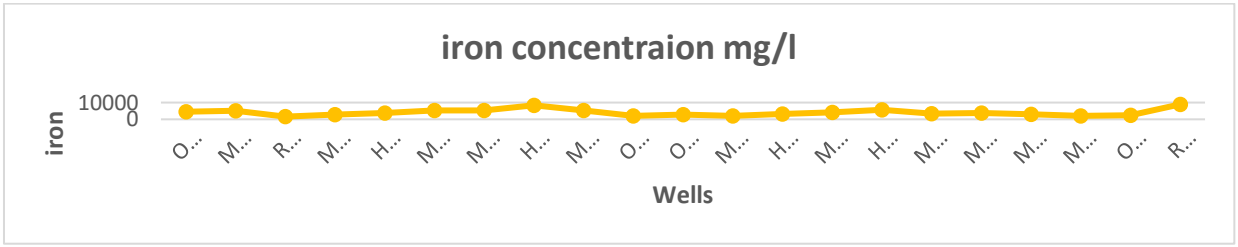

Figure III.18: Monitoring the concentration of iron for Cambrian water.

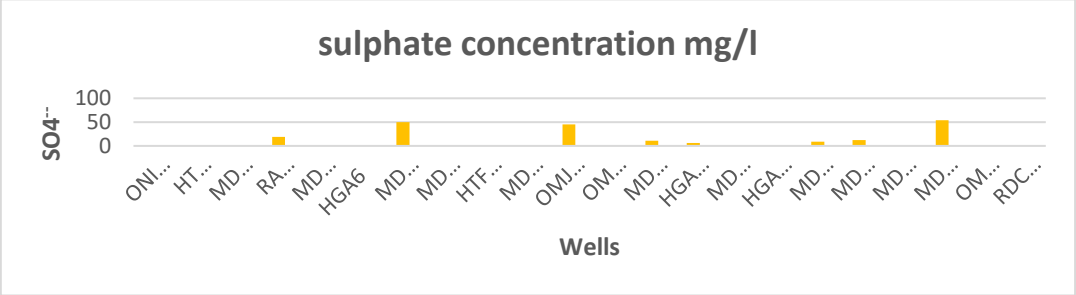

Figure III.19: Monitoring the concentration of sulphate for Cambrian water.

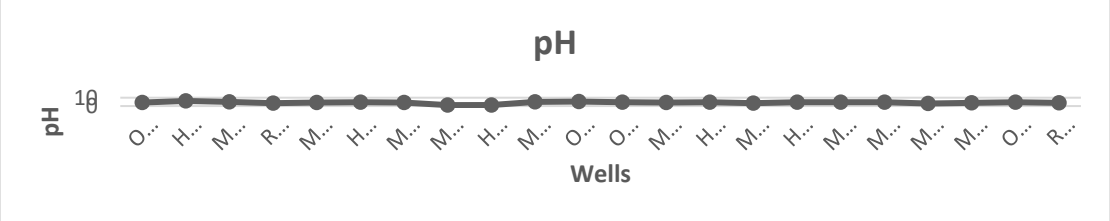

Figure III.20: Monitoring the variation of pH for Cambrian water.

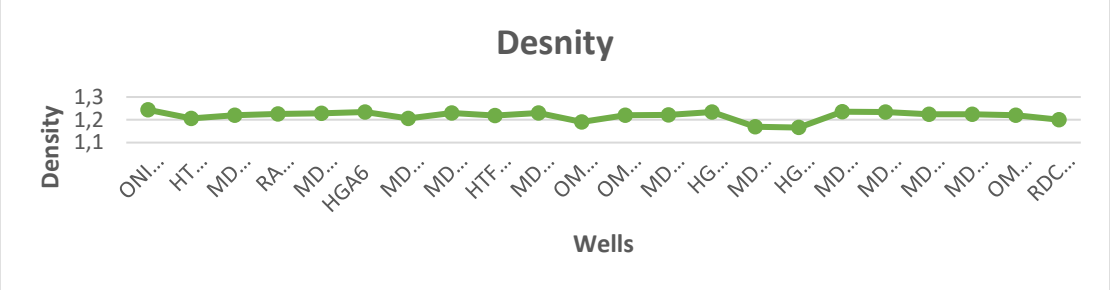

Figure III.21: Monitoring the variation of density for Cambrian water.

III.3 Cambrian/Albian mixtures analysis

III.3.1 Monitoring the concentration of the various elements of Cambrian/Albian mixtures water in the HMD field

In this part, we try to monitor the concentration of the various elements of water which sampled from 75 wells. The following figures represent the concentration of elements for different wells.

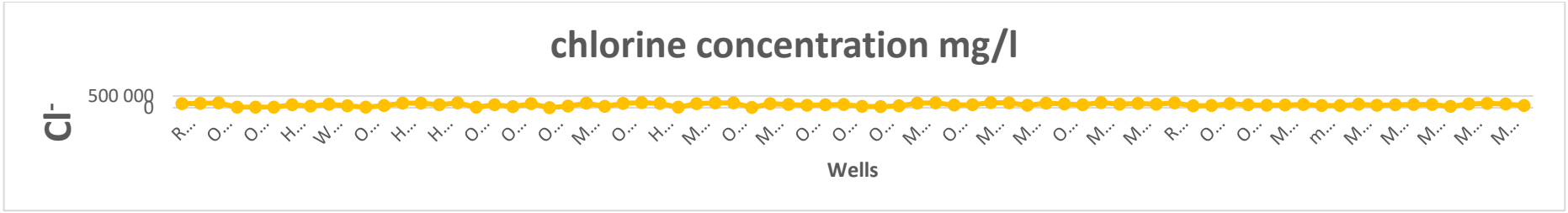

Figure III.25: Monitoring the concentration of chlorine for Cambrian/Albian mixtures water.

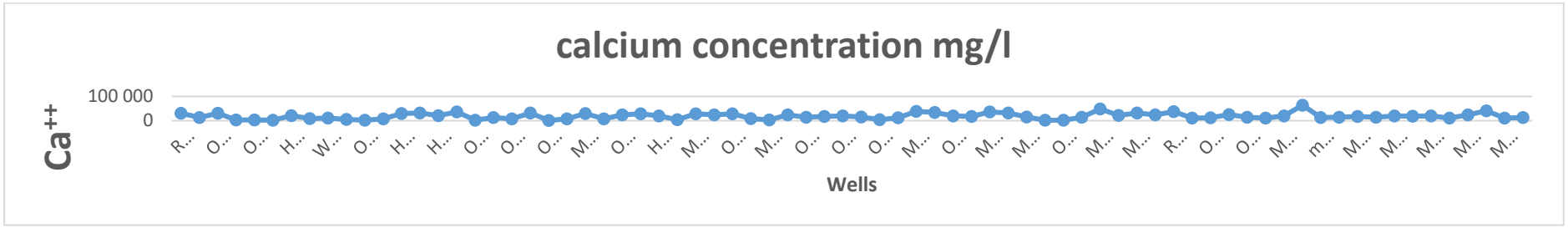

Figure III.26: Monitoring the concentration of calcium for Cambrian/Albian mixtures water.

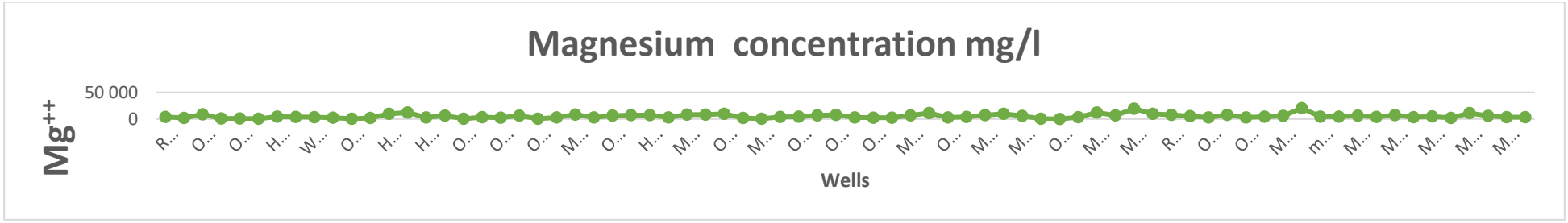

Figure III.27: Monitoring the concentration of magnesium for Cambrian/Albian mixtures water.

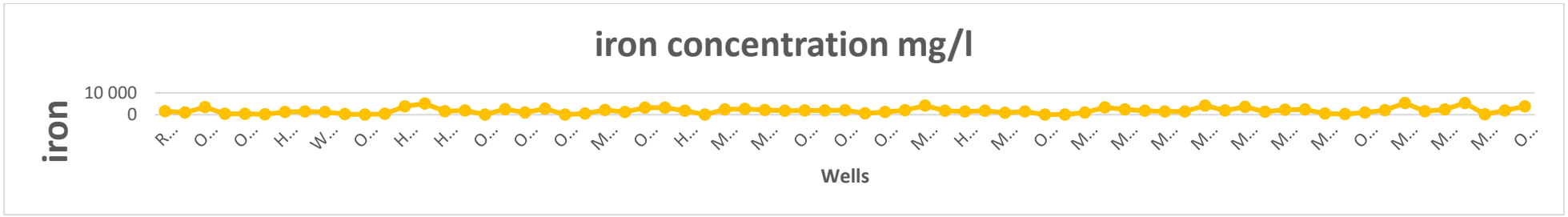

Figure III.28: Monitoring the concentration of iron for Cambrian/Albian mixtures water.

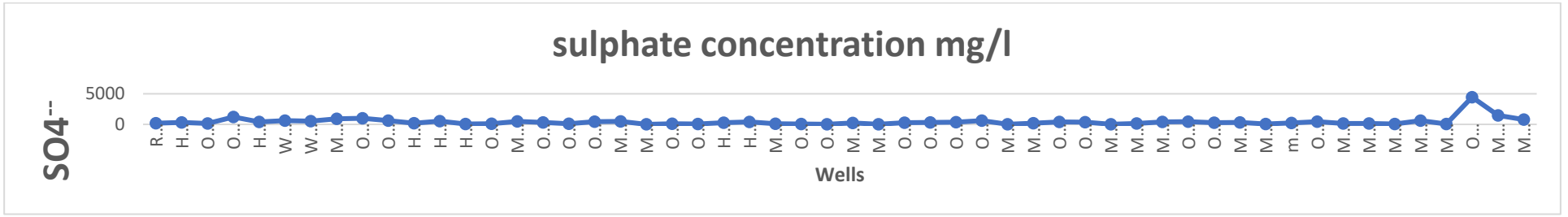

Figure III.29: Monitoring the concentration of sulphate for Cambrian/Albian mixtures water.

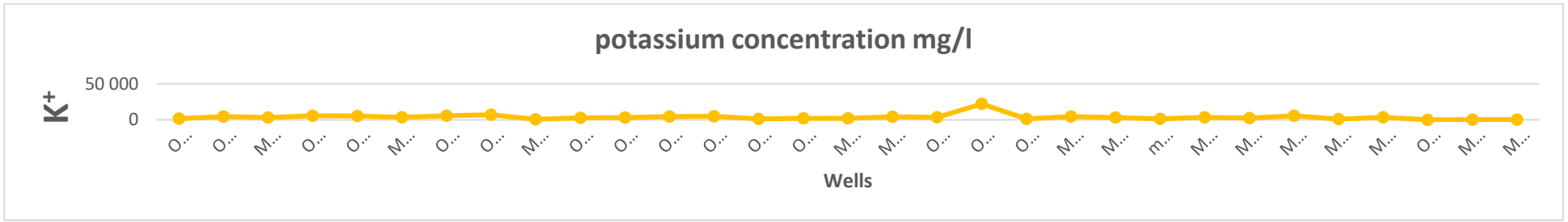

Figure III.30: Monitoring the concentration of potassium for Cambrian/Albian mixtures water.

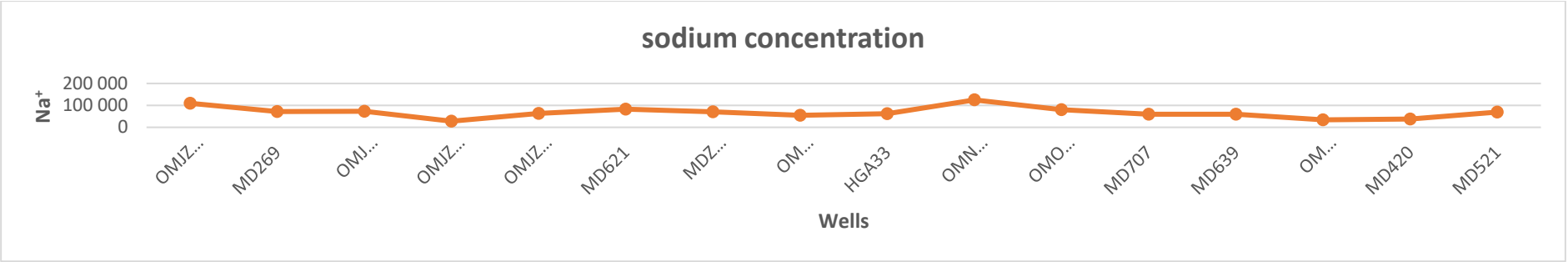

Figure III.31: Monitoring the concentration of sodium for Cambrian/Albian mixtures water.

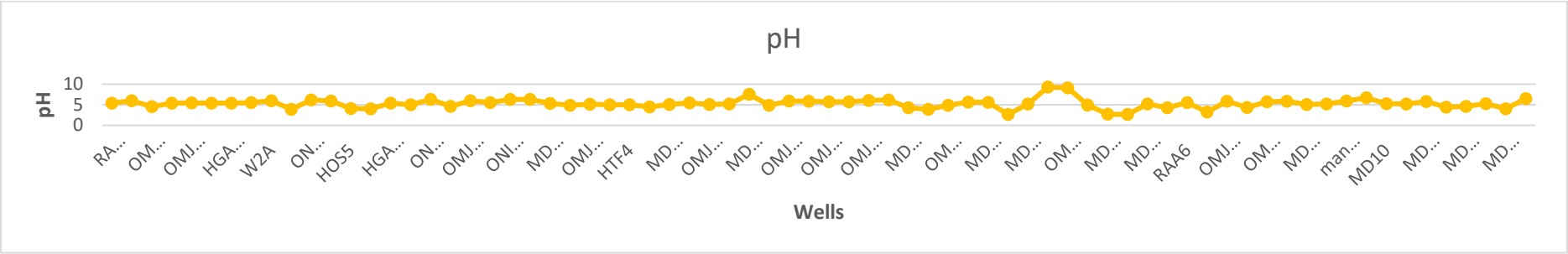

Figure III.32: Monitoring the variation of pH for Cambrian/Albian mixtures water.

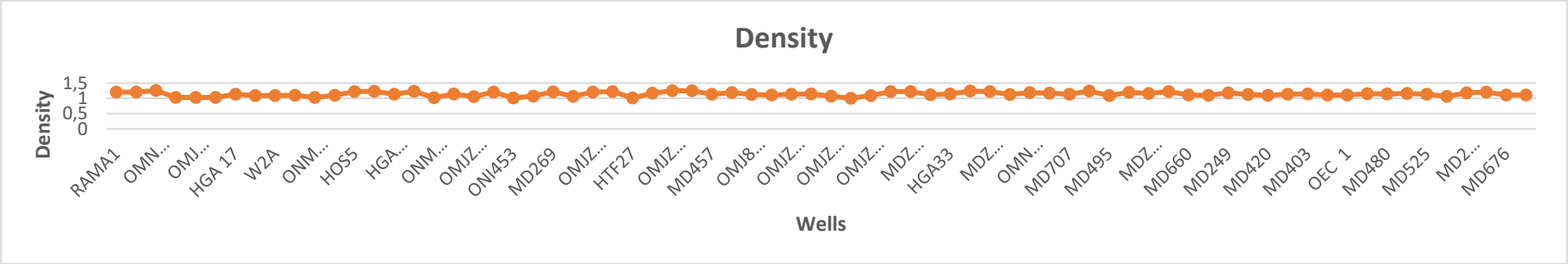

Figure III.33: Monitoring the variation of density for Cambrian/Albian mixtures water.

Part 2: Analyses of $BaSO_4$ deposits.

III.5 Analyses of deposit of MD 525 well

In this part, a deposit recovered from the MD 525 well production line will be analysed at the laboratory using the gravimetric method.

Figure III.39: MD 525 well deposit (Arbaoui, 2018).

The results of the analysis of the sample are summarized in the figure below.

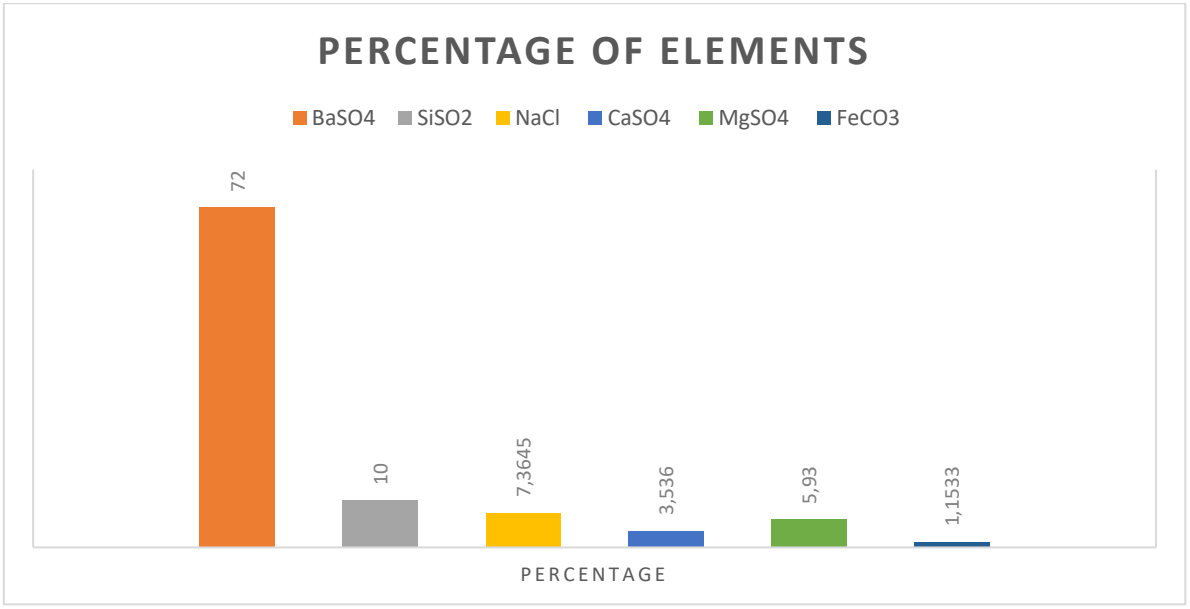

Figure III.40: Percentage of elements of MD 525 well deposit (Arbaoui, 2018).

Based on both qualitative (physical and chemical) and quantitative (acid attack and alkaline attack) analyses, the result confirms that the majority of deposition is $BaSO_4$.

III.6 Characterization of the scale

This study involved taking samples for analysis directly from several points in the field of HMD, E1B' surface, MFD E1C, Collector 14'', Zcina 30'' Valve, Line 6'' of MD 480, ONMZ 513 Wellhead, 2''7/8 liner of ONIZ 541 well.

III.6.1 XRD analysis

XRD analysis was conducted to verify the crystal phase formed in the different samples, and the measurement results were given in the form of intensity (peak). Radio crystallography analysis of the deposition samples revealed the following mineral phases:

- Sample N°1 : E1B' surface deposit.

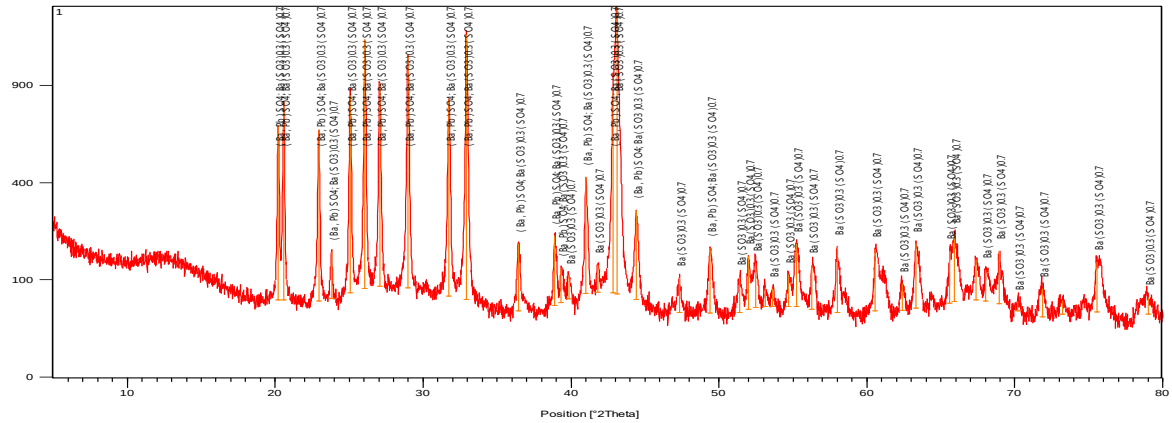

Figure III.41: XRD analysis of E1B' surface deposit.

- Sample N°2 : MFD E1C deposit.

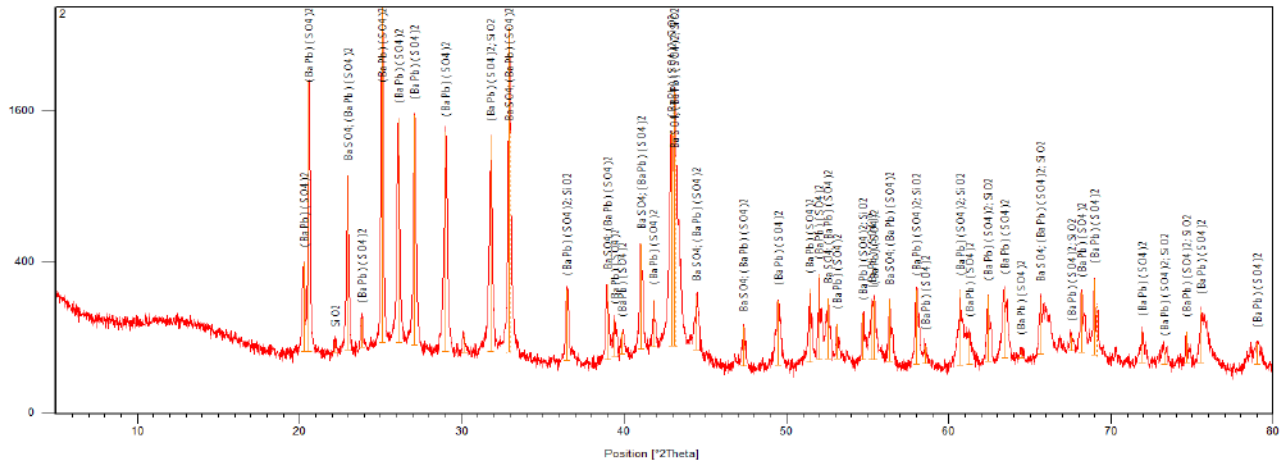

Figure III.42: XRD analysis of MFD E1C deposit.

- Sample N°3 : Collector 14''deposit.

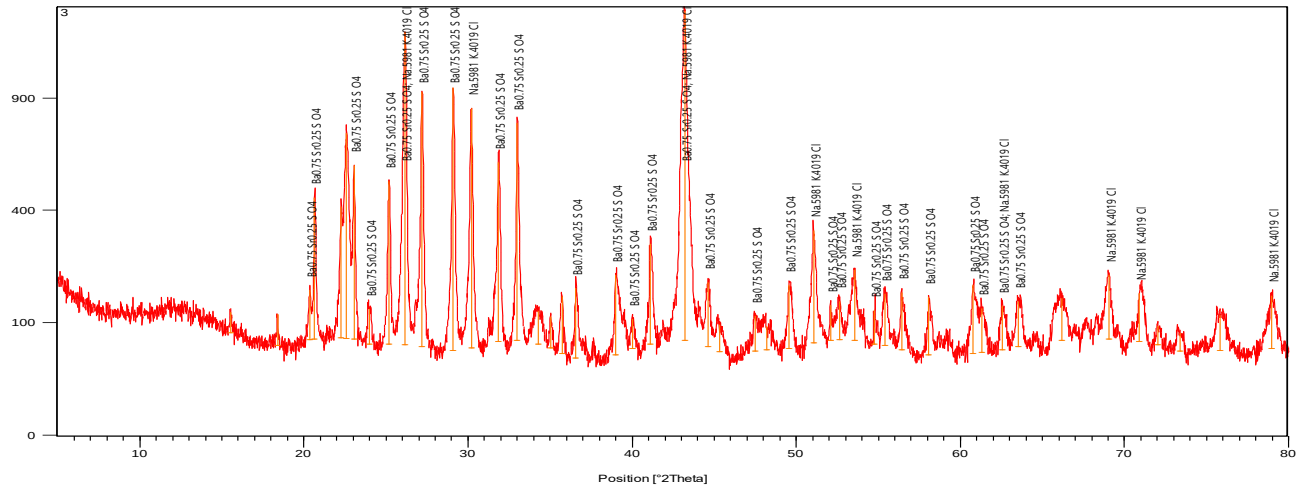

Figure III.43: XRD analysis of Collector 14''deposit.

Figure III.45: XRD analysis of Line 6'' of MD 480 deposit.

The scales on all the six filters are exposed to XRD analysis. The previous five figures provide direct experimental evidence of phase crystals formed in samples. The XRD spectrum contains intense peaks attributed to the barium sulphate $BaSO_4$ compound. In fact, the barite crystal sample is not the only mineral precipitated scales, therefore, we find other deposits such as SiO_2, NaCl, and KCl.

III.6.2 Scanning Electron Microscopy Analysis

The scaled core samples were examined by SEM to observe the particle size and morphology of the precipitates. The formation of $BaSO_4$ during flow of injection and formation waters in different equipment have been observed by Scanning Electron Microscopy (SEM). Detailed sample description and images performed on the solid sample by SEM-EDX analysis are shown below.

- Sample N°1 : E1B’ surface deposit.

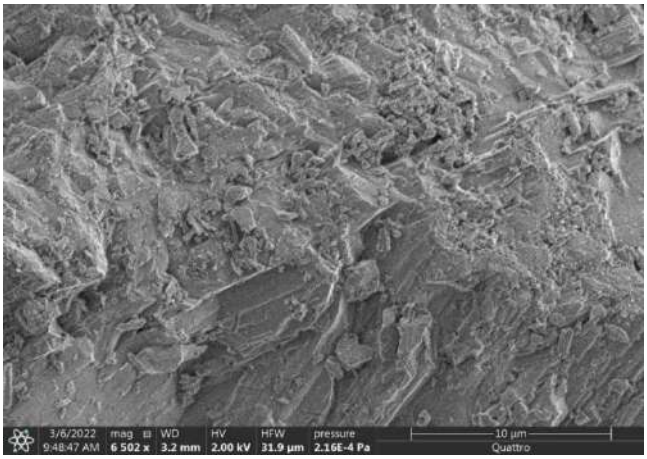

Figure III.46: SEM of E1B’ surface deposit.

- Sample N°2: Collector 14’’deposit.

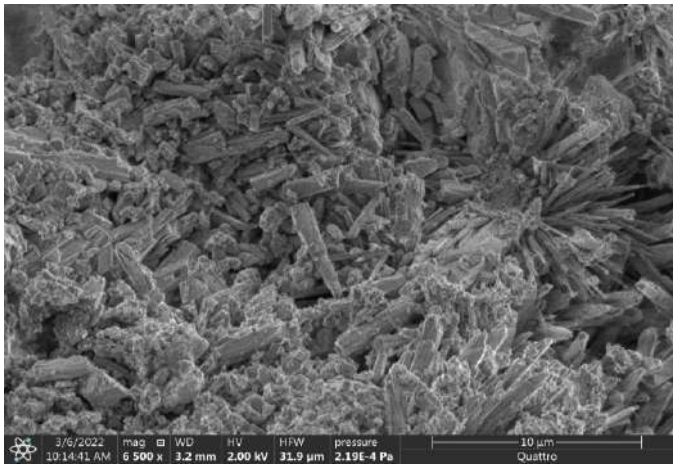

Figure III.47: SEM of Collector 14’’deposit.

- Sample N°3: Zcina 30’’ Valve deposit.

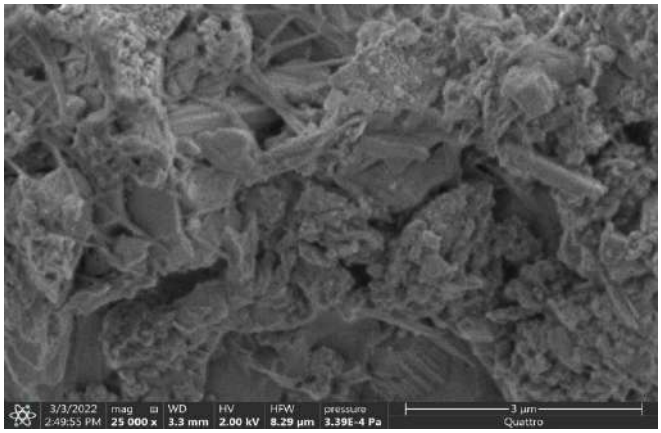

Figure III.48: Zcina 30’’ Valve deposit.

The previous figures show SEM images of scaling crystals precipitated from mixed injection water with formation water inside the production system in the field of HMD. the sample predominantly consists of barite, and minor amounts of quartz grains, $CaSO_4$ and $SrSO_4$ are observed.

III.7 Summary of deposit analysis results from 2009 to 2019 for the field of HMD.

The study of analysis of several deposits in the field of HMD in the period 2009-2019 helped in determining the predominant scales in this field, also zones and wells where each deposit is predominant. After monitoring deposits in the previously mentioned period, we draw the following graphs.

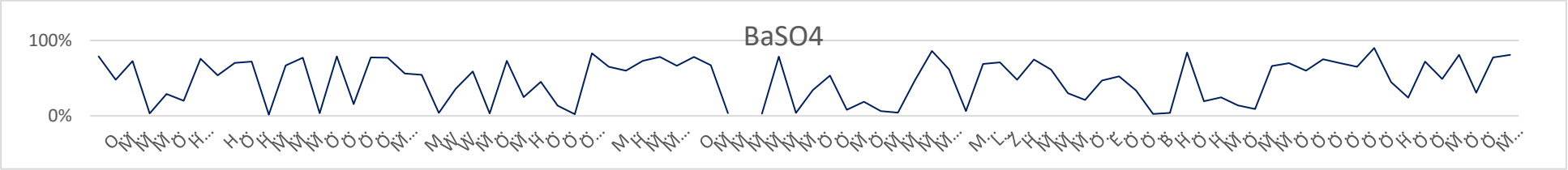

Figure III.51: $BaSO_4$ deposits in the HMD field.

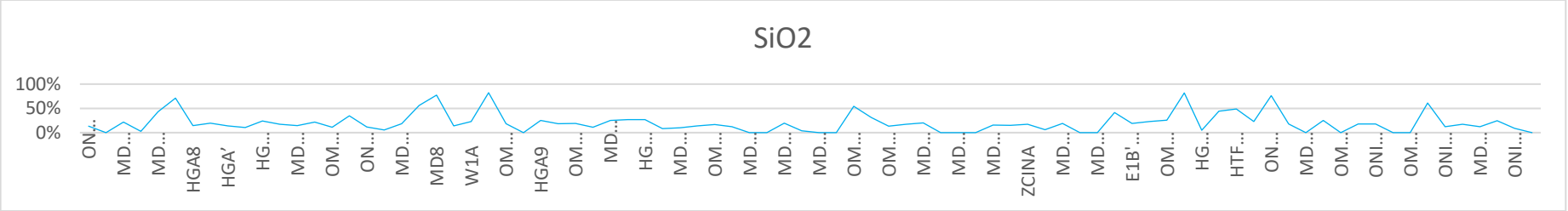

Figure III.52 : SiO_2 deposits in the HMD field.

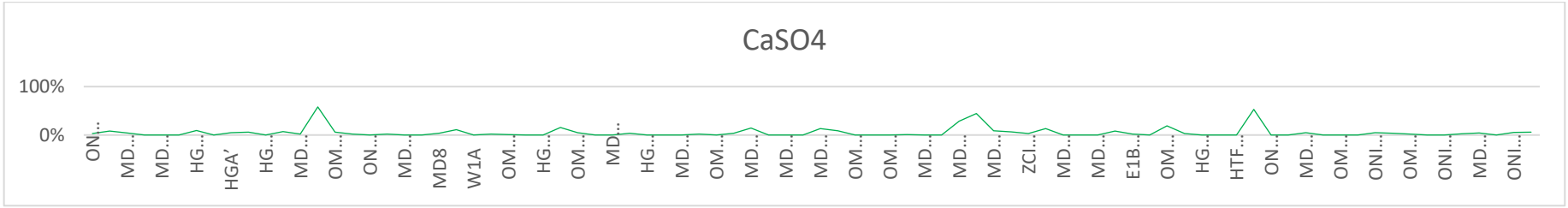

Figure III.53 : $CaSO_4$ deposits in the HMD field.

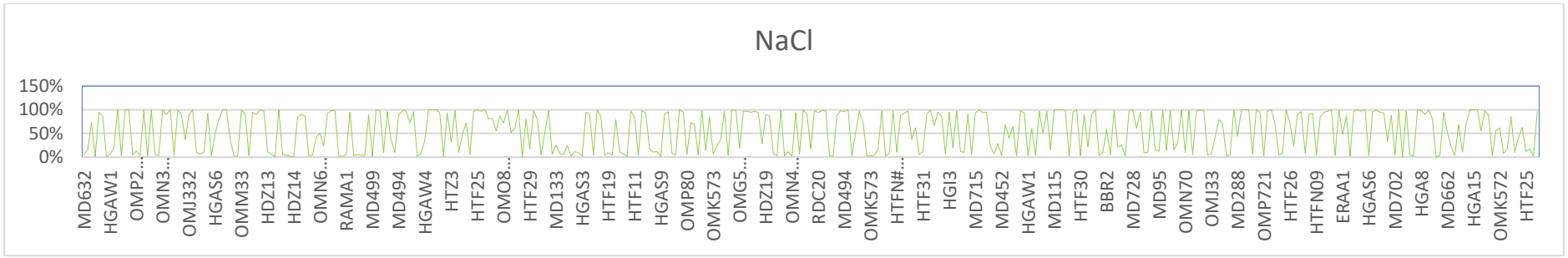

Figure III.54: NaCl deposits in the HMD field.

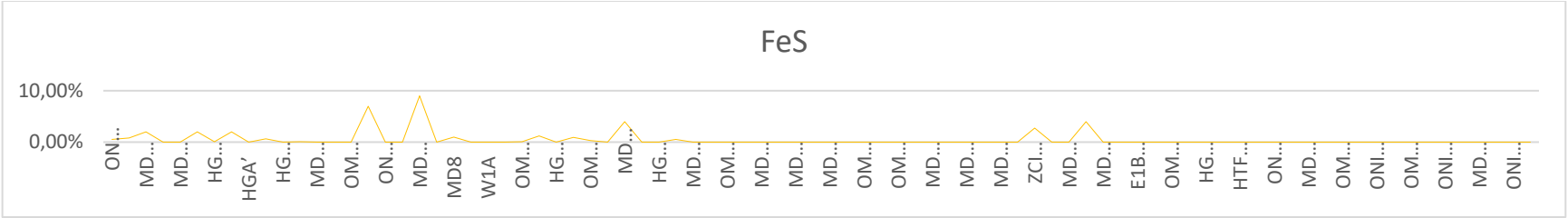

Figure III.55: FeS deposits in the HMD field.

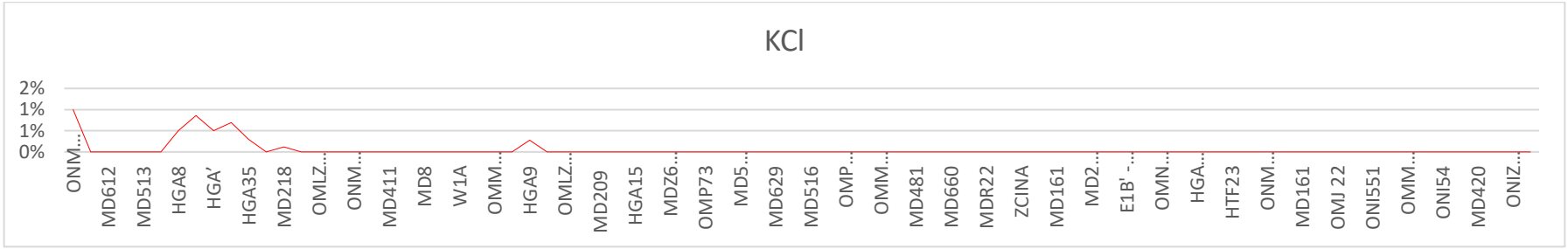

Figure III.56: KCl deposits in the HMD field.

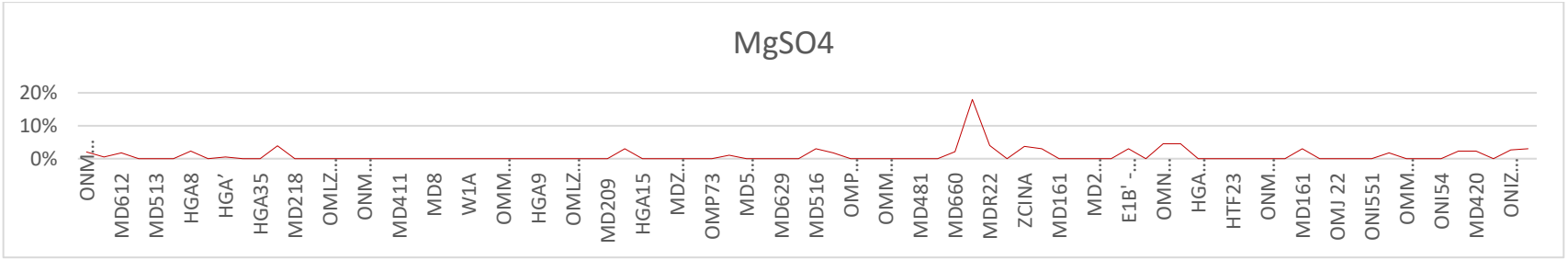

Figure III.57: $MgSO_4$ deposits in the HMD field.

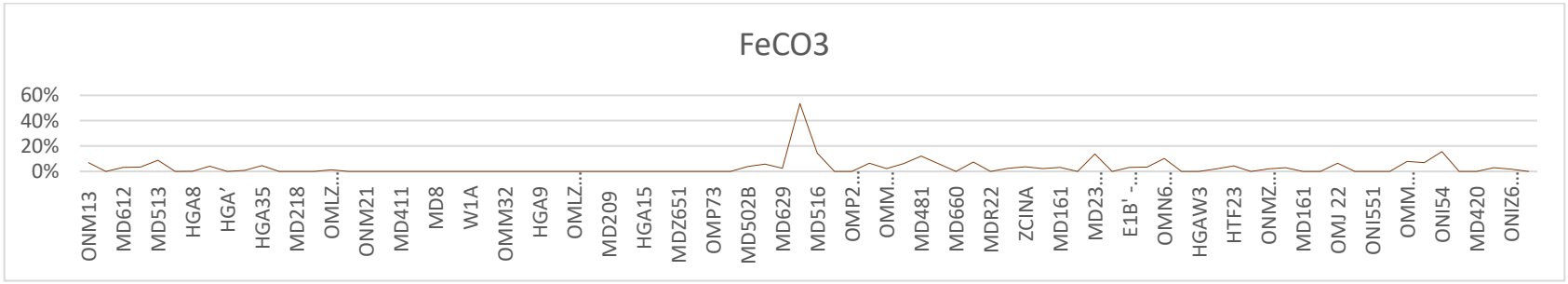

Figure III.58: $FeCO_3$ deposits in the HMD field.

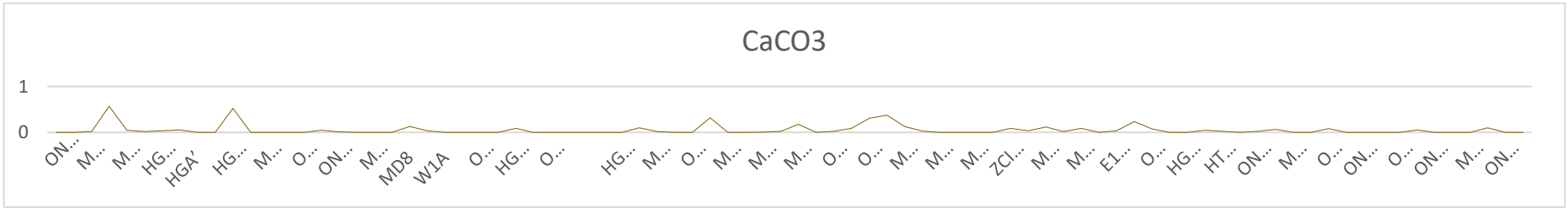

Figure III.59: $CaCO_3$ deposits in the HMD field.

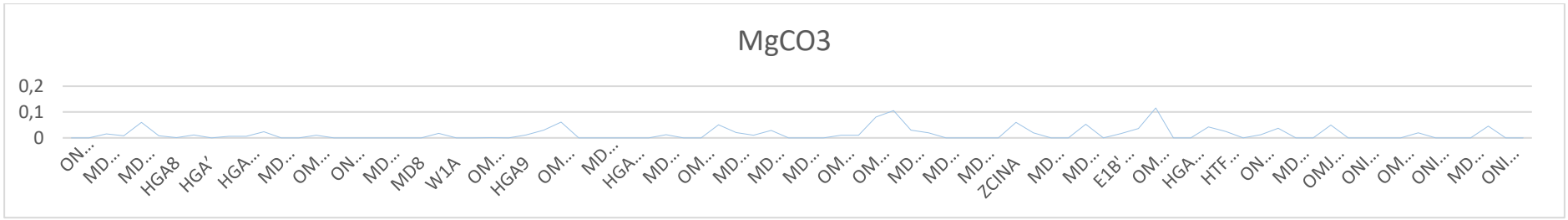

Figure III.60: $MgCO_3$ deposits in the HMD field.

According to the statics of the previous figure II.61, the predominant scale is NaCl deposit, where the majority of wells suffer from this problem, generally, they use a desalting system to avoid this deposit. The second deposit is $BaSO_4$ which represent the most dangerous and harmful one in a comparison with other deposits, actually they use inhibitors to treat this scale in HMD field. Other deposits represent minor percentage and less dangerous in this field.

Part 3: Treatment methods of $BaSO_4$ Deposition in the field of HMD

III.8 Treatments of $BaSO_4$ with AD 32 Inhibitor

The AD32 inhibitor is a deposition inhibitor used for the treatment of water circuits to prevent precipitation of calcium, strontium, barium, iron, and other cations salts in association with sulphates, carbonates, and oxides. The AD32 inhibitor is particularly recommended for crude oil lines and for water injection circuits to control the scale in tubing, pumps, and pipes. AD 32 Injected directly into the system to be inhibited, pure, or diluted in water, preferably in continuous injection using a dosing pump.

III.8.1 Monitoring of INIPOLE AD 32 in the HMD field

III.8.1.1 AD32 flow rate and consumption

The following table show the flow rate and consumption of AD 32 inhibitor for each station in the field of HMD.

Table III.6: Flow rate and consumption of AD 32 inhibitor for each station.

Station	**flow rate (m^3/h)**	**Consumption AD32 (l/min)**
Z14	28 - 30	0,09 - 0,1
CIS	4 - 8	0,01 - 0,02
W1C	12 - 16	0,04 - 0,05
HGA	5 - 10	0,021 - 0,042
CINA	26 - 28	0,08 - 0,09
ONI	25 - 28	0,104 - 0,116
OL6	27 - 30	0,103 - 0,115

III.8.1.2 Water consumption of stations and skids

The following figure represents the total consumption of water for stations and skids located in the field of HMD for the period 2011-2020, where the rate of consumption is in progress, especially in the last two years. High consumption of water is generally due to the increase in the number of wells that suffer from high salinity rate in this field.

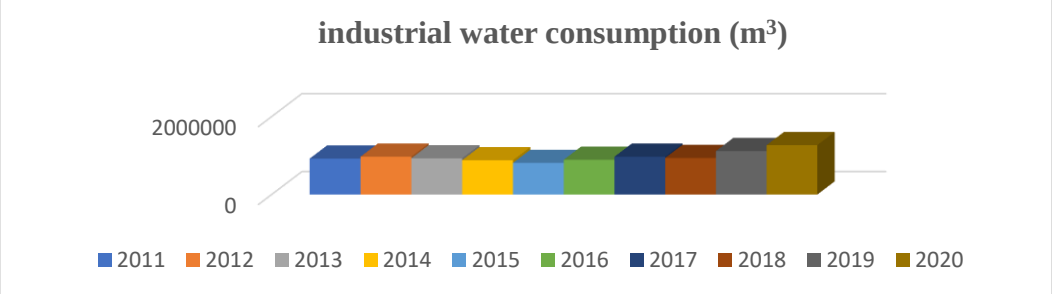

Figure III.62: Water consumption of stations and skids.

III.8.1.3 Consumption of AD32 inhibitor

The following histogram shows the consumption of AD32 for the period of 2011-2020 in the HMD field. We notice that the use of AD32 increases gradually until the year 2019, then

we can see a remarkable drop in the year 2020. This decrease is due to the discontinued importation of this product because of coronavirus.

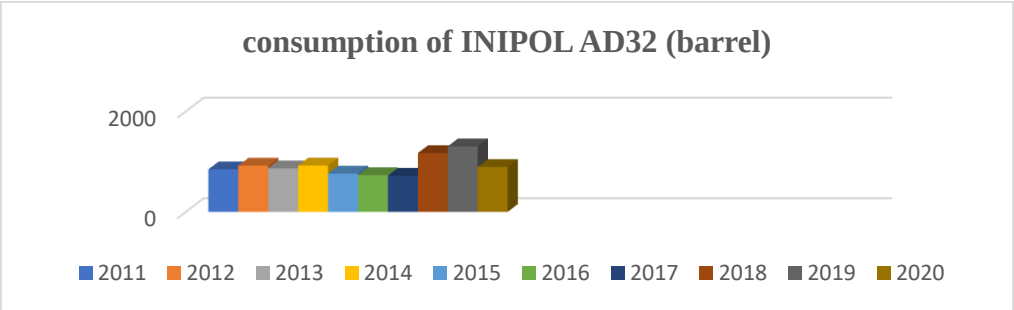

Figure III.63: Consumption of INIPOL AD 32 in HMD field.

II.8.1.4 The concentration of AD32 at the inlet and outlet of wells

The following two histograms show the variation of concentration of AD32 at the inlet and outlet of several wells in the field of HMD. Based on the monitoring of AD 32 concentration for a long time, we can notice that the concentration is dissimilar to the required one for industrial tests.

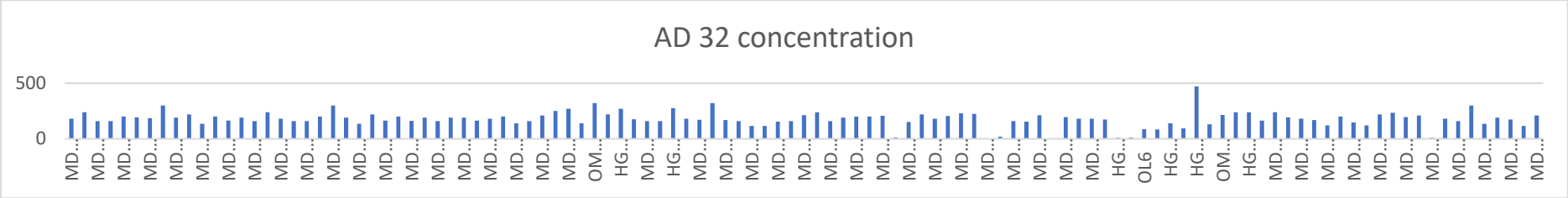

Figure III.64: Concentration of AD32 at the inlet of wells in HMD field.

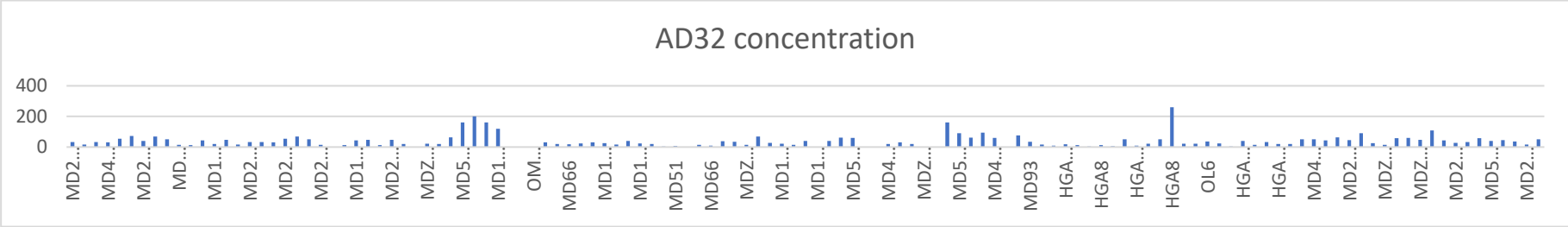

Figure III.65: The concentration of AD32 at the outlet of wells.

III.8.2 Evaluation of the effectiveness of AD32 inhibitor treatment in the HMD field

III.8.2.1 Study of the well ONIZ432

Based on the results of the ONIZ432 Well Gauging Tests, a potential drop in ONIZ432 was observed from 31/07/2017.

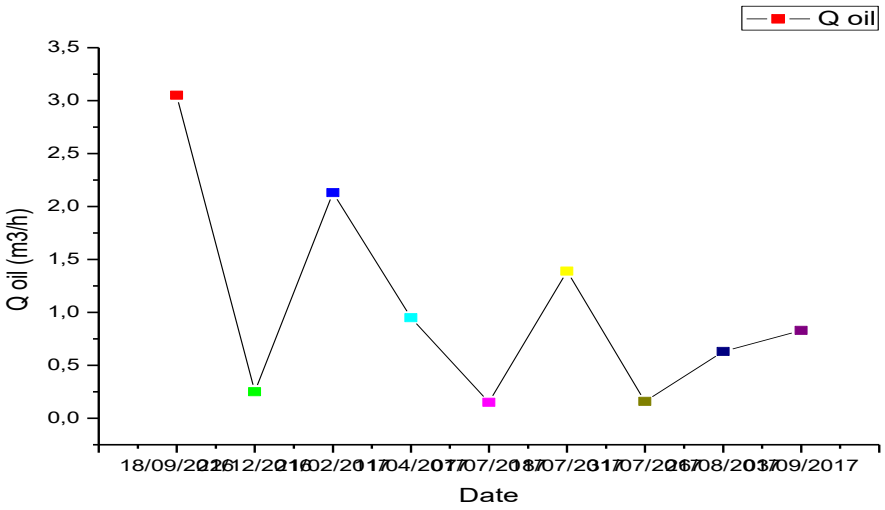

Figure III.66: Variation of oil rate of ONIZ432 well.

The laboratory results confirmed the presence of $BaSO_4$, Silica, Salts (NaCl), and $CaSO_4$ in the tubing and the near-wellbore. It is suspected because the incompatibility of the injected water (contains sulphate) and the formation water (contains barium) creates a $BaSO_4$ deposit.

Table III.7: Analysis results of sample of ONIZ432 well.

Well	Sampling point	Sampling date	Results
ONIZ432	3099 m	16/03/2017	3,7%Sels (NaCl) ,8 % CaSO4 47% BaSO4 41,2 % silice, the rest is a treatment product.

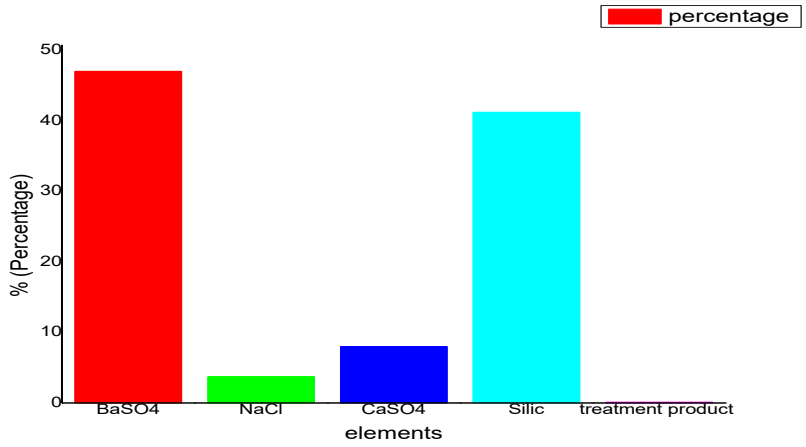

Figure III.67: Scales in ONIZ432 well.

Based on the results of the Gauging test, it can be concluded that:

- Disruption of production flow during the period (18/09/2016 to 18/07/2017)
- The decrease in flow rate from 1.39 m^3/h to 0.16 m^3/h corresponds to a drop of 1.23 m^3/h during the period (18/07/2017 to 31/07/2017) due to the precipitation of barium sulphate deposits.

The following table show the result test before connecting the well to the ONI skid (before treatment with the AD32 inhibitor).

Table III.8: Test results before connecting the well to the ONI skid

Date	D choke (mm)	Q Oil (m^3/h)	GOR (sm^3/sm^3)	Pressure (Kg/cm^2)			T Oil (°c)
				Wellhead	Pipe	Sep	
31/07/2017	15.08	0.16	9953	17.4	12.13	14.29	36

After connecting wells to skid ONI (after treatment with AD32 inhibitor), we find the following results:

Table III.9: Test results after connecting the well to the ONI skid

Date	D choke (mm)	Q Oil (m^3/h)	GOR (sm^3/sm^3)	Pressure (Kg/cm^2)			T Oil (°c)
				Wellhead	Pipe	Sep	
26/08/2017	15.08	0.63	2024	23.3	9.19	_	27
03/09/2017	15.08	0.83	1187	18.2	10.1	_	33

- ***treatment efficiency***

The determination of treatment effectiveness is made through the following relation:

$$E = (Q\ after - Q\ before) / (Q\ before) \qquad III.3$$

E : treatment efficiency

Q after : flow rate after treatment

Q before : flow rate before treatment

So; E = (0.63 – 0.16) /0.16 = 3.9375 E = 393.75

III.8.2.2 Study of wells HGA3, HGA9, HGA16 and HGA17

Oil production in the HASSI GEUTTAR region is assisted by the injection of fresh water to eliminate the formation of NaCl salt. This injection of water creates a problem of formation of barium sulphate deposits. Despite continuous injection into the HGA wells to dissolve the salt, the gauging tests show a net decrease in production flow during the following years in the wells (HGA3, HGA9, HGA16, HGA17), this decrease indicates tubing plugging.

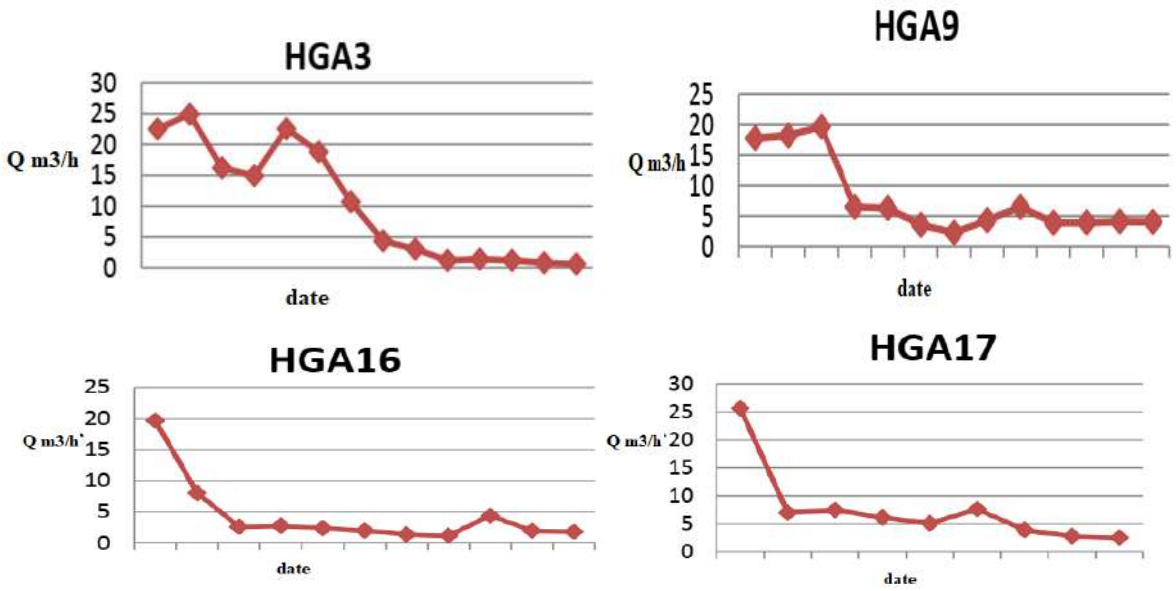

Figure III.68: Decrease in well oil flow (HGA3, HGA9, HGA16 and HGA17). (DATA Bank, SH ,2020)**.**

- ***Deposit analysis***

From the analysis of the samples, a considerable percentage of NaCl as well as $BaSO_4$ were found, which proves that the quantity of water injected is not suitable for effective desalination. Figures II.69 show the analyses of the samples of each well.

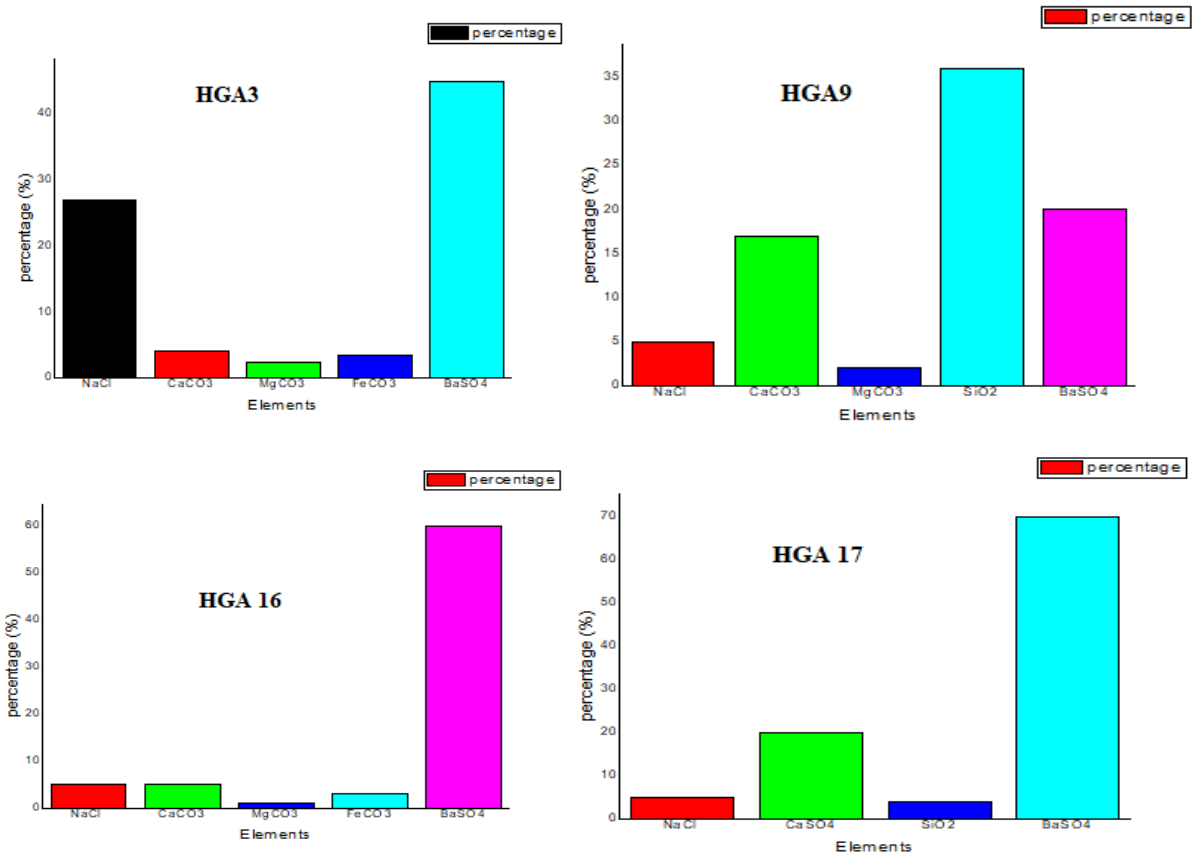

Figure III.69: Deposit analysis for HGA3, HGA9, HGA16 and HGA17 wells.

From the laboratory results, we notice that the concentration of AD32 at the inlet of the wells is disturbed, as its quantity at the outlet is insufficient, the amount of treatment is between 150 ppm and 160 ppm depending on that present in the reservoir; it is preferable to double the amount of treatment centre between 250 ppm-260 ppm to carry out the complete treatment of water located at the bottom and ensure a considerable concentration of phosphonate to finish the treatment in the upper part (the collections).

- ***Monitoring of AD 32 concentration***

Table III.10: Monitoring the concentration of AD 32 for different wells.

Wells	AD32 at inlet (ppm)	AD32 at outlet (ppm)
HGA3	276	40
HGA9	141	12
HGA16	85	4
HGA17	94	6
HGA8	270	20
HGA3	234	18
HGA9	220	30
HGA9	305	26
HGA17	370	30
HGA3	181	16
HGA9	182	40
HGA16	166	24
HGA17	194	20

The dosage monitoring shows that the amount of AD32 at the outlet is insufficient, in addition, the water arriving at the well is not well treated because the treatment of the HGA region requires a concentration of 250 ppm according to the industrial test. So, we will regulate these residual concentrations with optimized water flow, for this purpose, it is necessary:

- Monitor the concentration daily.
- Ensure a 250 ppm AD32 concentration at the inlet of the well to avoid perturbation of concentration.
- Ensure that the residual amount of AD32 is sufficient to complete the treatment until separation.

III.8.2.3 Study of wells HGA8, MD411, MD525

The following figure presents the analysis of the different samples of deposits in HGA8, MD411, and MD525 wells in the field of HMD.

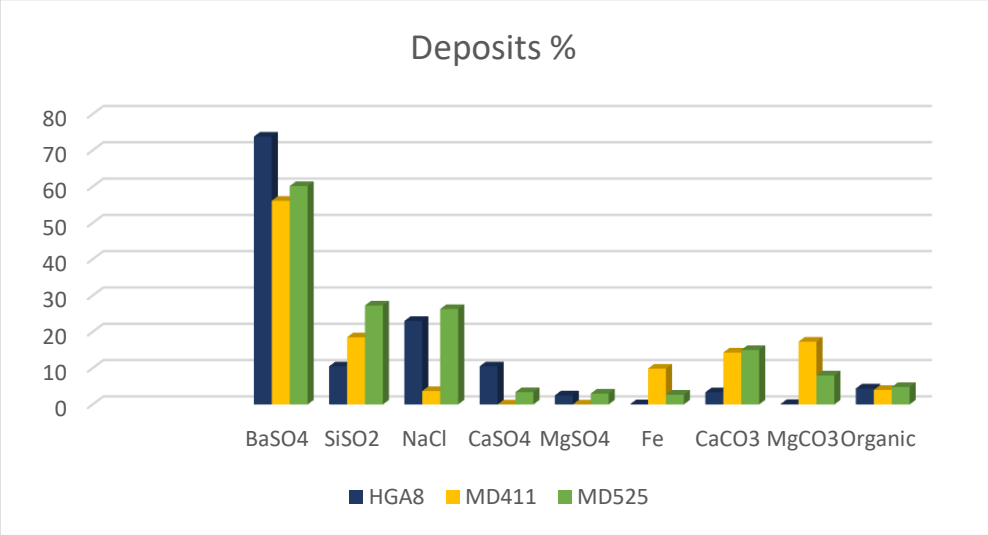

Figure III.70: Deposit analysis for HGA8, MD411, and MD525 wells.

The three wells HGA8, MD411, and MD525 formed a majority of $BaSO_4$, $SiSO_2$, NaCl, $CaCO_3$ deposits with low $CaSO_4$, $MgSO_4$ and organic deposits.

III.8.2.4 Comparative study between AD32 and other inhibitors

AD32 treatment product is the main inhibitor used in the Hassi Messaoud field against the formation of $BaSO_4$ precipitates. The table below shows the number of wells with the $BaSO_4$ deposition problem from 2016 to 2020 in the HMD field.

Table III.11: The number of wells with BaSO4 deposition problem in the HMD field (2016 - 2020).

Year	number of wells with BaSO4 deposition	Name of wells
2016	20	MDR11 - MD411 - MD516 - MD629 - OL6 - HGA 8 -MD316 - MD490 - OMM402 - MD155 - OMJ723 - HGA 16 - MD161 - MD262 - HGA9 - MD264 - MD480 - MD235 - MD660 - MD481
2017	15	MDZ651 - OML75 - OL6 - MD660 - ONIZ432 - HGA 16 -MD237 - OMN761 - HGAW3 - OMN601 - HTF23 - OMJ771 - MD612 - MD525 - MD474
2018	21	MD269 - OMJ22- HGA16 - OML822 - OMN41 - MD516 - MD439 - ONMZ751 - HGA8 - OMM 532 - ONI501 - ONIZ632 - MD480 - OMF502 - MD420 - OMN56B - OMG512 - OMLZ562 - MD525 - MD353 - ZCINA
2019	20	MD513 - HGA8 - OMM532 - OMP85 - MD353 - MD66 - OMO751 - MD421 - OMM302 - RDC26 - ONM234 - HGI4 - OMJ33 - MD676 - MD497 - HGAW5 - OMN601 - MD525 - ONI54 - ONIZ632
2020	35	MD201 - ONI45 - OML832 - ONM223 - MD413 - MD235 - MD218 - ONMZ473 - HGA7 - OML822 - OMN 442 - MD269 - ONI551 - OML832 - MD676 - ONIZ413 - ONM13 - MD235 - HGAW3 - MD387 - HGA8 - MD513 - HGA9 - MD685 - ONMZ513 - ONIZ432 - OMO36 - ONM471 - MD633 - MD413 -

According to the above table, the following interpretations may be mentioned:

- Before 2020, the number of wells with large amounts of barium sulphate precipitation was approximately 20 per year in the HMD field, which is primarily due to the injection of AD32 into the water circuits to avoid the formation of barium sulphates.
- During the year 2020, the significant increase in the number of wells with $BaSO_4$ deposits is explained by the lack of AD32 (due to exceptional circumstances, which is the start of the Covid-19 pandemic) and the use of other inhibitors that have not been as efficient as AD32.

From April 2020, an end of the stock of anti-deposit AD32 requires the use of other inhibitors of other oil fields (BBK, Ourhoud, GSA....). The table below expresses the requests for different amounts of inhibitors.

Table III.12: Deposition inhibitors used in HMD field during the year 2020. (DATA Bank, SH ,2020)

Products / Month	Biocide	Anti-deposit	Corrosion inhibitor
January	2	Zero stock	8 barrel Norust CR 486
February	Reception of 450 barrels of AD32		
		155 AD 32	4
March		42	8
April		114	24
	refund 60 AD 32 to the GSA group		
May		92	28
June		41	27
July	80 barrels of SCW 85375 (baker), GEA		
	5	64	
August	40 barrels CHIMEC 1264, BBK		
	12	40	
September	30 barrels CHIMEC 1264, BBK		
		35	
October	50 barrels CHIMEC 1264, BBK		
		13	
November	100 barrels SCALETREAT 837C, HBNS		

According to the table above, the various inhibitors that replaced AD 32 during its out of stock are SCW85375, SCALETREAT837C, CHIMEC1264, and even FQS113.

CHIMEC1264, as well as FQS113, were the two most used inhibitors in the field of Hassi Messaoud during the year 2020.

III.8.2.4.1 Study the wells MD413 and MD633

The wells understudy must be salty wells that require water injection. Over time, a production of the reservoir water appears in the well due to the Water Coning. The incompatibility between this formation water and the injection water used for desalination causes the formation of barium sulphates (formation water loaded with Ba^{2+}, and injected water loaded with SO_4^{2-}sulphate element).

- ✓ ***The well MD413***

The well MD413 is an oil production well located in central zone 15 drilled on 30/01/1987. The well-produced through 4 ½ inch tubing and is equipped with CCE 1 ”66 for further desalination of water.

The MD413 well have the following problems:

- Barium sulphate deposits;
- Calcium sulphate deposits;
- Salt deposition;
- And even magnesium sulphate deposits;

Regardless of who causes the frequent plugging, it always leads to a major drop in well production.

We found a potential drop in the MD413 well from 09/09/2020 (During this period, the deposit inhibitor used is CHIMEC1264). The laboratory analysis confirmed the presence of $BaSO_4$ in the tubing and the near-wellbore. It is suspected that the incompatibility of the injected water (contains sulphate) and the formation water (contains barium) creates a $BaSO_4$ deposit.

Table III.13: MD413 well sample analysis results

Well	Date of sampling	Point of sampling	Results
MD 413	17/10/2020	Exterior of CCE	100 % $BaSO_4$

Figure III.71: MD413 Well production profile - After the use of CHIMEC 1264 Inhibitor. (DATA Bank, SH ,2020)

Based on the results of the Gauging test, it can be noted that:

- Disruption of production flowrate during the period (09/09/2020 until 07/12/2020).
- The decrease in flow from 6.99 m^3/h to 4.1 m^3/h and then to zero flow rate (100% $BaSO_4$ deposition) is due to the precipitation of barium sulphate deposition after the use of CHIMEC 1264 (ineffective inhibitor).
- The increase in production flowrate from 07-12-2020 is justified by the elimination of the damage caused by barium sulphate using the curative treatment (Scale Blaster by the operation of Coiled Tubing in November 2020).

✓ ***The well MD633***

The MD633 well is an oil well located in Zone 24. It was drilled as a vertical well in June 2010, this well tends to precipitate salt, so it needs a continuous water injection to dissolve the salt. We noticed a decrease in oil flow of MD 633 well from 01/10/2020. Laboratory analysis results showed the existence of 54% ($BaSO_4$+Silica), 11% of salts (NaCl), and 35% of iron oxides.

Table III.14: MD633 well sample analysis results.

Well	Date of sampling	Point of sampling	Results
MD 633	11/10/2020	3416 m	11% of salts, 35% of iron oxides, the rest is insoluble residue ($BaSO_4$+Silica).

Figure III.72: MD633 Well production profile - After the use of CHIMEC 1264 Inhibitor (DATA Bank, SH ,2020)**.**

Based on the results of the Gauging test, we can report:

- Disruption of production flowrate from 01/10/2020.
- The decrease of the flow rate from 6 m^3/h to zero flow, which is the consequence of a clogging (11% Salts, 35% iron oxides, 54% $BaSO_4$ + silica), the decrease is due to the precipitation of barium sulphate deposits, Despite the use of CHIMEC1264 (ineffective inhibitor).

III.8.2.4.2 production shortfall

Unfortunately, the results obtained after the use of the new inhibitors were not satisfactory. They were interpreted as a drop in production at the wells having the problem of barium sulphate deposits. The following graph expresses the variation of the number of wells having the problem of $BaSO_4$ deposits during the year 2020 and also the production shortfall in the field of Hassi Messaoud:

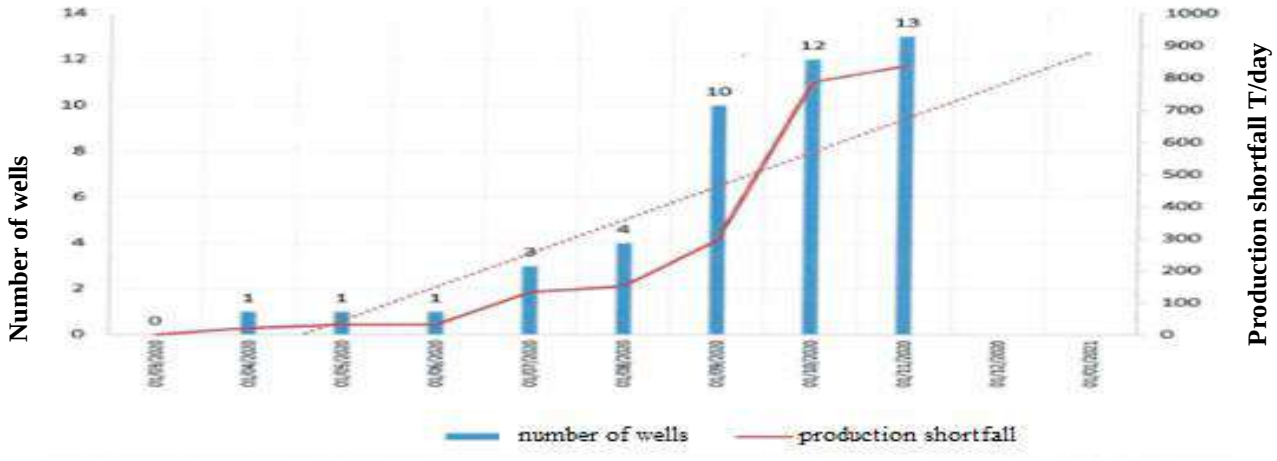

Figure III.73: The change in the production shortfall and the number of wells with the problem of barium sulphate deposition during the year 2020.

Figure III.73 shows that the increase in the number of wells with the $BaSO_4$ problem after the unavailability of AD32 in the year 2020 is mainly due to the use of new inhibitors that have proven to be ineffective. The previous figure confirms that with the use of the new inhibitors (such as CHIMEC 1264), the formation of barium sulphate deposits became enormous, and the production shortfall increased considerably.

Below are tables that express the variation of the production shortfall in the southern and northern fields of the Hassi Messaoud field.

Table III.15: Variation of production shortfall in the southern field.

Wells	*closing date*	*Q (m^3/h)*	*Production shortfall T/day*
HGA8	25/10/2020	2.85	54.7
HGA9	26/10/2020	2.67	51.3
HGA16	28/10/2020	3.26	62.6
MD235	10/04/2020	1.6	30.7
MD413	10/10/2020	6	115.2
MD513	26/09/2020	3.14	60.3
MD633	13/10/2020	4.74	91
MD612	30/10/2020	6	115.2
		Total	581

Table III.16: Variation of production shortfall in the northern field.

Wells	*closing date*	*Q (m^3/h)*	*Production shortfall T/day*
ONMZ473	08/07/2020	2.80	53.8
ONIZ632	10/08/2020	4	76.8
OML832	15/09/2020	1.5	28.8
ONM471	04/11/2020	2.45	30.7
ONMZ513	09/09/2020	2.63	47
MD513	26/09/2020	3.14	50.5
		Total	256.9

Total production shortfall due to the $BaSO_4$ deposits estimated by 838 tonnes.

The results obtained show that the addition of the new inhibitors reduces the production of the wells having large precipitates of $BaSO_4$. This decrease in the potential and inefficiency of these products in the field of Hassi Messaoud are due particularly to various factors:

- The heterogeneity of the reservoirs between the different fields; for example, the case of CHIMEC1264, which proved its effectiveness in the BBK field, but in the HMD field it is considered as ineffective inhibitor.

- Not all new inhibitors used are intended only for inhibition of $BaSO_4$ deposits. Among these products, some are intended for inhibition of $CaSO_4$ deposits, For example, SCALETREAT837C.
- Injection with the usual dosage (200 ppm for AD32) sometimes leads to overdoses and sometimes to lack of doses, what can be a strong argument of the ineffectiveness of the elements of treatment used (lack of doses hinders product efficiency, while overdose causes new yellowish deposition (phosphates)).
- Direct application of new inhibitors without industrial testing, which is due to stockout and inability to re-import AD32(border closures because of the global Covid-19 pandemic).

III.8.2.4.3 The economic result

The total production shortfall of the Hassi Messaoud field due to $BaSO_4$ was approximately 838 tonnes. One tonne of crude oil is between 7 and 9.3 barrels, the global average being about 7.6 barrels per tonne. The price of Algerian oil SAHARA Blend hit an average of 41 dollars per barrel in the second half of 2020. So, Hassi Messaoud's field has accumulated more than 260 thousand dollars in losses.

In addition, Scale-Blaster mechanical treatment operations by the Coiled tubing unit, which is used for cleaning barium sulphate deposits at the level of perforations and obstructions inside the tubing, it cost more than 250 thousand dollars for the operation (it can even go up to 400 thousand dollars). Therefore, the cost of curative treatment (applied by the Scale Blaster operation) during the period of the use of inhibitor injection of other oil fields has reached a cumulative amount of more than 3 million dollars.

In conclusion, the economic losses (mainly due to exceptional circumstances that created a shortage of the indispensable AD32 inhibitor against BaSO4 deposit formation) were approximately $3.5 million in this period.

III.8.2.4.4 Results of the comparative study

The purpose of this part is to study the formation and inhibition of $BaSO_4$ deposition by the use of AD32 inhibitor and other new inhibitors. The results obtained in this study have revealed the importance of the anti-deposition mentioned above and its effectiveness in relation to other products on the prevention of deposit formation.

Based on the various results obtained in this study, it was concluded that:

The new inhibitors used in the HMD field (SCW85375, SCALETREAT837C, CHIMEC1264, and FQS113) to replace AD32 are ineffective.

An excess of inhibitor may have an inverse effect where there is the formation of other deposits that come from the inhibitor.

In the end, we give the solutions that we see effective to preventing the formation of these sulphate deposits, which are:

- The construction of two large tanks (one north and one south of HMD) filled with water treated by the anti-deposition for use in water plugs.
- Water flow control and AD 32 inhibitor concentration.
- Perform industrial testing of new inhibitors before they are injected into the system to be inhibited.
- Make a list of inhibitors (already tested and validated) to use in case of stock shortage of the main inhibitor AD32.

III.8.3 problems of treatment with AD32 inhibitor in the field of HMD

Several factors affected the effectiveness of AD32 inhibitor in the field of HMD, such as:

- The generalization of water treatment injected in salt wells in the HMD field.
- The lower or higher concentration of the test dose (overdosage and insufficient dosage) is due to dilution during transport, improper mixing in treatment facilities, or leakage in the pipeline.
- Unknown problems in the process of pumping injected water (discontinuous pumping).
- Heavy inhibitor particles (settling).
- The influence of temperature and pressure on the inhibitor (inactive).
- Incompatibility between the treatment products used in the HMD field.
- Water plugs that are not treated by the anti-deposit AD32 (Table III.17)

Table III.17: Control of the AD32 concentration of some wells treated by water plugs.

Wells	Concentration of AD32 ppm
MD443	0
ONMZ212	0
OMOZ232	0
MD 573	0

III.8.3.1 Anti-deposition concentration control in the HMD field

The variation in desalination water flow directly affects the concentration of the chemical AD32 deposition inhibitor in the water. Each time a line of the network is clogged or, a salt well is closed, the water flows automatically decreases, and consequently, the concentration of the product increases, which gives us an overdose of the product. On the other hand, any dilution or leakage in the pipeline is conduct to an insufficient dosage.

The following tables represent the monitoring in the laboratory of inhibitor sent to the salted wells for confirmation and adjustment. As observed, the concentration of AD32 changes due to external factors, so we need to correct it to the right dosage.

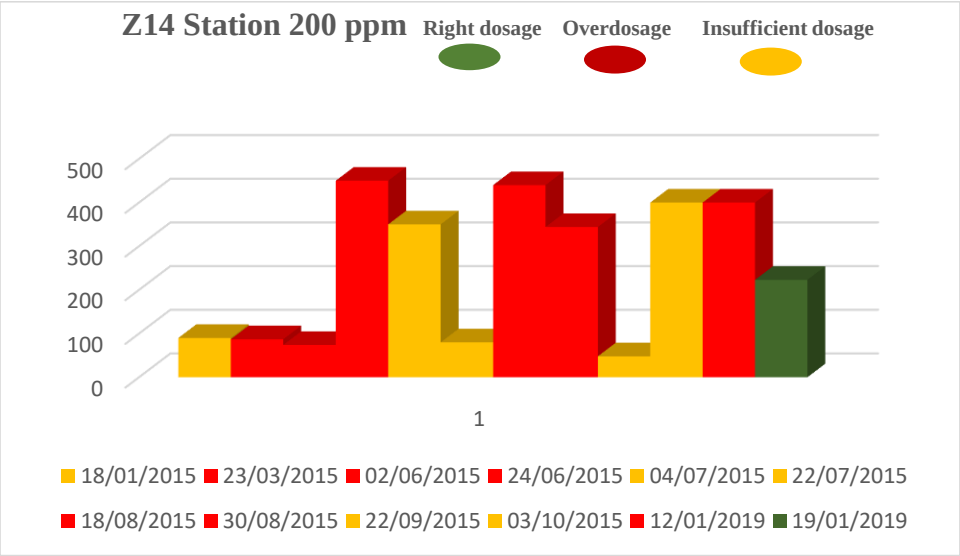

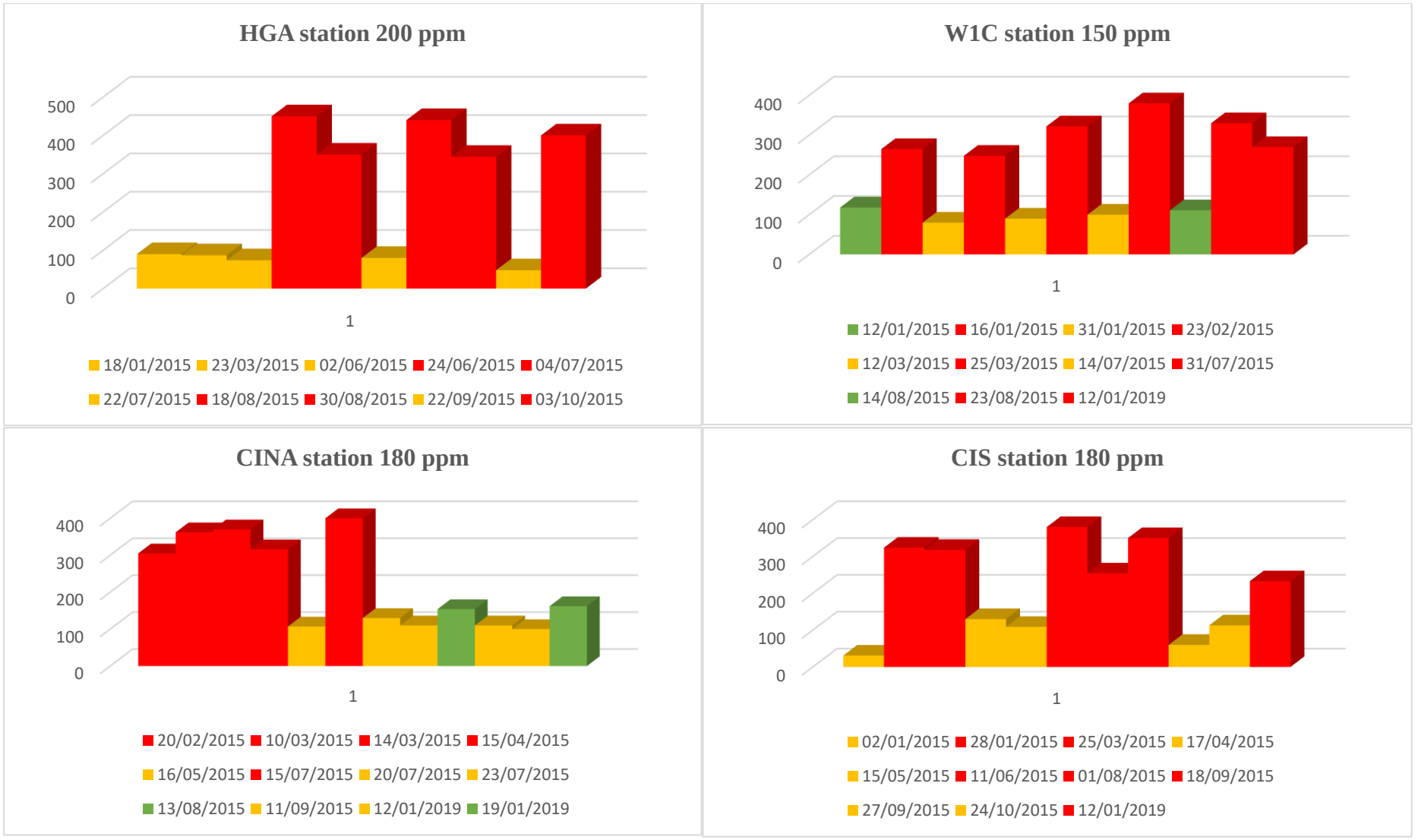

Figure II.74: Monitoring the concentration of AD 32 for desalting stations.

Table III.18: Monitoring the concentration of AD 32 for skids

Date	Skid HP	Concentration of AD32 ppm
09-01-19	MD421	130
	ONI	400
	W1CHP	350
	W1CHP	151

Right dosage Overdosage Insufficient dosage

Problem due to repeated disturbances of treated water flow causing overdose in AD32 treatment product, which leads to yellowish deposition (phosphates).

The main causes of the overdose problem are:

- The state of BSB pumps
- Leaks caused by line corrosion
- Salt well closures and openings

Figure II.75: Treatment product deposits.

The results of the analysis of the deposits carried out at the laboratory showed the presence of corrosion products (FeS and iron oxides) caused by SRB sulphate-reducing bacteria and treatment products caused by overdose.

Table III.19: Analysis results of deposits recovered from blockage lines.

Wells	Results
CINA 4''pipeline	75% Organic deposit 1.1 % FeS iron sulphides rest: Treatment products
MD 488	35.42 % Iron oxides 33.37% Organic deposit 23.16 % Iron sulphides FeS 06 % Treatment products
Water line between MD288 and MD 93	33% Organic deposit Rest % Treatment products
MD320, purge valve 4"	100% treatment products
Water Line MD10	65% Organic deposit Rest: majority of treatment products

III.8.4 Study the compatibility between the treatment products used in the HMD field

To prevent problems that may arise from the use of two or more products at once, a compatibility study between products used simultaneously in oil production is necessary. Possible incompatibility between two or more products may lead to production problems (foaming, deposits, loss of efficiency, and clogging of pipes).

We present the results of compatibility testing of three treatment products currently in use in the HMD region. These are the corrosion inhibitor Cortron CP 7130 of the firm Champion Technology, the bactericide FQS THPS 75 of FQS, and the anti-deposit INHIPOL AD32 of CECA.

✓ ***The method***

The method used is that proposed by the IFP (Production and treatment of salted crude oils, Éditions TECHNIP), which consists of mixing equal volumes of products under the conditions of the test and studying the behaviour of the mixture after one minute, 03 hours, and 48 hours of contact.

The tests were conducted under ambient conditions at 04°C and 70°C.

✓ ***Results***

We observed different results by mixing the three treatment products then by mixing them in pairs under different conditions of temperature and contact time. The following figures summarize the results and the visual observations of the tests carried out.

We use the following mixtures:

X (AD32+FQS THPS75+CORTRON CP 7130), A (AD32+FQS THPS 75), B (AD32+CORTRON CP 7130), C (FQS THPS 75+CORTRON CP 7130).

✓ ***Interpretation of results***

The three treatment products: the corrosion inhibitor Cortron CP 7130 of the firm Champion Technology, the bactericide FQS THPS 75 of FQS, and the deposit INIPOL AD32 of CECA, represented by the mixture X, are incompatible with each other at ambient temperature and 04°C, with the formation of persistent mosses that tend to consistency. At 70° C, the mixture has two phases: a phase with a dominant volume and a second phase with a volume less than the initial volume of each of the three products. In such a situation, with phase separation and where initial volumes are not preserved, incompatibility of the mixture is likely, and further investigation is necessary.

Mixture A (AD32+ FQS THPS 75) has always been compatible in all test conditions (temperature variation and contact time variation).

Mixture B (AD32+ Cortron CP 7130) is incompatible with ambient temperature and at 04°C, where it exhibits a significant formation of persistent foams. At 70°C, the foams disappear, but the initial volumes of the phases are not preserved. The same conclusion for the X mixture is valid.

Mixture C (FQS THPS 75+ Cortron CP 7130) shows two phases of different volumes under test conditions. This mixture may also be incompatible, and where further investigations are necessary.

III.9 Evaluation of the effectiveness of the ENMAX device in the field of Hassi Messaoud

Currently there is a severe problem in Hassi Messaoud field due to the formation of barium sulphate, asphaltene in the wells and the oil pipeline network. This problem leads to line blockage and oil production decrease. Approximately 200 km pipelines are replaced every year due to the problem of scale deposition. The ENMAX device was installed on the flowline of well MD-411 on 01/03/2017 for free trail to evaluate the performance and effectiveness of this device.

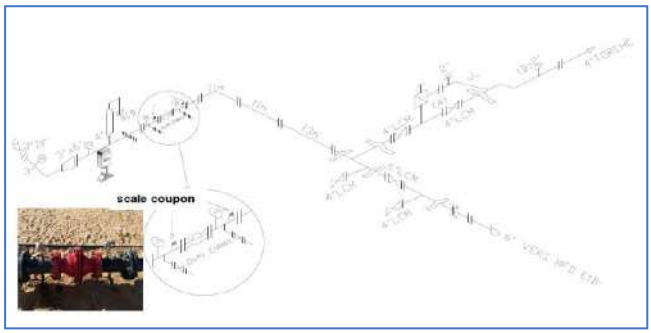

Figure III.81: Installation of the ENMAX device on the flowline of MD411 well.

III.9.1 Deposits on the 6'' flowline of well MD-411 before ENMAX installation

Photos below show the deposits formation on the flowline of well MD-411 before ENMAX installation on the flowline of well MD-411.

Figure III.82: Deposits formation on the flowline of well MD-411.

The graph below indicates the analysis of sample taken from the flowline of well MD-411 before installing the ENMAX device. Sample was taken from 6" flowline of well MD-411.

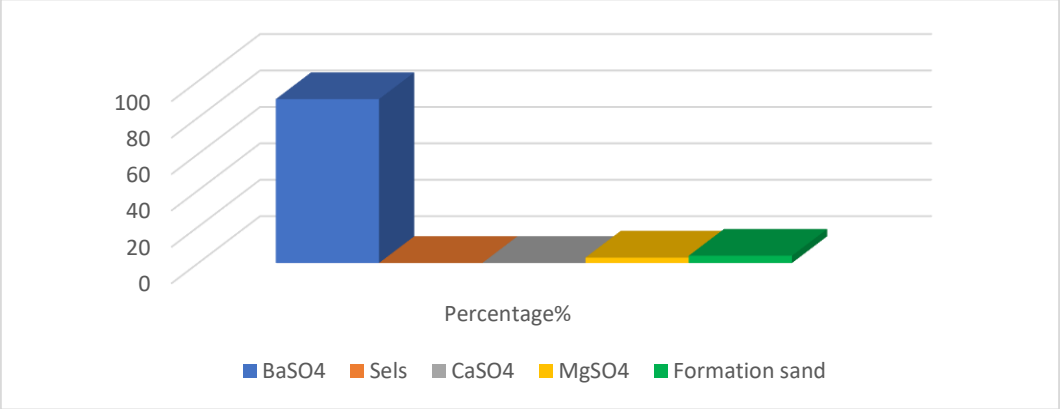

Figure III.83: Sample analysis of the scale found in the flowline of well MD-411.

III.9.2 Evaluation of the ENMAX 6''device

The evaluation of the 6'' ENMAX device installed on the flowline of well MD-411 includes the following parameters:

III.9.2.1 Pressure reading upstream and downstream ENMAX and flowrate daily reading

The figure below indicates the following:

- Daily pressure reading upstream and downstream the 6'' ENMAX device installed on the 6'' flowline of well MD-411.
- Daily oil flowrate for well MD-411.
- Daily wellhead pressure for well MD-411.

III.9.2.2 Laboratory analysis of upstream and downstream 6'' ENMAX device

Samples were taken upstream and downstream ENMAX device installed on the flowline of well MD 411, then they were analysed at laboratory. The sample analysis includes pH, Fe, scale inhibitor concentration calcium, magnesium, hardness, and total dissolved solids. Hardness was computed from the analysis of cations: Ca^{++} and Mg^{++}. There are slightly differences between the analysis upstream and downstream of the 6'' ENMAX device.

The figures below indicate the results obtained from the sample analysis upstream and downstream ENMAX device installed on the flowline of well MD-411.

III.9.2.3 Scale coupons analysis upstream and downstream 6'' ENMAX device

Scale coupon was installed upstream and downstream the 6'' ENMAX device which installed on the flowline of well MD-411. The third scale coupon was installed in the bypass corrosion of MD411 at about 62 m from ENMAX for comparison.

After dismantling the 6'' ENMAX device from the flowline of well MD-411, the scale coupon upstream and downstream of the 6'' ENMAX device was dismantled for complete analysis.

It has been found that there is a slightly difference between the laboratory analysis of the scale coupon upstream and downstream of the ENMAX device installed on the flowline of well MD-411..

From the scale weight, it can be noticed the following:

- There is no big difference in the amount of scale formed on the surface of the scale coupons upstream & downstream ENMAX device installed on the flowline of well MD-411.
- Same predominant item which is $BaSO_4$ mixed with silica.
- The difference between two values (scale coupons upstream and downstream ENMAX device) is due to the high organic content may be caused by bio corrosion leading to high corrosion rate.

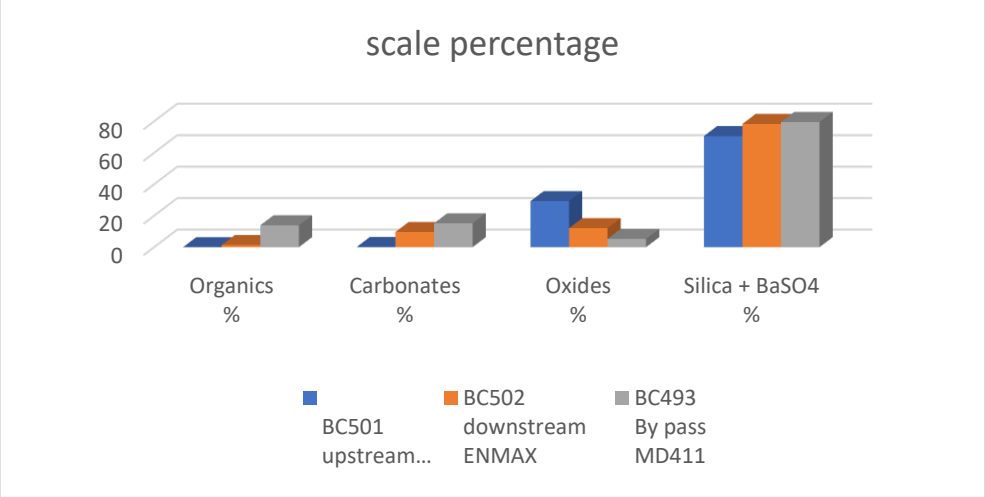

Figure III.96: Scale percentage.

III.9.2.4 Visual inspection of upstream and downstream of 6'' ENMAX device

Visual inspection for the flowline of well MD-411 was conducted before ENMAX device installation and after dismantling ENMAX device.

The photos below indicate the deposits formation before installation the ENMAX device on the flowline of well MD-411 and after dismantling ENMAX device.

- ✓ ***Deposits on the 6'' flowline of well MD-411 before ENMAX installation***

Photos below show the deposits formation on the flowline of well MD-411 before ENMAX installation on the flowline of well MD-411.

Figure III.97: Scales found in the flowline of well MD-411.

- ✓ ***Deposits on the flowline of 6'' well MD-411 after dismantling ENMAX device***

The photo below indicates the downstream of the flowline of well MD-411 after dismantling the ENMAX device. From the photos below you can notice that no deposits were found on the flowline downstream of the dismantled ENMAX device.

Figure III.98: 6'' flowline of well MD-411 downstream of NMAX device after dismantling the device.

The photo below illustrates the upstream flowline of well MD-411 after dismantling the 6'' ENMAX device. From the photo below it can be noticed that there are deposits accumulated upstream 6'' ENMAX device.

Figure III.99: 6'' flowline of well MD-411 upstream of NMAX device after dismantling the device.

III.9.2.6 Scale Measurements after dismantling 6'' ENMAX device

The accumulation of the deposits on the flowline of the well MD-411 was checked after dismantling the 6'' ENMAX device (upstream and downstream the ENMAX device).

It can be noticed the following points:

- No deposits were found on the flowline of well MD-411 after dismantling the ENMAX device (downstream dismantled ENMAX device).
- There are deposit accumulations on the flowline of well MD-411 after dismantling the ENMAX device (upstream dismantled ENMAX device).
- It has been found that the ENMAX device was working well as no deposits accumulated downstream the dismantled 6'' ENMAX device.

III.9.3 Comparison of scale measurements before and after ENMAX device installation

A comparison was made between the measurements of the deposits accumulations before installing the ENMAX device on the flowline of well MD-411 and after dismantling the ENMAX device from the flowline of well MD-411. The results of the comparison can be summarized as follow:

It has been found deposits accumulate before installing the ENMAX device on the flowline of well MD-411. The thickness of deposits on the bottom section of the flowline of well MD-411 was 1.5 cm, while the thickness of the upper section was 0.5 cm.

No deposits accumulated inside the 6'' flowline of well MD-411 downstream of the ENMAX device according to the visual inspections after dismantling the device.

It has been noticed that there were deposits accumulations were found after dismantling the ENMAX device upstream part of the dismantled ENMAX device.

Figure III.100: Deposit inside ENMAX device.

Pressure drop across the ENMAX device was almost 0.5 bar according to daily monitoring of the pressure reading upstream and downstream of the device.

General Conclusion

General Conclusion

The scaling problem is widespread and common in the oil and gas sector worldwide. The formation of barium sulphate deposits is one of the most common problems in the HMD field. These mineral deposits result from the incompatibility between the injected water (Albian) rich in sulphates SO_4^{-2} and the formation water (Cambrian) rich in barium Ba^{+2}.
This study allows us to better understand how to analyse water and deposits, determine the nature of this deposit, and evaluate methods used to treat the precipitation of barium sulphate deposits in Hassi Messaoud field.

Different sets of experiments and analyses were performed to determine the quality and the characteristics of three types of waters in the field of HMD (Albian, Cambrian and mixture). The obtained results help in better understanding the behaviour of water and predict the possible deposits that may occur in this field. The potential quality issues in the injection water process were defined as the ionic composition of the water, chemical incompatibilities such as scales and precipitates, and suspended solids content. The incompatibility of the Albian and Cambrian waters of the HMD field was determined by the gravimetric method.

Analysis of different solid samples from several points in the field of HMD, especially from damaged equipment and pipelines, confirms the existence of $BaSO_4$ scales with a high percentage. Thus, the results illustrate the dangers of these deposits, which classify as the second deposit after the predominant scale NaCl in the HMD field. The evaluation of the current method of treatment which is the use of AD 32 inhibitor on several wells in the HMD field, shows that the efficiency of treatment is not optimal in multiple wells. Limitation of AD32 generally, due to numerous factors and operational conditions such as; variation of concentration of AD32 (Overdosage and insufficient dosage), the effect of some parameters on the process of inhibition, incompatibility between the treatment products used in the HMD field, and the absence of an accurate study that evaluate this inhibitor, especially the economic aspect. Although the previous inconveniences, AD 32 is considered the best inhibitor in comparison with the other types, such as; SCW85375, SCALETREAT837C, CHIMEC1264, and FQS113. A comparative study carried out during the period of covid 19 pandemic in 2020 confirm the failure of various inhibitors that replaced AD 32 during its out of stock.

The new device ENMAX was installed and tested in the flowline of MD 411 well to solve this severe deposit, but the results were unsatisfying because of several factors such as; the flowline of MD 411 is already treated with AD 32, ENMAX caused a drop in pressure of the line, this device may block the pipeline especially when deposits accumulate inside it.

General Conclusion

Recommendations

Based on the results and conclusions obtained from this study, the following suggestions for future work in the same field are recommended:

- A compatibility study of the products used simultaneously in the HMD field is indispensable.
- Continuous control of AD32 concentration by sampling is required due to the instability of the efficiency of the inhibitor.
- Stop the generalization of injection water treatment in the whole zones of the field, and specify each well with a special treatment.
- More coordination between the departments in charge of controlling the concentrations of the anti-deposit in case of a change in water flow.
- Construction of two big tanks (in the north and south of HMD) filled with anti-deposit treated water for use in water plugs.
- An industrial test is necessary for other types of inhibitors to replace AD32 in the case of stockout.
- Enmax devices need more tests and evaluation to confirm the capacity of treatment of this tool.

References

References

Alwi, N., Salleh, I.K., Irvine-Fortescue, J., Graham, G.M., Dyer, S., Wright, R., Simpson, C., Kidd, S and Stalker, R. Scale and Scale Inhibitor Challenges for an Alkaline Surfactant Polymer Flood in a Seawater Flooded Reservoir, SPE 164058, SPE International Symposium on Oilfield Chemistry, The Woodlands, Texas, USA, April 2013.

Amjad, Z., Inhibition of barium sulfate precipitation: Effects of additives, solution pH, and supersaturation water treatment, 9 (1994) 47-56, china ocean press-printed in beijing

Aoun, M., Plasari, E., David, R., Villermaux, J. Are barium sulphate kinetics sufficiently known for testing precipitation reactor models? Chemical Engineering Science, 1996. 51(10): p. 2449-2458.

Aoun, M., Plasari E., David R., Villermaux J., A simultaneous determination of nucleation and growth rates from batch spontaneous precipitation, J. Chem. Eng. Sci. 54 (1999) 1161.

Arbaoui M.A., Hacini. M., Barium Sulphate Deposits, Technologies and Materials for Renewable Energy, Environment and Sustainability, TMREES18, 19–21 September 2018, Athens, Greece, Energy Procedia (2018).

Archibald, D. D, Gaber, B. P.; Hopwood, J. D.; Mann, S.; Boland, T. J. Atomic force microscopy of synthetic barite microcrystals. Cryst. Growth 1997, 172, 231.

Azizi, J., Shadizadeh, S.R., Manshad, A.K. and Jadidi, N. Effects of pH and Temperature on Oilfield Scale Formation. Iranian Journal of Oil & Gas Science and Technology, Vol. 7 (2018), No. 3, pp. 18-31

Bader, M.S.H., Sulfate scale problems in oil fields water injection operations, Desalination 201 (2006) 100–105.

Bertero, L., Chierici, L. G., Gottardi, G., Mesini, E. and Mormino, G. (1988). Chemical Equilibrium Models: Their Use in Simulating the Injection of Incompatible Waters. SPE Reservoir Engineering. February 1988, 288 – 294.

Bezerra, M., C. M., Khali, N. C. and Rosario, F. F. (1990). Barium and Strontium Sulfate Scale Formation due to Incompatible Water in the Namorado Field, Campos Basin, Brazil. The SPE latten American production engineering conference. October 14 – 18. Rio Janetro: SPE 21109, 1 – 5.

BinMerdhah, A.B., Yassin A.M., Formation Damage Due To Scale Formation In Porous Media Resulting Water Injection, Emirates Journal for Engineering Research, 13 (3), 69-79 (2008).

BinMerdhah, A.B., Yassin AA. M, Muherei M.A., Laboratory and prediction of barium sulfate scaling at high-barium formation water, Journal of Petroleum Science and engineering 70 (2010) 79–88.

BinMerdhah, A.B Inhibition of barium sulphate scale a thigh barium formation water, Journal of Petroleum Science and Engineering 90–91 (2012) 124–130.

BinMerdhah, A.B scale formation in oil reservoir during water injection at high-barium and high-salinity formation water, Journal of Applied Sciences, 7(21), 3198-3207, 2007

Boak, L.S (2012). *Factors that impact scale inhibitor mechanisms*, [Doctoral dissertation, Institute of Petroleum Engineering, Heriot-Watt University]. https://core.ac.uk/download/pdf/77035500.pdf

Boak, L.S., Graham, G.M. and Sorbie, K.S.: "The Influence of Divalent Cations on the Performance of BaSO4 Scale Inhibitor Species", SPE 50771, SPE International Symposium on Oilfield Chemistry, Houston, Texas, 16-19 February 1999.

References

Bromley, L — A Thermodynamic property of strong electrolytes in aqueous solutions, AIChE J. 19 (1973) 313.

Charlot, G., — "Les méthodes de la chimie analytique". Masson & CIE, 1966.

Chen H.J., — Henrichsen, C.J., Burnside, C.A., Widener, M.: "Assessment of Barite Scaling Potentials, Sulfate Removal Options and Chemical Treating Strategies for the Tombua-Landana Development", SPE 106480, International Symposium on Oilfield Chemistry, Houston, Texas, USA, 27 February – 2 March 2007.

Connell, D — 1983. *Prediction and Treatment of Scale in North Sea Fields.* Heriotwatt university: M.E. Thesis.

Crabtree, M., — Eslinger, D., Fletcher, P., Miller, M., Johnson, A., King, A. (1999). Fighting Scale–Removal and Prevention. *Oilfield Review*,11(3), 30-45.

Christian, R. — Prévention et inhibition des dépôts de sulfates dans les installations pétrolières, Institut français du pétrole, publication 1996.

Cowan J. C — Weintritt, D. J., (1976). *Water-formed scale deposits*. Gulf Publishing Company, Houston.

Dai, H., — Shi, W., Kan, A.T., Zhang, N. and Tomson, M.: "Thermodynamic Model Improvements for Common Minerals at High Temperature, High Pressure and High TDS with Mixed Salts", SPE 164045, SPE International Symposium on Oilfield Chemistry, The Woodlands, Texas, USA, April 2013.

Dean, J.A — Patnaik, P., 2004. Dean's Analytical Chemistry Handbook. McGrawHill, New York.

Dégremont — Water treatment handbook - 1991 sixth edition Degremont.

Dia, M, A., — Lo, S, M., Pontié, M., Bagan, H., Diawara, C, K., Rumeau, M. Étude de faisabilité d'un nouveau procédé d'adoucissement des eaux par échange d'ions à usage domestique, C.R. chimie 9 (2006).

Dyer, S.J. — Graham G.M., Sorbie K.S.: Factors affecting the thermal stability of conventional scale inhibitors in HP/HT reservoirs. SPE Int. Symp. Oilfield Chemistry. SPE 50717, Houston, 1999, USA.

El-Said M., — Ramzi M., and Abdel-Moghny T., "Analysis of Oilfield Waters by Ion Chromatography to Determine the Composition of Scale Deposition, "Desalination, 2009, 249, 748–756

Emmons, D. H., — Graham, G. C., Holt, S. P., Jordan, M. M., Lorcardel, B., 1999. Onsite, near- real-time monitoring of scale deposition. SPE Publication 56776.

Frenier, W.W., — Ziauddin, M. Formation, removal, and inhibition of inorganic scale in the oilfield environment 2008, Richardson, Tex.: Society of Petroleum Engineers. 230.

Flouret J — (2013), *Étude et modélisation d'un réacteur de coprécipitation innovant pour le traitement d'effluents liquides radioactifs*, [doctoral dissertation, Université de Lorraine, France].

Gillow, J. — M. Hay and J. Horst. In Situ Sulfate Mine Water Treatment – Practical Engineering in the Field, 2014.

Graham, G. M., — Boak, L. S., Sorbie, K. S., 1997. The influence of formation calcium on the effectiveness of generally different barium sulphate oilfield scale inhibitors. Presented at the SPE International Symposium on Oilfield Chemistry, Houston, USA, 18-21. SPE Publication 37273. February 1997a

Graham, G.M — Mackay, E.J., Wattie, I and Boak, L.S.: "Scale Inhibitor Selection Criteria for Downhole (SQUEEZE) Application in a High Volume Horizontal Well in a Fractured Chalk Reservoir", SPE 65025, International Symposium on Oilfield Chemistry, Houston, Texas, 13- 16 February 2001b.

Graham, G.M., — Boak, L.S. and Sorbie, K.S.: "The Influence of Formation Calcium and Magnesium on the Effectiveness of Generically Different Barium Sulphate Oilfield Scale

References

	Inhibitors", SPE Production and Facilities, Vol. 18, Issue No. 1, pp. 28 - 44, February 2003c.
Granier, J.F	Granier J-F, 1998., propriété des fluides de gisement, tome 2,
Hadia N.,	Chauhari L., Mitra S. K., Vinjamur M. et al., "Experimental Investigation of Use of Horizontal Wells in Waterflooding," Journal of Petroleum Science and Engineering, 2006, 56, 303-310)
Hennessy, A.J.B.,	Graham G.M. The effect of additives on the co-crystallisation of calcium with barium sulphate. Journal of Crystal Growth 237–239 (2002) 2153–2159.
Imhmed, S.A.A.,	Application of magnetic susceptibility measurements to oilfield scale management, Institute of Petroleum Engineering Heriot Watt, University Edinburgh, Scotl and, UK April 2012.
James, R.W.,	Wood, W.A. The Crystal Structure of Barytes, Celestine and Anglesite. Proceeding of the royal society, A, Vol.109.
Jones, F.,	Oliveira A., Rohl A.L., Parkinson G.M., Ogden M.I. and Reyhani M.M., investigation into the effect of phosphonate inhibitors on barium sulfate precipitation J. Cryst Growth, 237-239(2002) 424-429.
Jones, F.,	Stanley A., Oliveira A., Rohl A.L., Reyhani M.M., Parkinson G.M. and Ogden M.I., The role of phosphonate speciation on the inhibition of barium sulfate precipitation, J. Cryst. Growth, 249 (2003) 584- 593.
Jones F.,	Jones, P., Ogden M.I, Richmond W.R., Rohl, A.L, Saunders M. The interaction of EDTA With barium sulphate. Journal of colloid and interface science 316, 553-561. 2007
Jordan, M.M.,	Graff, C.J. and Cooper, K.N.: "Development and Deployment of a Scale Squeeze Enhancer and Oil-Soluble Scale Inhibitor to Avoid Deferred Oil Production Losses During Squeezing Low-water Cut Wells, North Slope, Alaska", SPE 58725, SPE International Symposium on Formation damage control, Lafayette, Louisiana, 23-24 February 2000.
Jordan, M.M.,	Sorbie, K S., Jiang, P., Yuan, M., Todd, A. C., Taylor, K., Hourston, K.E., Ramstad, K.,. Mineralogical controls on inhibitor adsorption/desorption in Brent group sandstone and their importance in predicting and extending filed squeeze lifetime. Presented at the European Production Operations Conference and Exhibition, Aberdeen, UK, 15-17 March. SPE Publication 27607, 141-153. 1994
Kan, A.T.,	Zhang, N., Shi, W., Wang, K., Wang, L., Yan, C., Yan, F. and Tomson, M.B.; Interrelationship of CO2, weak acids, bases and pH in scale prediction and control, SPE 164127, SPE International Symposium on Oilfield Chemistry, The Woodlands, Texas, USA, April 2013.
Kieffer, R.,	Mangina, D., Puela, F., Charcosseta, C. Precipitation of barium sulphate in a hollow fiber membrane contactor: Part II The influence of process parameters, Chemical Engineering Science 64 (2009) 1885 – 1891.
Lalmi, Z.	(2008), *Inhibition de la déposition des sels insolubles au niveau des installations industrielles et des puits pétroliers de la région Ourhoud*, [Magister dissertation, university of Ouargla].
Lembarki., A.	L'impact des dépôts sur la production, mémoire de fin de formation, IAP, 2017.
Lindlof, C. J. and Stoffer, G. K.	A case study of sea water injection incompatibility. Journal of Petroleum Technology, July 1983 1256 – 1262.
Mabrouk, A.	(2012). *Caractérisation des résines échangeuses d'ions d'intérêt pour les réacteurs à eau sous pression : Application et validation d'un modèle dédié*. Autre. [Doctorale dissertation, Ecole Nationale Supérieure des Mines de Paris, 2012. France.].
Mackay, J. E.,	Modelling In-Situ Scale Deposition: The Impact of Reservoir and Well Geometries and Kinetic Reaction Rates. SPE Production and Facilities. February 2003, 45 – 56.

References

Mavredaki, E., Neville A., Sorbie K., Assessment of barium sulphate formation and inhibition at surfaces with synchrotron X-ray diffraction (SXRD), Applied Surface Science 257 (2011) 4264–4271.

Moghadasi, J., Jamialahmadi, M., Muller-Steinhagen, H., Sharif, A., Izadpanah, M. R., 2002. Formation damage in Iranian oilfields. Presented at the SPE International Symposium and Exhibition on Formation Damage Control, Lafayette, USA, 20-21 February SPE publication 73781, 9 pp. 2002

Moghadasi, J., Jamialahmadi, M., Muller-Steinhagen, H., Sharif, A., Ghalambor, A., B Izadpanah, M. R., Motaie, E.,. Scale formation in Iranian oil reservoir and production equipment during water injection. Presented at the 5th International Oilfield Symposium and Exhibition, Aberdeen, UK, 29- 30 January 2003. SPE Publication 80406, 14 pp. 2003a

Moghadasi, J., Jamialahmadi, M., Muller-Steinhagen, H., Sharif, A., Scale formation in oil reservoir and production equipment during water injection (Kinetic of CaSO4, and CaCO3 crystal growth and effect on formation damage). Presented at the SPE European Formation damage Conference, The Hague, Netherlands, 13-14 May. SPE Publication 82233, 12 pp. 2003b

Moghadasi, J., Muller-Steinhagen, H., Jamialahmadi, M. and Sharif, A (2004a). Model study on the kinetics of oil field formation damage due to salt precipitation from injection. Journal of Petroleum Science and Engineering. 43: 201– 217.

Moghadasi, J., Jamialahmadi, M., Muller-Steinhagen, H., Sharif, A. (2004b). Formation Damage Due to Scale Formation in Porous Media Resulting from Water Injection. The SPE International Symposium and Exhibition on Formation Damage control. February 18-20. Lafayette, Louisiana: SPE 86524, 1 – 11.

Monnin, C. A thermodynamic for the solubility of barite and celestite in electrolyte solutions and seawater to 200 ◦C and 1 kbar, Chem. Geol., 153 (1999) 187.

Montgomerie, H. (2014). *Novel inhibitor chemistry for oilfield scale application*. [Doctoral thesis, University of Huddersfield].

Moritz, A. P., Neville, A., 2000. A novel approach for monitoring of CaCO3 and BaSO4 scale formation. SPE Publication 60189.

Nancollas, G. H., Liu, T. S. (1975). Crystal Growth and Dissolution of Barium Sulfate. Society of Petroleum Engineers Journal. December 1975, 509 – 516.

Nancollas, G.H. Oilfield Scale: Physical Chemical Study of its Formation & Prevention, International Symposium on Chemicals in the Oil Industry, UK, 143-164, 1985.

Nielsen A.E Homogenous nucleation in barium sulphate precipitation. Acta Chemica Scandinavica 15, 441-442. 1961.

Nielsen A.E The kinetic of crystal growth in barium sulphate precipitation. Acta Chemica Scandinavica 12(5), 951-958 . 1958,

Nielsen A.E., and Toft, J.M. electrolyte crystal growth kinetic, Journal of crystal growth 67,652-664. 1984.

Pina, C. M., Becker, U.; Risthaus, P.; Bosbach, D.; Putnis, Molecular-scale mechanisms of crystal growth in barite A. Nature 1998, 395, 483. (13)

Pina, C. M., Bosbach, D.; Prieto, M.; Putnis, A. J. Microtopography of the barite (0 0 1) face during growth: AFM observations and PBC theory Cryst. Growth 1998, 187, 119.

Putnis, A., Putnis, C. V. SPE Int. Symp. Oil Field Chem. 29094 1995, February, 773

Quddus A. Allam, I.M. : "BaSO4 Scale Deposition on Stainless Steel", Desalination, 127, p219-224, 2000.

Raymond, D Traitements des eaux, deuxième édition, revue, Edition de l'école polytechnique de Montréal 1999.

References

Rondon, V.C (2010). *Étude Des Mécanismes De Libération D'actifs Nano disperses. Application Au Traitement De Puits*, [Doctoral thesis, University of Bordeaux I].

Rosseinsky, D.R the solubilities of sparingly soluble salts in water Part5.-the solubility of barium sulphate at 25 °C. Transactions of the Faraday Society 54, 116-118. 1958.

Shaw, S.S., Sorbie, K.S.: "Structure, Stoichiometry and Modelling of Calcium Phosphonate Scale Inhibitor Complexes for Application in Precipitation Squeeze Processes", SPE 164051, SPE International Conference on Oilfield Scale, Texas, USA, 8-10 April 2013a.

Shaw, S.S., Sorbie, K.S.: "Scale Inhibitor Consumption in long-Term Static Barium Sulphate Inhibition Efficiency Tests", SPE 164052, SPE International Conference on Oilfield Scale, Texas, USA, 8-10 April 2013b.

Skoog, D. A., D. M. West, F. J. Holler, "Chimie analytique ". 7e édition, 1997.

Smith, P.S., Clement Jr. C.C., and Mendoza Rojas, A. (2000). Combined Scale Removal and Scale Inhibition Treatments. The 2000 second International Symposium on Oilfield Scale. January 26 – 27. Aberdeen, UK: SPE 60222, 1 –6.

Smith, R.P. 1976. *The prediction of multi component ion exchange equilibria with particular reference to the system involved in the recovery of uranium*, [doctoral dissertation, University of Natal, Durban, South Africa].

Strachan, J. C., Heath, M.S., White, K., Williams, G., Strong, A. and Bell, K. (2004). Experience With Pre-Emptive Squeeze Treatments on BM Magnus with Aqueous Based Scale Inhibitors. The sixth International Symposium on Oilfield Scale. May 26 – 27. Aberdeen, UK: SPE 87462, 1 – 13.

Sweeney F.M. Cooper, S.D.: "The Development of a Novel Scale Inhibitor for Severe Water Chemistries", SPE 25159, SPE International Symposium on Oilfield Chemistry, New Orleans, Los Angeles, 2-5 March 1993.

Teghidet, H (2012). *Etude de la cristallisation contrôlée de la calcite par voie électrochimique. Effet des ions étrangers au système calcocarbonique sur la nucléation-croissance de la calcite*, [doctoral dissertation, Université Pierre et Marie Curie paris vi France].

Todd, A. C., Yuan, M. D., Prediction of sulphate scaling tendency in oilfield operation. SPE production Engineering Journal, February, 63-72. 1989.

Tomson M.B., Fan, C., Lu, H., Zhang, P, Al-Saiari, H. and Kan, A.T.: "Integration of Kinetics into Scale Prediction Software, Scale Soft Pitzer", SPE International Symposium on Oilfield Chemistry, The Woodlands, Texas, USA, 20-22 April 2009.

Uehara-nagamine, E and Armenante, P.M. Effect of process variables on the single-feed semi batch precipitation of barium sulphate. Chemical engineering research and design, 79 (8), 979-988.2001.

Vetter, J.O., Kandarpa, V., & Harouaka, A. (1982). Prediction of Scale Problems Due to Injection of Incompatible Waters. Journal of Petroleum Technology, 34(02), 273–284.

Vetter, J.O., Farone W.A., Veith E, Lankford S., Calcium carbonate scale considerations: a practical approach. Presented in the International Symposium of Production Technology, Lubbock, 16-17 November1987. SPE Publication 17009. 1987.

Vicum L. Mazzotti M., Baldyga J., Applying a thermodynamic model to the non-stochiometric precipitation of barium sulfate, Chem. Eng. Technol. 26 (3) (2003) 325.

Wong, D.C.Y., JAWORSKI, Z., and NIENOW, A. W. Barium sulphate precipitation in semi-batch reactors. Chemical engineering research and design, 81(8), 874-880.2003.

Yuan, M.D. Barium Sulfate Scale Inhibition in Deepwater Cold Temperature Environment, SPE 68311, 3rd International Symposium on Oilfield Scale, Aberdeen, UK, 30-31 January 2001.

Yuan, M.D.,

References

Todd A.C. and Sorbie K.S., Sulphate scale precipitation arising from seawater injection: a prediction study, Marine and Petroleum Geology Volume 11 Number1; 1994.

Data bank, Sonatrach DP IRARA, Hassi Messaoud, 2019.

Appendices

APPENDIX A

A.1 The functions of ENMAX CPRS

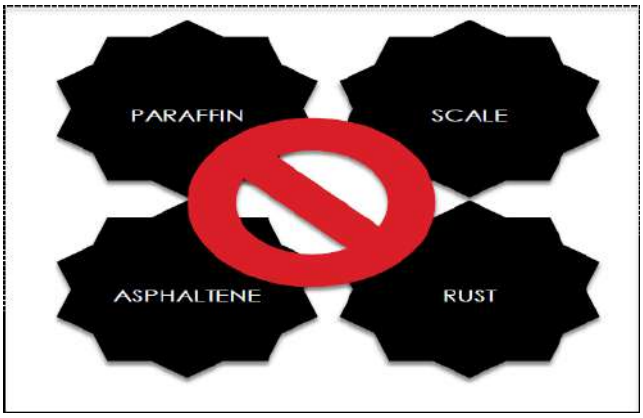

Figure A.I: Main function of ENMAX.

A.2 Types and sizes of the downhole unit

The following table summarizes the type and dimensions of the downhole unit as follow :

Table A.1: Types and dimensions of downhole unite

Downhole unit	**Bar Style**			**Disc Style**		
D ext	2-3/8"	2-7/8"	3-1/2"	2-3/8"	2-7/8"	3-1/2"
D ext of cartridge	1.66"	1.66"	1.66"	2"x10	2.5"×10	3"X10
Flow rate (GPM)	90	90	90	90	100	120

A.3 Types and sizes CPRS surface units

a. Drum style

It has the following size:

Table A.2: sizes of ENMAX/ Drum style

D ext Fixed	D ext Variable
2" × 2"	2"×3"
3" × 3"	3"×4"
4" × 4"	4"×6"
6" × 6"	6"×8"
8" × 8"	8"×10"
10" ×10"	10"×12"
12" ×12"	

Figure A.2: ENMAX / Drum style

b. Online Style

Table A.3: sizes of ENMAX/ online style

D ext Fixe	D ext Variable
2" × 2"	2"×3"
3" × 3"	2.5"×3"
4" × 4"	3"×4"
6" × 6"	4"×6"
8" × 8"	4"×8"
10" ×10"	6"×8"
12" ×12"	6"×10"
14" ×14"	8"×10"
16" ×16"	8"×12"
18" ×18"	10"×12"
20" ×20"	10"×14"
12"×14"	
12"×16"	
14"×16"	
14"×18"	
16"×18"	
16"×20"	

Figure I.62: ENMAX / online sty

Figure A.3: ENMAX / online style

Note: Nominal pressures and variations in outside diameter must be designed to match the working conditions.

A.4 1 The test steps

On 01/03/2017, the installation of the ENMAX tool in flowline 6'' of well MD-411. The following Parameters were taken daily:

- Pressure upstream and downstream of ENMAX 6'', Daily oil flowrate and Wellhead pressure of MD-411 well;
- on 16/07/2017, The free trial period was completed and the ENMAX device was dismantled successfully from the flowline of well MD-411.
- The scale coupon upstream & downstream the ENMAX device was dismantled for complete analysis.
- Visual inspection upstream &downstream the ENMAX device was performed

- The deposits accumulations were measured downstream the ENMAX device after dismantling the
- ENMAX device from the flowline of well MD-411.
- Comparison needs to be conducted for the deposits accumulation before and after installing the ENMAX device on the flowline of well MD-411.

Table A.4: Pressure and flow rate daily reading of well MD 411.

Evaluation of Scale Prevention Device (ENMAX) on the flowline of well MD-411					
Date	Wellhead pressure , bar	Well oil flowrate , m3/day	Pressure Upstream ENMAX device, bar	Pressure Downstream ENMAX device , bar	Remarks
01/03/2017	34.28	128.27	16	16	
02/03/2017	35.70	188.76	16	16	
03/03/2017	37.75	192.88	16	16	
04/03/2017	35.18	182.81	16	16	
05/03/2017	34.61	182.44	16	16	
06/03/2017	34.46	183.12	16	16	
07/03/2017	34.56	174.26	16	16	
08/03/2017	33.99	184.30	15.5	15	• Found a small leak in the pressure gauge after ENMAX device and need to be fixed (reading is not correct). • Sample was taken before and after the device and sent to the laboratory for analysis.
09/03/2017	34.06	177.70	15.5	15	
10/03/2017	34.14	175.21	15.5	15	It's recommended to conduct Bouchon D'eau for the flowline of well MD-411 to avoid salt formation on the holes of the device.
11/03/2017	34.63	182.76	16	15.5	Bouchon D'eau for the flowline of well MD-411 was conducted this morning and found the same pressure drop across the device. Further investigation is in progress.
12/03/2017	34.32	178.35	15.5	15	
13/03/2017	33.73	172.78	15.4	15	
14/03/2017	33.75	170.79	16.5	16	
15/03/2017	33.61	169.91	16	15.5	
16/03/2017	34.22	174.43	16	15.5	
17/03/2017	33.60	169.09	16	15.5	
18/03/2017	33.31	131.86	15.5	15	
19/03/2017	33.45	133.71	14	13.5	
20/03/2017	33.28	128.37	15.5	15	
21/03/2017	33.90	127.93	14.5	14	
22/03/2017	35.53	133.76	16	15.5	
23/03/2017	34.84	130.95	15.5	15	
24/03/2017	33.64	127.38	16	15.5	
25/03/2017	34.03	131.09	16	15.5	
26/03/2017	34.10	130.02	15.5	15	
27/03/2017	32.80	123.30	16.5	16	

28/03/2017	34.63	134.11	16	15.5	
29/03/2017	32.87	126.50	16	15.5	
30/03/2017	33.50	119.12	16	15.5	
31/03/2017	33.77	118.96	16.5	16	
01/04/2017	32.49	125.46	15.5	15	
02/04/2017	32.22	169.27	16	15.5	Juggage was conducted on the well : oil 7.75 m3/hr., GOR 609 and water is zero
03/04/2017	33.95	174.72	15	14.5	
04/04/2017	33.12	166.70	15	14.5	
05/04/2017	32.60	165.27	15	14.5	
06/04/2017	33.91	178.10	15.5	15	
07/04/2017	32.34	174.97	15.5	15	
08/04/2017	34.19	181.11	15.5	15	
09/04/2017	32.92	176.47	15	14.5	
10/04/2017	31.54	173.29	15	14.5	
11/04/2017	33.58	187.41	15.5	15	
12/04/2017	33.54	189.31	15	14.5	
13/04/2017	36.60	204.91	17	16	The pressure gauges were purged and check
14/04/2017	34.10	190.41	16	15.5	
15/04/2017	33.03	182.16	16	15.5	
16/04/2017	33.56	181.80	16	15.5	
17/04/2017	33.28	171.90	15.5	15	Bouchon D'eau for the flowline of well MD-411 was conducted
18/04/2017	32.88	175.49	16	15.5	
19/04/2017	31.54	164.46	16	15.5	
20/04/2017	31.54	172.91	16	15.5	
21/04/2017	32.35	169.14	15.5	15	
22/04/2017	31.91	169.05	15.5	14.5	
23/04/2017	33.32	179.75	16.5	16	
24/04/2017	33.46	182.07	16	15.5	
25/04/2017	32.83	173.62	16	15.5	
26/04/2017	34.28	180.89	16.5	15.5	
27/04/2017	32.98	183.14	16.5	16	
28/04/2017	34.56	189.40	17.5	16.5	
29/04/2017	33.67	186.36	17.5	16.5	
30/04/2017	32.95	187.17	16.5	16	Bouchon D'eau for the flowline of well MD-411 was conducted
01/05/2017	33.79	180.64	16	15.5	
02/05/2017	33.28	180.30	16.5	16	
03/05/2017	33.61	184.06	16	15.5	
04/05/2017	32.18	173.64	16	15.5	
05/05/2017	33.56	182.29	16	16	
06/05/2017	33.66	181.07	16.5	16	
07/05/2017	32.58	187.74	17	16	
08/05/2017	33.45	189.92	17	16	
09/05/2017	32.64	184.79	18	17.5	
10/05/2017	33.10	193.92	16.5	16	
11/05/2017	31.79	183.72	16.5	16	
12/05/2017	31.07	182.61	16	16	
13/05/2017	29.25	171.68	16.5	16	
14/05/2017	31.27	187.87	16	15.5	
15/05/2017	29.68	175.21	16	15	
16/05/2017	31.10	178.06	16	15.5	
17/05/2017	30.29	168.67	15	14	
18/05/2017	33.76	122.33	16.5	16	Bouchon D'eau for the flowline of well MD-411 was conducted
19/05/2017	33.80	189.47	16.5	16	
20/05/2017	31.18	172.31	16.5	16	
21/05/2017	31.38	176.96	15.5	15	
22/05/2017	32.42	181.86	15.5	15	
23/05/2017	31.99	175.66	16.5	16	
24/05/2017	30.36	165.14	16.5	16	
25/05/2017	32.97	178.78	16	15.5	
26/05/2017	30.35	167.47	16	15.5	
27/05/2017	29.08	163.41	16	15.5	
28/05/2017	29.45	166.55	15.5	15	
29/05/2017	31.86	178.76	15	14	
30/05/2017	33.19	183.98	16	15	
31/05/2017	33.55	182.29	16.5	16	Bouchon D'eau for the flowline of well MD-411 was conducted.
01/06/2017	31.77	174.58	16	15.5	End of three month free trail.
02/06/2017	31.07	181.01	16.5	16	
03/06/2017	32.24	181.17	15.5	15	
04/06/2017	31.45	176.95	16.5	16	
05/06/2017	31.98	174.53	15.5	15	
06/06/2017	32.19	177.43	16.5	16	
07/06/2017	31.36	171.70	16.5	16	
08/06/2017	32.29	176.49	17	16.5	
09/06/2017	33.97	181.52	16.5	16	
10/06/2017	33.52	181.73	16.5	16	
11/06/2017	34.00	184.11	16	15	
12/06/2017	33.53	185.51	16	15	
13/06/2017	33.89	188.64	16	16	Bouchon D'eau for the flowline of well MD-411 was conducted.
14/06/2017	34.39	186.71	16.5	16	
15/06/2017	33.65	180.84	16.5	16	
16/06/2017	33.60	187.50	16	16	
17/06/2017	33.02	183.70	15	14.5	
18/06/2017	33.95	187.84	16	15.5	

19/06/2017	33.28	183.70	16.5	16	
20/06/2017	33.11	183.50	16	15.5	
21/06/2017	33.28	183.08	16.5	16	
22/06/2017	33.51	185.60	16	15.5	
23/06/2017	33.26	182.37	16	15.5	
24/06/2017	32.13	179.25	16.5	16	
25/06/2017	33.22	177.21	17	16	
26/06/2017	32.71	179.47	16	15.5	
27/06/2017	33.01	183.24	16	15.5	
28/06/2017	32.24	180.95	16	15.5	
29/06/2017	33.08	182.01	16	15.5	
30/06/2017	36.97	125.08	16	15.5	Bouchon D'eau for the flowline of well MD-411 was conducted.
01/07/2017	35.08	194.99	16	15.5	
02/07/2017	34.87	164.80	16	15.5	
03/07/2017	33.58	156.99	16	15.5	
04/07/2017	33.40	157.34	16.5	16	
05/07/2017	33.76	161.31	16.5	15.5	
06/07/2017	33.13	157.09	16	15.5	
07/07/2017	33.38	159.15	16	16	
08/07/2017	33.24	163.39	16	15.5	
09/07/2017	32.62	158.42	16	15.5	
10/07/2017	32.73	156.24	16	15.5	
11/07/2017	34.21	163.21	16	16	
12/07/2017	33.10	157.26	16	16	
13/07/2017	33.60	166.29	16	16	
14/07/2017	33.31	156.75	16	16	
15/07/2017	31.98	151.29	17	17	
16/07/2017	30.89	144.68	15.5	15	
17/07/2017	31.06	130.10	15	14.5	The device was dismantled and a spool was installed on the flowline instead. Well was closed for 4 Hrs.

Notes:
1- The daily flowrate and Wellhead pressure of Well MD-411 were taken from the Sonatrach databank (Corrected Figures).

Table 3-1 Pressure, flowrate Daily reading for well MD-411

APPENDIX B

B.1 Estimated residual AD32 (output)

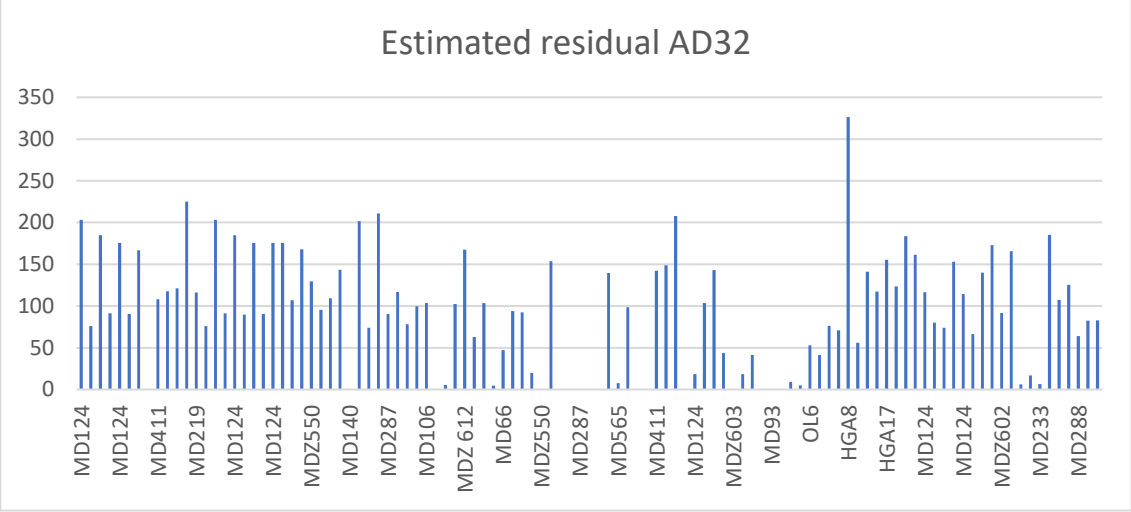

Figure B.1: Estimated residual AD32 at the output of wells.

B.2 TSS at the outlet of wells

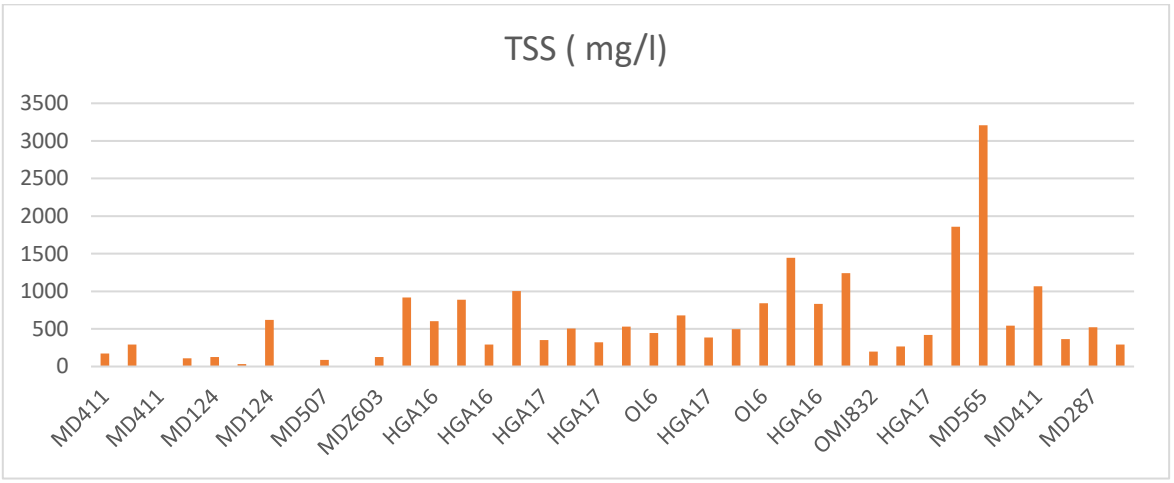

Figure B.2 : TSS at the outlet of wells.

B.3 The SO_4 concentration at the outlet

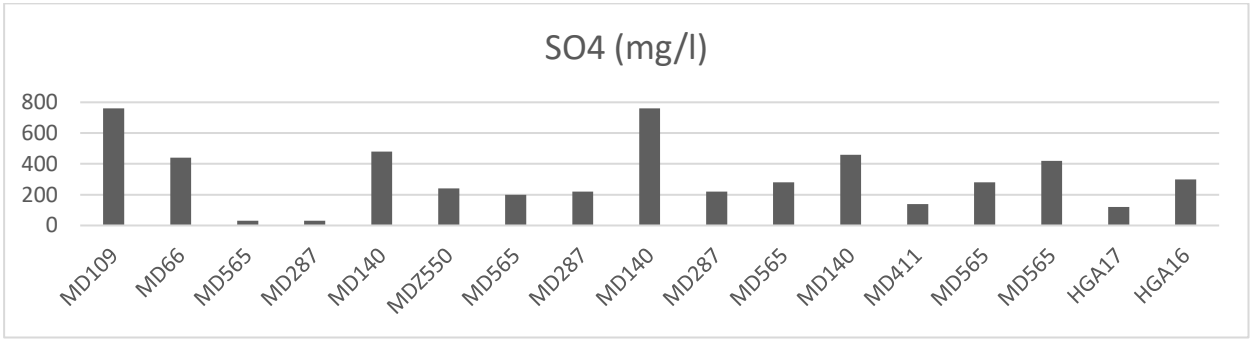

Figure B.3: The concentration of SO_4 at the outlet of wells.

B.4 The estimated percentage of Albian water at the outlet

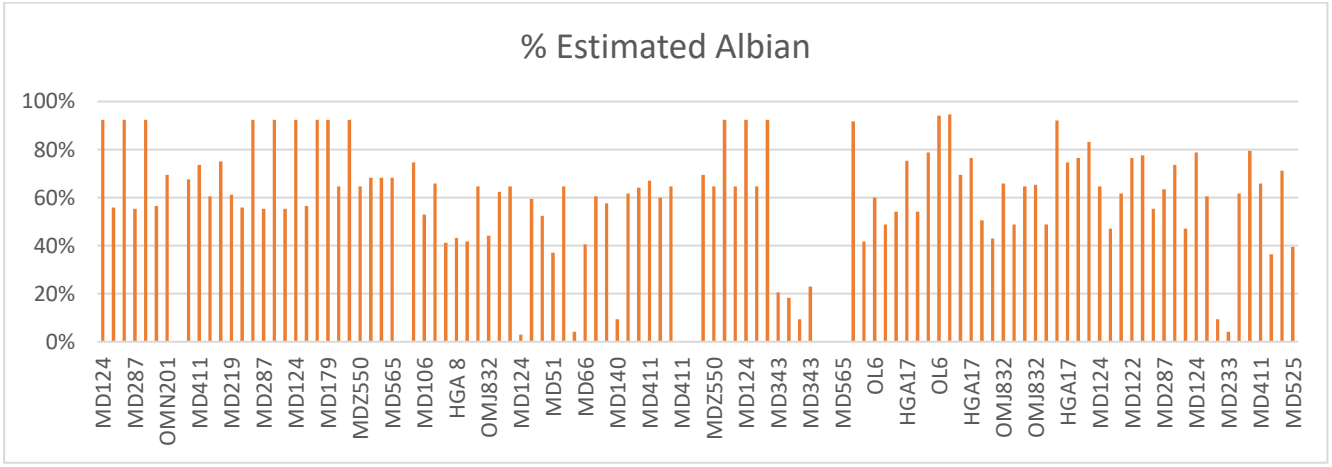

Figure B.4: The estimated percentage of Albian water at the outlet.

APPENDIX C

C.1 Study of the well ONIZ432

Well test

The main purpose of the test is to measure the production flow rate, the wellhead pressure, the pipe pressure, and the separator, this test allowed us to obtain other parameters such as the GOR, and the oil temperature. The results of the ONIZ432 well-gauging tests are shown in Table C.1.

Table C.1: Results of well test of ONIZ432 well.

Date	D choke (mm)	Q oil (m^3/h)	GOR (sm^3/sm^3)	Pressure (Kg/cm^2)			T oil (°c)
				wellhead	Pipe	Sep	
18/09/2016	15	3.05	1162	26.49	17.73	17.19	22
22/12/2016	15.08	0.25	41221	24.1	21.1	_	_
21/02/2017	15.08	2.13	1360	33.4	17.6	_	_
11/04/2017	15.08	0.95	2288	25.75	15.92	16.38	21
07/07/2017	15.08	0.15	5218	32	18	5.3	34
18/07/2017	15.08	1.39	530.27	381	26.1	13.6	34
31/07/2017	15.08	0.16	9953	17.4	12.13	14.29	36
26/08/2017	15.08	0.63	2024	23.3	9.19	_	27
03/09/2017	15.08	0.83	1187	18.2	10.1	_	33

Figure C.1 : Well production profile of ONIZ432.

C.2 Study of the well MD413

Table C.2 : The latest well operations on well MD413.

Date	Opérations	Details
28/11/2020	OPERATION_SPECIALE	Kick Off CCE
21/11/2020	OPERATION_SPECIALE	Scale blaster + Tube clean
20/10/2020	WIRELINE	Contrôle
14/10/2020	WIRELINE	Contrôle
09/10/2020	SNUBBING	-----

Below is a detailed map of the location of well MD413 relative to other nearby wells.

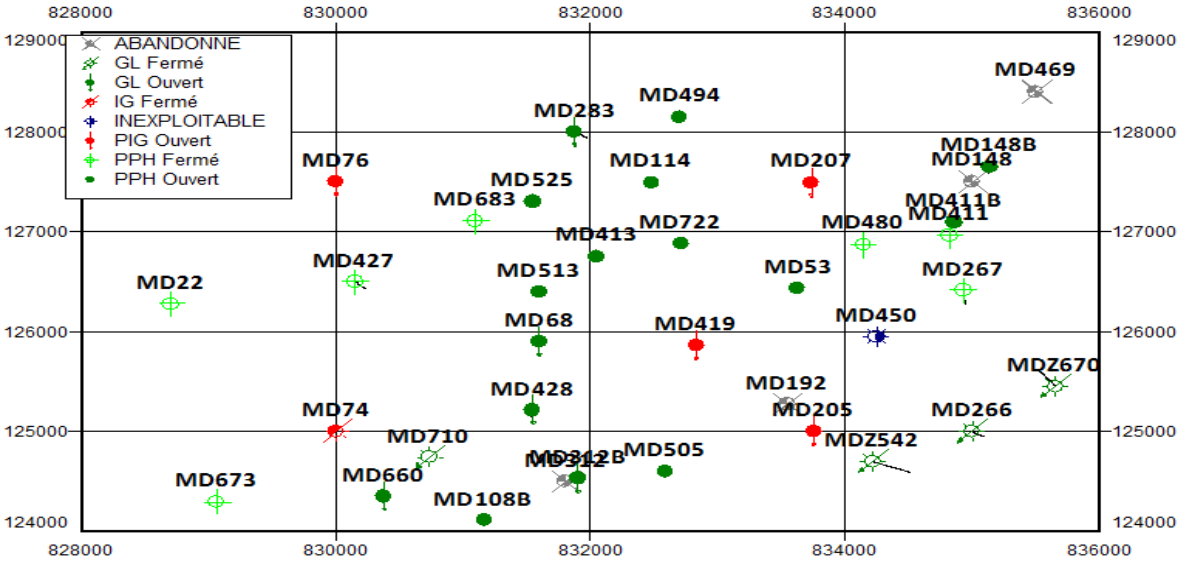

FigureC.2 : Map of location of MD413.

C.3 study of the well MD633

Below is a detailed map of the location of well MD413 relative to other nearby wells.

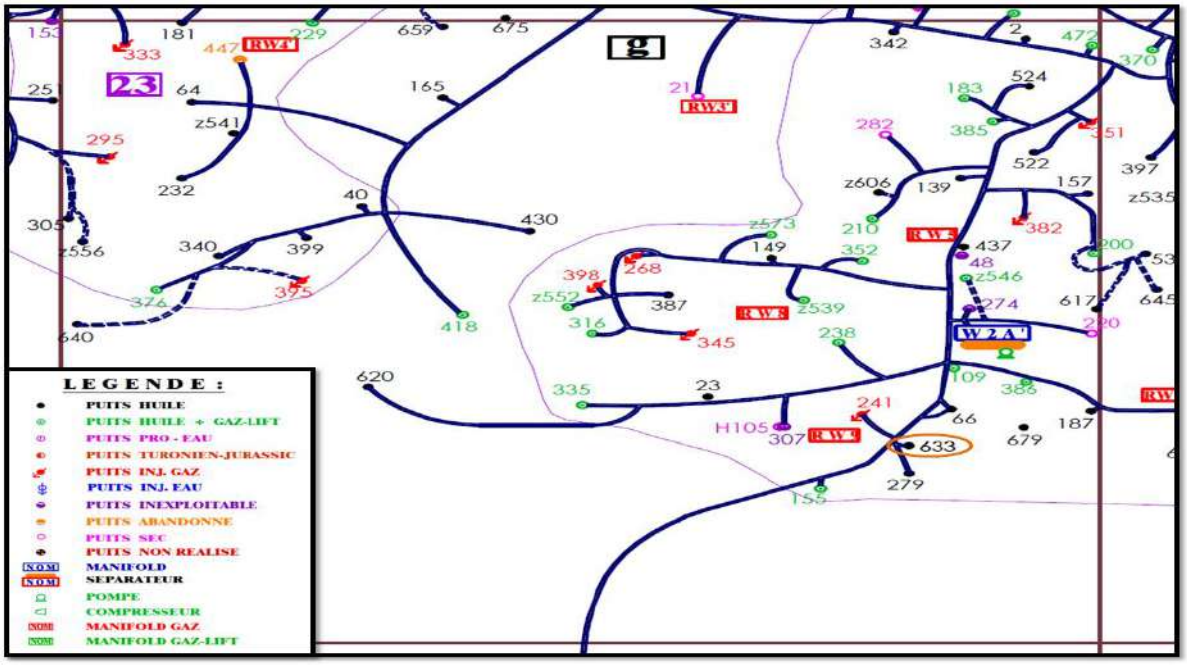

Figure C.3 : Map of location of MD633.

The table below shows the latest operations on well MD633.

Table C.3 : The latest well operations on well MD633.

Date Début	Opérations	Sous/opérations
13/10/2020	SNUBBING	-----
11/03/2019	OPERATION_SPECIALE	Mise en production
07/03/2019	OPERATION_SPECIALE	Mise en production
23/02/2019	WIRELINE	Controle
22/02/2019	WIRELINE	Instrumentation

APPENDIX D

Table D.1 below shows the costs of the various Scale-Blaster operations intended for the curative treatment of $BaSO_4$ deposits in the field of Hassi Messaoud during the period of unavailability of the AD32 (April 2020 to December 2020).

Table D.1 : The costs of Scale-Blaster operations for the curative treatment of $BaSO_4$ deposits.

N°	Wells	Zone	Date	Comments	costs (dollar)
1	MD	1B	08-avr-20	CT ScaleBlaster and TubeClean during Snubbing	250 250,00
2	MD	HZN	01-mai-20	CT ScaleBlaster during Snubbing	/
3	MD	2S	09-mai-20	CT ScaleBlaster & TubeClean during Snubbing	/
4	OMP	11	29-mai-20	CT ScaleBlaster and TubeClean	303 875,00
5	HGAW	HZP	30-juin-20	CT Scale blaster and Tube Clean	321 890,00
6	MD	HZS	20-oct-20	CT ScaleBlaster and TubeClean during Snubbing	278 850,00
7	MD	14	26-oct-20	CT ScaleBlaster and TubeClean	303 875,00
8	MD	15	11-nov-20	CT ScaleBlaster and TubeClean during Snubbing	417 838,04
9	MD	15	22-nov-20	CT ScaleBlaster and TubeClean during Snubbing	393 250,00
10	ONM	15	25-nov-20	CT ScaleBlaster and TubeClean during Snubbing	423 541,50
11	MD	14	16-déc-20	CT ScaleBlaster and TubeClean during Snubbing	429 000,00

Table D.2: monitoring the variation of AD 32 inhibitor for stations of HMD field.

Dates	*[AD32]*
	Station Z14 (200 ppm)
12/05/2014	130
01/01/2015	**560/430**
11/01/2015	**306**
04/02/2015	**365**
17/03/2015	**23**
19/06/2015	**110**
26/07/2015	**380**
29/08/2015	**400**
02/10/2015	**65**
16/10/2015	**86**

12/01/2019	**400**
19/01/2019	**223**
	Station HGA (200 ppm)
18/01/2015	**90**
23/03/2015	**87**
02/06/2015	**74**
24/06/2015	**450**
04/07/2015	**350**
22/07/2015	**80**
18/08/2015	**440**
30/08/2015	**344**
22/09/2015	**48**
03/10/2015	**400**
	Station W1C (150 ppm)
12/01/2015	**118**
16/01/2015	**265**
31/01/2015	**80**
23/02/2015	**248**
12/03/2015	**90**
25/03/2015	**322**
14/07/2015	**100**
31/07/2015	**380**
14/08/2015	**111**
23/08/2015	**330**
12/01/2019	**270**
	Station CINA (180 ppm)
20/02/2015	305
10/03/2015	362
14/03/2015	370
15/04/2015	316
16/05/2015	107
15/07/2015	400
20/07/2015	130
23/07/2015	110
13/08/2015	154
11/09/2015	110
12/01/2019	100
19/01/2019	162

	Station CIS (180 ppm)
02/01/2015	**31**
28/01/2015	**324**
25/03/2015	**318**
17/04/2015	**130**
15/05/2015	**109**
11/06/2015	380
01/08/2015	254
18/09/2015	350
27/09/2015	**60**
24/10/2015	**113**
12/01/2019	**233**